Final Report to

Geophysical Modeling for Studying Acquisition and Processing Methods in the Deepwater Gulf of Mexico

RFP2007DW2001

Subcontract 07121-2001

January 3, 2014

Peter Pangman, Principal Investigator
Michael Fehler, Project Manager
Charles Meeder, Technical Consultant

SEG Advanced Modeling Corporation
8801 S. Yale, Suite 500
Tulsa, Ok 74137
918-497-4614
jmadole@seg.org
www.seg.org

LEGAL NOTICE

This report was prepared by Mike Fehler and Chuck Meeder as an account of work sponsored by the Research Partnership to Secure Energy for America, RPSEA. Neither RPSEA members of RPSEA, the National Energy Technology Laboratory, the U.S. Department of Energy, nor any person acting on behalf of any of the entities:

a. MAKES ANY WARRANTY OR REPRESENTATION, EXPRESS OR IMPLIED WITH RESPECT TO ACCURACY, COMPLETENESS, OR USEFULNESS OF THE INFORMATION CONTAINED IN THIS DOCUMENT, OR THAT THE USE OF ANY INFORMATION, APPARATUS, METHOD, OR PROCESS DISCLOSED IN THIS DOCUMENT MAY NOT INFRINGE PRIVATELY OWNED RIGHTS, OR

b. ASSUMES ANY LIABILITY WITH RESPECT TO THE USE OF, OR FOR ANY AND ALL DAMAGES RESULTING FROM THE USE OF, ANY INFORMATION, APPARATUS, METHOD, OR PROCESS DISCLOSED IN THIS DOCUMENT.

THIS IS A FINAL REPORT. THE DATA, CALCULATIONS, INFORMATION, CONCLUSIONS, AND/OR RECOMMENDATIONS REPORTED HEREIN ARE THE PROPERTY OF THE U.S. DEPARTMENT OF ENERGY.

REFERENCE TO TRADE NAMES OR SPECIFIC COMMERCIAL PRODUCTS, COMMODITIES, OR SERVICES IN THIS REPORT DOES NOT REPRESENT OR CONSTIITUTE AND ENDORSEMENT, RECOMMENDATION, OR FAVORING BY RPSEA OR ITS CONTRACTORS OF THE SPECIFIC COMMERCIAL PRODUCT, COMMODITY, OR SERVICE.

Principal Investigator
Peter Pangman, SEG Advanced Modeling Corporation, Director of Geophysics

_____ Date: _____

Table of Contents

ABSTRACT 8
EXECUTIVE SUMMARY 10
PROJECT MANAGEMENT 13
EARTH MODELS 16
Model Overview 16
Elastic Tilted Transverse Isotropic (TTI) Earth Model 18
Gravity Earth Model 21
Resistivity Earth Model 22
Elastic Earth Model 22
Additional Model Information 23
Figures 25
NUMERICAL SIMULATION 37
Numerical Simulation Issues 37
AUS Simulations 37
TTI Simulations 38
Elastic Simulations 38
Figures 40
SEISMIC ACQUISITION 43
Simulations Conducted Prior to the Beginning of the SEAM Phase I RPSEA Project 44
Acoustic Absorbing Upper Surface Data 47
Tilted Transverse Isotropy 50
Elastic Data 55
Figures 64
GRAVITY 83
SEAM Gravity Model 83
Figures 91
CONTROLLED SOURCE ELECTROMAGNETICS 98
SEAM Resistivity Model 98
CSEM Acquisition Geometry 99
CSEM Simulation Issues 99
CSEM Data 100
Data Distribution 101

Figures 102
MAGNETOTELLURICS 108
Magnetotelluric Simulation 108
Receiver Positions and Numbering 108
Output Data 109
Output Data Format 110
Simulation Issues 110
Data Distribution 111
Figures 112
QUALITY CONTROL 115
QC of Seismic Simulations 115
Vendor Qualification 115
QC Conducted by Simulation Vendors 118
QC Conducted by a QC Vendor 118
Evaluation Specifications for Near-Surface Trace Data 118
Evaluation Specifications for VSP Trace Data 120
Evaluation Specifications for Seafloor Trace Data 120
QC Conducted by Technical Project Manager 121
Issues Identified During QC 121
QC on Classic Data Sets Composed of Selected Traces from Selected Shots 122
Figures 124
DATA COMPRESSION 128
Evaluation of Compression of Elastic Data Set 130
Evaluation of Compression of the WAZ and NAZ AUS and TTI Classic Data Sets 131
Use of Decompression Code 132
Figures 134
IMPACT TO PRODUCERS 143
TECHNOLOGY TRANSFER 144
CONCLUSION 145
RECOMMENDATIONS 147
FIGURES AND TABLES 148
REFERENCES 158
LIST OF ACRONYMS AND ABBREVIATIONS 159
TABLE OF SYMBOLS 161

APPENDICES 164
Appendix A - Technology Transfer 164
APPENDIX B - Shot & Receiver Locations and Numbering 167
Appendix C – SEG-Y Header Definitions 175

ABSTRACT

The objective of this project is to contribute to the evolution of geophysical imaging technology by providing realistic benchmark geological models and associated synthetic seismic and potential field data which will allow the industry and researchers to effectively and efficiently assess seismic (and other data) acquisition and processing techniques for generating images of hydrocarbon reservoirs beneath massive, complex salt bodies located in deepwater regions. Better subsurface imaging enhances the industry's ability to successfully explore and develop hydrocarbon resources and produce them for the consumer.

Synthetic geophysical data sets were acquired by numerical simulation over the SEAM numerical earth model, a realistic representation of a 60 block area of the sub-salt exploration challenge in the deepwater Gulf of Mexico.

These data sets are:

1. Acoustic Seismic with Absorbing Sea Surface Data Sets: This variable density acoustic data set was acquired over a large area of the SEAM model, selected so as to optimize research into seismic acquisition techniques and the development of imaging algorithms for sub-salt exploration and development challenges. The Absorbing Sea Surface is a non-physical boundary condition but is the condition that most geophysical processors convert their data to using processing algorithms called multiple-elimination techniques. The data set generated by SEAM will allow the testing of multiple elimination techniques.

2. Controlled-Source Electromagnetic (CSEM), Magnetotelluric (MT), and Gravity Data Sets: These complementary data sets were acquired over the full SEAM model. They are available in a form that, when combined with the acoustic and elastic seismic, will enable research into joint inversion methods for enhanced subsurface interpretation of structure, rock and fluid properties.

3. Tilted Transverse Isotropic (TTI) Data Set: This data set was acquired to facilitate research into the identification of effects of TTI on data processing and imaging subsalt for the enhancement of exploration and development. This data set includes 'streamer' pressure sensor data in addition to 4 component data collected in 4 'boreholes' penetrating the seafloor.

4. Elastic Seismic Data Set: This data set was acquired over a carefully selected sub-area of the SEAM model to facilitate research into the identification of elastic effects on data quality, the development of approaches to remove elastic "noise" from acoustic data sets, and improved methods for elastic data processing. The data set includes seafloor 4 component, wellbore 4 component, as well as 'streamer' pressure sensor data.

The data were quality controlled, archived, and distributed to the SEAM participating companies and is available to the public after September 1, 2013 at www.seg.org/SEAM.

EXECUTIVE SUMMARY

Synthetic geophysical data sets were acquired over the SEAM Phase 1 numerical earth model, which is a realistic representation of a 60 block area of the sub-salt exploration challenge in the deepwater Gulf of Mexico. These data sets were acquired using numerical simulation codes selected through rigorous validation procedures. Each data set was run through a quality control procedure. 'Classic data' subsets of these data were generated to be more readily distributed and accessible. Both the classic and full data sets have been archived and are available upon request.

The primary goals of the SEAM Project are to:

- Design and generate synthetic model 3D geophysical data that represent exploration and subsurface characterization challenges to the consortium members, including but not limited to:
    - Imaging and illumination
    - Coherent noise reduction
    - Field acquisition strategies
    - Rock property estimation
    - Reservoir description and monitoring
    - Joint geophysical inversion approaches
    - Share the high cost effort of substantial model design and synthetic data generation.
    - Provide a forum to discuss geophysical problems of interest to the consortium members and the industry at large.
    - Advance the art of modeling and computation by testing and comparing modeling code for accuracy and efficiency.
    - Provide data sets for industry benchmarks and educational purposes.
    - Further the science of geophysics for the public benefit.

All seismic data sets are stored according to industry best practice standards in SEGY format. Non-seismic data sets are stored in formats that allow ease of access.

Four general types of data have been simulated:

1. Acoustic Seismic with Absorbing Sea Surface Data Set: This variable density acoustic data set was acquired over a large area of the SEAM model, selected so as to optimize research into seismic acquisition techniques and the development of imaging algorithms

for sub-salt exploration and development challenges. The Absorbing Sea Surface is a non-physical boundary condition but is the condition that most geophysical processors convert their data to using processing algorithms called multiple-elimination techniques. The data set generated by SEAM will allow the testing of multiple elimination techniques.

2. Controlled-Source Electromagnetic (CSEM), Magnetotelluric (MT), and Gravity Data Sets: These complementary data sets were acquired over the full SEAM model. They are available in a form that, when combined with the acoustic and elastic seismic data generated by SEAM, will enable research into joint inversion methods for enhanced subsurface interpretation of structure, rock and fluid properties.

3. Acoustic Transverse Isotropic (TTI) Seismic Data Set: This data set was acquired to facilitate research into seismic processing and imaging of the subsurface for enhanced sub-salt exploration and development challenges. Including this property in imaging improves the structural and stratigraphic image quality and resolution and positions the image more accurately in space, both laterally and vertically. This data set includes 'streamer' pressure sensor data in addition to 4 component data collected in 4 'boreholes' penetrating the seafloor.

4. Elastic Seismic Data Set: This data set was acquired over a carefully selected sub-area of the SEAM model to facilitate research into the identification of elastic effects on data quality, the development of approaches to remove elastic "noise" from acoustic data sets, and improved methods for elastic data processing. This includes simulation of streamer hydrophone (pressure sensor) data, seafloor four component data, and Vertical Seismic Profile (VSP wellbore) four component data.

This final report includes a description of the geological and numerical considerations for the development the SEAM Phase I model, descriptions of all data sets including acquisition design parameters and the goals for these acquisition plans, the numerical simulations, descriptions of the numerical validation procedures developed for confirming the reliability of the numerical simulations, descriptions of the QC conducted for each data set and implementation results, and how to obtain copies of the data.

A detailed technical report for the Phase I component of the SEAM project, which preceded the work here, contains information that is complimentary to this report and available through the SEG at www.seg.org/SEAM (see Fehler and Keliher, 2011).

A project management plan was in effect to insure the objectives were met and a program of technology transfer took place throughout the life of the project.

Funding for this project is provided by RPSEA through the "Ultra-Deepwater and Unconventional Natural Gas and Other Petroleum Resources" program authorized by the U.S. Energy Policy Act of 2005. RPSEA (www.rpsea.org) is a nonprofit corporation whose mission is to provide a stewardship role in ensuring the focused research, development and deployment of safe and environmentally responsible technology that can effectively deliver hydrocarbons from domestic resources to the citizens of the United States. RPSEA, operating as a consortium of premier U.S. energy research universities, industry, and independent research organizations, manages the program under a contract with the U.S. Department of Energy's National Energy Technology Laboratory.

PROJECT MANAGEMENT

The project management plan included:

- An organized function driven structure consisting of the SEAM Board of Directors with oversight and financial control of the project.

- A Management Committee consisting of a representative from each participating Oil and Gas Company and Industry Service Providers. This Committee was chaired by one of the company representatives elected by the Members of the Management Committee.

- A Project Manager, Michael Fehler, was employed to coordinate and manage the project activities. This included working with all the Technical Committees and Management Committee, and responsibility for the activity of subcontractors.

- To assist the Project Manager and advise the Management Committee, six Technical Committees were established. These committees were made up of technical expert volunteers from the participating companies to assist with technical support, model building, acquisition design, evaluation of numerical methods, methods of data storage, and any other technical issues. Each committee had two co-chairmen. In addition, the committee co-chairs worked together to maintain cohesion and integrate the work of all the Technical Committees.

- The Technical Committees included:

    - Model Design Committee
    - Numerical Design Committee
    - Acquisition Design Committee
    - Non-seismic Design Committee
    - Execution Committee
    - Data Storage and Distribution Committee

The Model Design Committee was responsible for making decisions concerning the SEAM model, and performing the work to construct the model. The Model Committee was co-chaired by Richard Day (COP) and Joe Stefani (Chevron) and consisted of members Dean Stoughton (BHP), Edward Naylor (BHP), Kevin Bishop (BHP), and Mark Gordon (Repsol). Additional conversations, help, and feedback came from Joachim Blanch (BHP), Jacques Leveille (Hess), Scott Morton (Hess), and John Anderson (XOM).

The Numerical Design Committee was responsible for setting numerical parameters, evaluating vendor tests results, and determining the seismic wavelet; Co-chaired by John Anderson (XOM) and Scott Morton (Hess). Members included Robert Bloor (ION), Nizar Chemingui (PGS), Joakim Blanch (BHP), Arthur Cheng (Halliburton), Elive Menyoli (Marathon), and Joe Stefani (Chevron).

The Acquisition Design Committee was responsible for defining the acquisition parameters for each seismic data set based on the objectives and properties of the model and for recommending Classic Data Sets. The Acquisition Design Committee was led by Co-Chairs: Adam Seitchik (Devon) and Chuck Meeder (Marathon). Members included Laurent LeMaistre (TOTAL), Nick Moldoveanu (WesternGeco), Tim Brice (WesternGeco), Roger Sollie (Statoil), Paul Williamson (TOTAL).

The Non-seismic Design Committee was responsible for design of all non-seismic simulations of gravity, CSEM and MT. The Non-seismic committee included co-chairmen Michael Frenkel (EMGS), and Neville Barker (OHM). Members included Irina Filina (Hess), Neda Bundalo (Marathon), and Shangli Ou (XOM).

The Execution Committee defined quality control procedures and assisted the Project manager with quality control. This committee was co-chaired by John Weigant (Geotrace) and Wenying Cai (Repsol). Members included Nicola Bienti (ENI), Ron Kerr (Devon), and Mihai Popovici (3DGeo).

The Data Storage and Distribution Committee defined and evaluated alternatives for data archiving and distribution. Co-chairmen were Stew Levin (Halliburton) and Ray Gedaly (Repsol).

While we list affiliations of committee members during the time that they served on committees, please note that several of the listed affiliations are no longer valid.

Monthly activity and budget reports were filed with RPSEA and the project was reviewed at the regular Ultra Deepwater TAC meetings. The Management Committee met at least every quarter.

The SEAM Phase I-RPSEA Management Committee Representatives at the conclusion of the project are as follows:

John	Anderson	ExxonMobil Upstream Research Co.
Marcelo	Benabentos	Nexen Petroleum USA Inc (Dallas)
Joakim	Blanch	BHPBilliton Petroleum (Americas), Inc
Robert	Bloor	GX Technology
Shon	Bourgeois	Marathon Oil Company
Nizar	Chemingui	PGS Americas
Arthur	Cheng	Halliburton/Landmark
Mike	Cogan	Statoil
Henri	Houllevigue	Total E&P USA Inc.
Alan	Huffman	Sigma^3 Integrated Reservoir Solutions
Paulo	Johann	Petrobras
Dana	Jurick	Devon Energy Corporation
Eugenio	Loinger	Eni S.p.A.
Lucy	MacGregor	OHM Rock Solid Images
Brian	Macy	ConocoPhillips Company
Scott	Morton	Hess Corporation
Shkelqim	Muskaj	Repsol USA, Inc.
Jon	Rasmussen	EMGS (Electromagnetic Geoservices ASA)
Joseph	Stefani	Chevron Energy Technology Company
Bruce J.	VerWest	CGGVeritas Services (USA) Inc
David	Walraven	Anadarko Petroleum Corporation
Peter	Wang	WesternGeco L.L.C
Mai	Yang	Maersk Oil America Inc
Gary	Yu	Geotrace Technologies, Inc.

EARTH MODELS

SEAM's goal was to produce earth models and simulations on those models to advance the state of the art in multiple geophysical disciplines. The model is not only large, it is highly complex with realistic faults, overturned beds, overhanging salt, density diffractors to generate diffracted multiples, turbidite fans, and braided stream channel reservoirs. Some compromises had to be made due to limitations of model building tools available and due to the need to provide a gridded model for use during simulation. An attempt was made to make the best model possible for the SEAM project given the limitations in hardware, software, and time available. The development and details of stratigraphy, structure and construction of this model are covered in the book published by the SEG ' SEAM Phase 1: Challenges of Subsalt Imaging in Tertiary Basins, with Emphasis on Deepwater Gulf of Mexico' by M. Fehler and P. J. Keliher in 2011 (online ISBN 978-1-56080-294-5).

To be useful in multiple disciplines, the model was designed to capture as much physics and realism as possible. This requires internal consistency across the domains of rock properties (e.g., fundamental properties like percent shale and porosity), the intermediate level elastic and electromagnetic properties (compressional and shear velocity, density, horizontal and vertical resistivities, etc.) and the output simulations [or "modeling"] of seismic, electromagnetic, and gravity phenomena. By rooting the ultimate simulation back to fundamental rock properties, any changes in the latter are guaranteed to change all the elastic and other properties automatically, consistently, and with the appropriate correlations. Figure 1-1 is a schematic that outlines the general philosophy of the model building, model simulation, and use of the resulting data for geophysical investigations.

Model Overview

Five earth models were generated in SEAM Phase I to simulate a realistic earth model of a salt canopy region of the Gulf of Mexico complete with fine-scale stratigraphy that includes oil and gas reservoirs. The model represents a 35 km EW x 40 km NS area and 15 km deep, and the base grids are 20 m x 20 m x 10 m (x,y,z) except that the initial Acoustic model was on a 10m x 10m x 10m grid. The model is large and highly complex with realistic faults, overturned beds, overhanging salt, density diffractors to generate diffracted multiples, turbidite fans, and braided stream channel reservoirs. All model properties are derived from fundamental rock properties including v-shale (volume of shale) and porosities for sand and shale that follow typical compaction gradients below water bottom. Hence, properties have subtle contrasts at macro-layer boundaries, especially in the shallow section, generating very realistic synthetic data. The model files include the horizons, faults, fundamental rock properties, and the property grids of P-velocity, S-velocity, density, anisotropy orientation, and resistivity. The models can be used to verify processing and imaging test results, or for simulation of additional

acquisition geometries to suit specific applications. Descriptor files containing indices for geological units, locations of reservoirs, vshale, sand and total porosity are also available so different petrophysical parameterizations may be used to generate different geophysical models by interested users.
The geophysical models that were developed include:

1) Acoustic isotropic earth model,
2) Elastic TTI Earth Model,
3) Elastic Earth Model,
4) Gravity Earth Model,
5) Resistivity Earth Model.

All models are available separately or combined.

Note that the Elastic TTI model distribution has the S-velocities as originally developed, with a minimum value of approximately 120 m/s. The Elastic Earth Model distribution is the model used for simulation of the SEAM Phase I RPSEA elastic data set. For the elastic simulations, the minimum S-wave velocity was set at 600 m/s by transforming all S-wave velocities in the originally designed model having velocities between 100 and 800 m/s into a range between 600 and 800 m/s. The Elastic TTI Earth Model contains 21 binary files each approximately 21 GB. These files provide not only geophysical properties of the model but also give gridded geological and petrophysical properties of the model. This distribution also includes the resistivity models that were provided to vendors for use in the CSEM and MT simulations.

The Acoustic Isotropic Earth Model used for the Acoustic Absorbing Upper Surface (AUS) data simulations is the same as the one used for the Acoustic Free Surface (see Fehler and Keliher, 2011). For the SEAM Phase I RPSEA project, a new model was built that is slightly different from the one used for the acoustic and acoustic AUS simulations. The models are almost identical except for the overturned sediment raft immediately below a portion of the salt body. Due to lack of complete documentation in how the initial acoustic model was constructed, it was not possible to identically match this portion of the model when the full elastic TTI model was constructed. For this reason, all SEAM Phase I RPSEA simulations were conducted on a consistent model that was built from scratch. All geological descriptor files that are available are for this newer version of the model

The rugose salt body, shown in Figure 1-2, is the most prominent feature of the earth model. The salt, embedded in a sedimentary system, is not entirely homogeneous. The heterogeneity within the salt structure and the sedimentary layers are detailed in the "Geologic Features" section of Fehler and Keliher (2011). Complexity of the salt body is illustrated in Figures 1-3a and 1-3b showing the east and west flanks of the salt. Some of the simulated data sets extend over the entire data volume but other more detailed data

sets focus on the area of salt overhang and the grotto seen in Figure 1-3b. The data sets and their location on the model are described in detail in the Seismic Data Acquisition Section.

There are seventeen bodies defined within the model (Figure 1-4). Some of the complexity includes the heterogeneous salt at the top of the salt body, overturned sediments beneath the salt, and salt sutures. Turbidite and channel reservoirs were overlaid on the Pleistocene and Miocene intervals. These represent realistic reservoirs in geometry, shale content, and rock properties. Examples of the shape and Vshale volume variation within the turbidites are illustrated in Figure 1-5. Thin sheets of turbidite sequences were stacked and the distribution of their cumulative vertical sum in the model is shown in Figure 1-6. The stacked sum of channel sequences is also visible in this figure.

Elastic Tilted Transverse Isotropic (TTI) Earth Model

The SEAM TTI model is closely related to the SEAM Isotropic acoustic variable density model. The structural components of the two models are identical. The TTI elastic model has, besides the Vp and density, ρ, of the acoustic model, added the parameters Vs, ε, γ, δ, Dx, and Dy for an elastic anisotropic model. The variables D_x^{tti} and D_y^{tti}, are the x and y components of the dip which are equivalent to the direction angles θ, ϕ of the symmetry axis of anisotropy. The use of Dx and Dy to describe bed dip is defined below and in the README that accompanies the model files. Some information from that README file also appears below.

Vp = Compressional wave velocity
Vs = Shear wave velocity
ρ = density
E,γ, and δ are Thomsen's weak anisotropy parameters (Thomsen, 1986).
ε = P-wave anisotropy; the fractional difference of Vp in the vertical (or bed-normal) and horizontal (or bed parallel) directions
γ = S-wave anisotropy; the fractional difference of Vs in the vertical (or bed-normal) and horizontal (or bed parallel) directions
δ = the crucial anisotropic parameter for near-normal P-wave propagation
See also G. Mavko, T. Mukerji, and J. Dvorkin,1998.

Both the isotropic and anisotropic models have the same physical size; namely 35Km in the E-W direction, 40Km N-S and 15Km in depth. The parameters for the anisotropic model are stored on a regular x-y-z grid spacing of 20x20x10m, whereas the isotropic model is preserved on a 10x10x10m grid.

The TTI model also has saved rock physics parameters for shale fraction, Vsh, and total and effective porosity ϕ^{τ}, ϕ^{ε}. There is a discussion in the SEAM Phase I report (Fehler and Keliher, 2011) on the relationship between the rock physics parameters and the physical parameters that control wave propagation. Non-seismic parameters for the bed parallel and bed normal resistivities, Rn and Rp were developed. These parameters were used to generate vertical and horizontal resistivity files using the approach described in Fehler and Keliher (2011).

The Vp and Density volumes for the isotropic and TTI model will be similar but not identical. Besides the obvious use of different mesh sizes there were some differences in the model construction process. The 10m grid size and large volumes of the isotropic model forced some extra interpolation to achieve the 10m sampling that was not necessary for the TTI model.

Non-geologic model features included in the density model that may prove useful when validating imaging are the high density SEG logo imprinted at the base of the model and some deep diffractors that are centered at Z=13500 as well as some shallow diffractors. These features were imprinted to the density as the last step in constructing the model. The locations of the density diffractors are described in Fehler and Keliher (2011).

A unique feature of this model in the industry is the relationship of the axis of anisotropy relative to the dip, (structural and stratigraphic). Most models are built, or derived from the seismic data during the imaging process, to have the TTI axis of symmetry normal to the bed dip. The SEAM TTI model is more realistic for the Gulf of Mexico and other Tertiary Basins where velocity is a function of depth and compaction as well as stratigraphic layering. To represent this in the model, the TTI axis is tilted towards the vertical from the bed dip for the less compacted, shallower intervals and is also based on shale content.

Two versions of the dips are available, the stratigraphic dips and the TTI dips. The TTI dips are a weighted version of the stratigraphic dip. The TTI dip multiplies the stratigraphic dip by a layer based weight 'W_s' that is in the range 0-1. See Table 1-1 for the values of the weight function. The weight factor W_s serves to bend the unit normal of the symmetry axis towards the vertical for values less than one. A value of zero yields a vertical symmetry axis.

$$D_x^{tti} = W_s D_x$$

$$D_y^{tti} = W_s D_y$$

The anisotropy parameters ε, δ, and γ were computed from the value of Vsh and a region dependent parameter epsMax, delMax, gamMax. See Table 1-1 for the values of the anisotropic parameters.

$$\varepsilon = V_{sh} * \ epsMax$$

$$\gamma = V_{sh} * \ gamMax \qquad (1)$$

$$\delta = V_{sh} * \ delMax$$

Table 1-1. Layer dependent parameters for setting anisotropy variables. GeoIndex is Geology unit index shown in Figure 1-4. Other parameters are defined in the text.

Region	GeoIndex	Ws	epsMax	delMax	gamMax	
Basement	1	0	0.000	0.000	0.000	
MomSalt	2	0	0.000	0.000	0.000	
Cretaceous	3	1	0.150	0.075	0.150	
OligocenePaleoge	4	0.9	0.130	0.065	0.130	
LowerMiocene	5	0.8	0.100	0.050	0.100	
MiddleMiocene	6	0.7	0.120	0.060	0.120	
UpperMiocene	7	0.7	0.110	0.066	0.121	
Pliocene	8	0.6	0.100	0.050	0.100	
Pleistocene	9	0.6	0.080	0.040	0.080	
Water	10	0	0.000	0.000	0.000	
Salt	15	0	0.000	0.000	0.000	
InvLowerMiocene	11	1	0.100	0.050	0.100	
InvOligoPaleog	12	1	0.120	0.060	0.120	
InvCretaceous	13	1	0.130	0.065	0.130	
Salt Sutures	14	0.7	0.090	0.045	0.090	
Het Salt	17	0	0.000	0.000	0.000	

Relation of dips to axis of symmetry and direction angles

The TTI symmetry axis is given from two parameters Dx and Dy as follows. Given a surface z = f(x,y), or F(x,y,z) = f(x,y) – z, whose local in-line dip D_x and cross-line D_y at (x,y,z) are defined as:

$$D_x = \frac{\partial f}{\partial x}$$

$$D_y = \frac{\partial f}{\partial y} \qquad (2)$$

$$\hat{n} = \frac{(D_x, D_y, -1)}{N} \qquad (3)$$

where $N(D_x, D_y) \equiv \sqrt{1 + \ D_x^2 + D_y^2}$

If we are given D_x and D_y , then we may recover ϕ, θ as shown in the following that makes use of the symmetry axis expression in terms of the direction angles. We note that equation (4) has forced the dip into the range 0-90 degrees. We also note that the sign of the normal vector is ambiguous. The choice of negative z component implies the upward pointing normal.

$$\hat{n} = \left(\frac{D_x}{N}, \frac{D_y}{N}, -\frac{1}{N}\right) = (\sin\theta\cos\phi\ , \sin\theta\sin\phi, \cos\theta)$$

$$\cos\theta = \frac{1}{N} \Rightarrow \theta = \cos^{-1} 1/N \text{ and } \sin\theta = \sqrt{1 - \frac{1}{N^2}} \text{ or } N\sin\theta = \sqrt{N^2 - 1} = \tan\theta$$

$$D_x = N\sin\theta\cos\phi = \tan\theta\ \cos\phi$$

$$\phi = \cos^{-1} {D_x}/{\sqrt{N^2 - 1}} \qquad (4)$$

$$D_y = N\sin\theta\sin\phi = \tan\theta\ \sin\phi$$

$$\phi = \sin^{-1} {D_y}/{\sqrt{N^2 - 1}}$$

We summarize the relationship between dip-x and dip-y and the angles.

$$D_x = {n_x}/{n_z} = \tan\theta\ \cos\phi$$

$$D_y = {n_y}/{n_z} = \tan\theta\ \sin\phi \qquad (5)$$

TTI Model Section was modified from the file SEAM _TTI_Model.doc 12/7/2010 by Richard Day.

Gravity Earth Model

The SEAM Phase I gravity simulation was calculated from a 40x40x20 (x,y,z) meter size voxet cell density volume. The original density model, the Acoustic Isotropic Earth Model, (dx=dy=dz=10m) was resampled to a grid size of 40 m in each horizontal direction and 20 m in depth in order to comply with the software requirement for a file size as well as to make a consistent voxet size of the EM model. The resampling of the density voxet has no measurable impact on the final results. Densities within the model vary from 1.003 g/cm^3 to 3.140 g/cm^3 The latter high density is the density of the SEG

logo embossed in the base of the model. The low density is water. The model used for gravity simulation is included with the simulated gravity data, but the model is also available separately.

Resistivity Earth Model

The SEAM resistivity model has Vertical Transverse Isotropic (VTI) anisotropy in the background, while a large salt body is isotropic and homogeneous with resistivity 100 Ωm. The model is further described in the CSEM Section of this report.

The resistivity model that was built at the time that the TTI model was constructed had bed-normal and bed-perpendicular resistivity values. Resistivity values in the horizontal and vertical directions were required for the CSEM simulation and resistivity in the horizontal direction was needed for the MT simulation. The rotation from bed-normal and bed-perpendicular resistivity to vertical and horizontal resistivity required making an assumption about the resistivity tensor. The rotation used and assumptions made in choosing the approach for doing the rotation are described in Fehler and Keliher (2011).

Elastic Earth Model

In the original elastic model, the shear wave velocity near the sea floor was as low as 120 m/s based on rock physics. During the construction of the model, considerable effort was made to evaluate measurements of S-wave velocity near the seafloor. While measurements are few and uncertainties are large, there is reason to believe that values as low as 10s of m/s are possible. For practical reasons of density of spatial sampling required for simulation and excessive travel time (simulation time), the velocities for the Vs model used for elastic simulation were scaled to values more manageable for today's state-of-the art in wave equation computer simulation. Numerous methods for scaling the velocities were discussed and some rejected because they induced unreasonable effects in the model including Vp/Vs ratios with little or no contrast between lithologies, and simple truncation at a set Vs was non-geological and not acceptable. The minimum Shear velocity in the elastic simulation model was set to 600 m/s. The model was modified to meet this criteria through linear adjustment of the velocities. The linear compression approach compresses the impedance contrast but leaves some impedance and Vp/Vs ratio contrast in the model in the shallow and reservoir intervals. An example shear velocity cross-section in the model as originally built is shown in Figure 1-7. The linear compression (Figure 1-8) was applied to all shear velocities from 100 m/s to 800 m/s throughout the model. Shear velocities over 800 m/s were unchanged. Figure 1-9 shows the adjusted shear velocities on the same cross section as shown in Figure 1-7. The shear velocity and impedance contrasts are reduced but contrasts are still apparent at most of the depth intervals. The original Vp/Vs ratio for this section is shown in Figure 1-10 which exhibits a large range of Vp/Vs values from very high at the seafloor to more

typical sediment values of near 2.0. The Vp/Vs ratio after the linear compression of Vs (Figure 1-11) shows a reduction of the high ratios near the seafloor, a reduction in the variation of Vp/Vs but reasonable contrasts due to lithology variations are still apparent.

Additional Model Information

Some non-geologic features were added to the model to provide additional detailed tests for simulations and imaging. These include some point diffractors and insertion of the SEG logo at the base of the model defined by density variations from the background sediment densities (Figure 1-12).

The correct model must be used with each data set due to the variations in the models that were made to meet the needs of each type of simulation. The model files contain

1. Acoustic isotropic earth model (10m x 10m x 10m)
    a. Compressional wave interval velocity
    b. Density

2. Elastic TTI Earth Model (20m x 20m x 10m). Consists of 22 files as follows
    a. Compressional wave interval velocity
    b. Shear wave interval velocity
    c. Density
    d. Stratigraphic dip-X
    e. Stratigraphic dip-Y
    f. Geoindex for geology
    g. Geoindex including reservoir index
    h. Geoindex before salt added
    i. Effective porosity
    j. Total (sand plus shale) porosity
    k. Vshale
    l. Bed normal resistivity
    m. Bed parallel resistivity
    n. Vertical Resistivity
    o. Horizontal Resistivity
    p. Vertical Resistivity decimated to (20,20,40) m grid in (E,N,D)
    q. Horizontal Resistivity decimated to (20m x 20m x 40m) m.
    r. TTI dip-X
    s. TTI dip-y
    t. Delta
    u. Epsilon
    v. Gamma

3. Elastic Earth Model used for Elastic Simulations (20m x 20m x 10m)
    a. P-wave velocity
    b. Shear wave velocity
    c. Density

4. Gravity Earth Model (40m x 40m x 20m)
    a. Density

5. Resistivity Earth Model (40m x 40m x 20m).
    a. Vertical resistivity
    b. Horizontal resistivity

Figures

Figure 1-1. Rooting the SEAM model in rock properties: from geology and petrophysics to geophysics. Figure from Joe Stefani, Chevron.

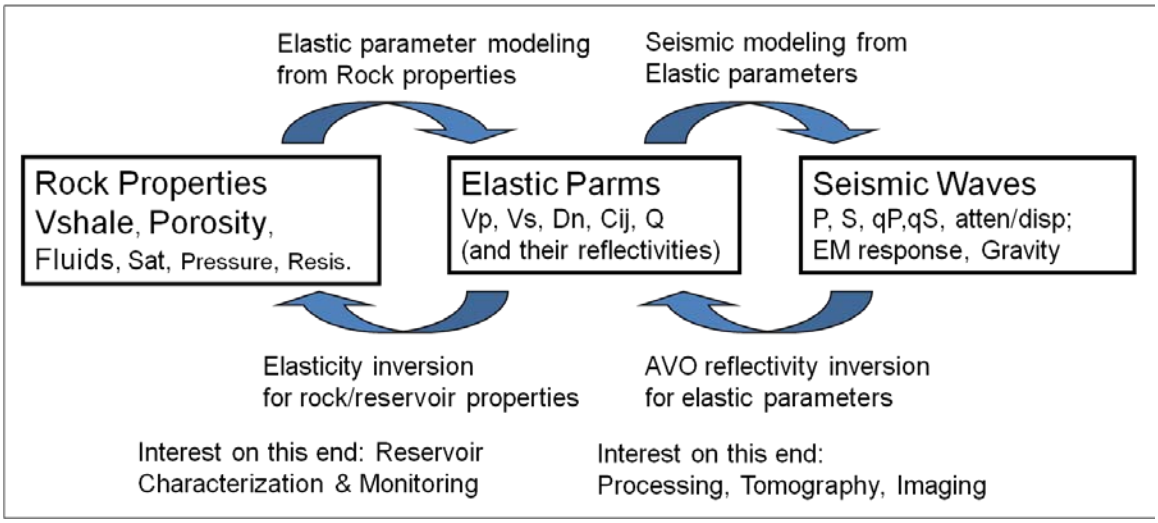

Figure 1-2. A view looking down upon the top of the complex 3D salt body. Shown around the salt is a depth slice at Z=7500 m from the gridded P-wave velocity, Vp. The white and red rectangle defines the bounds of the 35 km E-W by 40 km N-S model. The salt body surfaces extend beyond the model for gridding purposes. From Fehler and Keliher (2011).

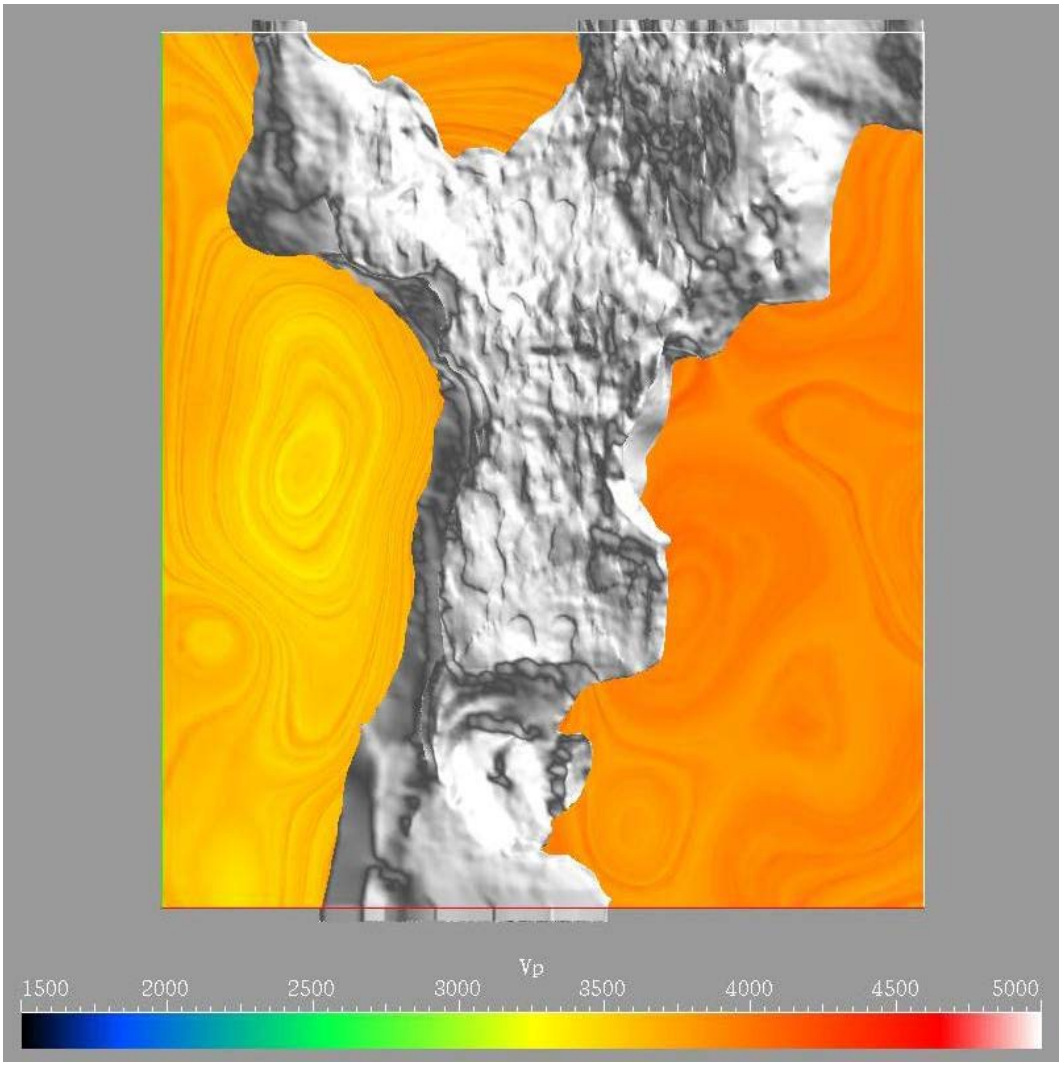

Figure 1-3a. View towards the west of the eastern flank of the main salt body. Overhangs are seen from this perspective as well as the root stalk of the salt that ties to the mother salt which is not shown. The white rectangle measures 40 km by 15 km with north to south running right to left. From Fehler and Keliher (2011).

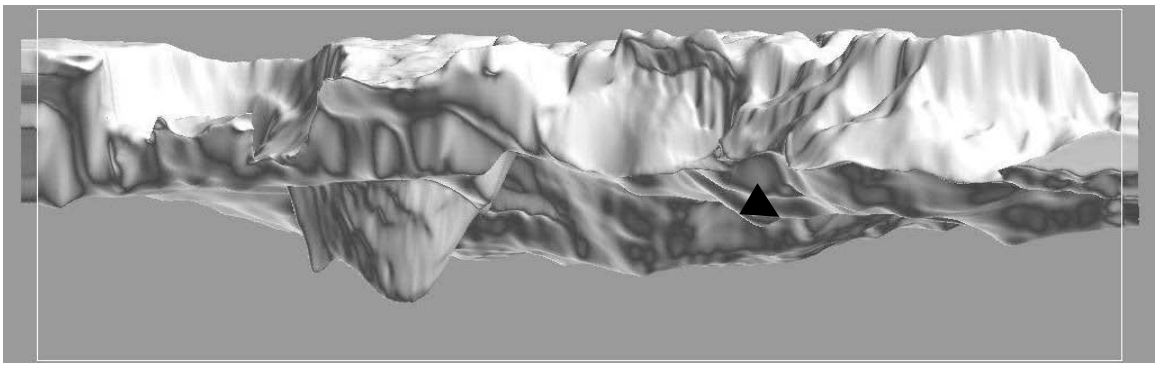

Figure 1-3b. View towards the east of the western flank of the main salt body. Overhangs and a grotto are seen from this perspective. The white rectangle measures 40 km by 15 km with north to south running left to right. The grotto and salt overhang area is the focus of some of the limited area data sets. Modified from Fehler and Keliher, 2011.

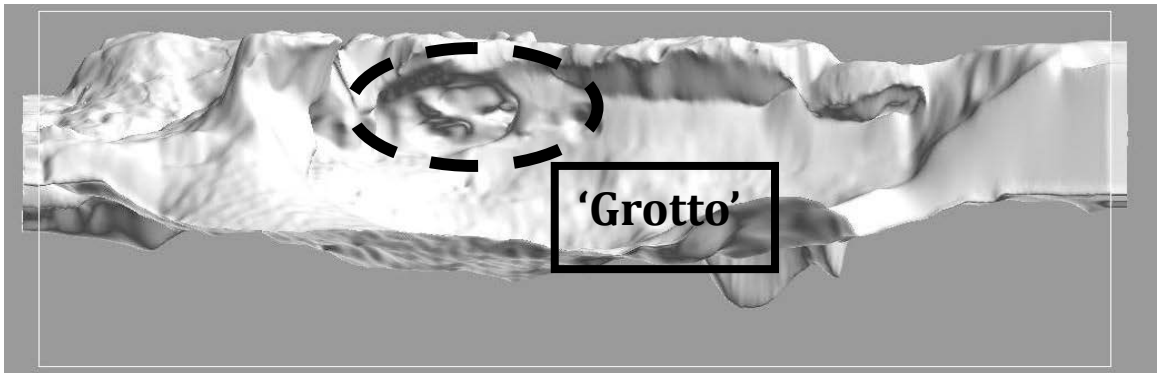

Figure 1-4. GeoIndex values on model cross section. GeoIndex values are:1=Basement, 2=Mother Salt, 3=Cretaceous, 4=Oligocene-Paleogene, 5=Lower Miocene, 6=Middle Miocene, 7=Upper Miocene, 8=Pliocene, 9=Pleistocene, 10=Water, 11=Inverted Lower Miocene, 12=Inverted Olig-Paleogene, 13=Inverted Cretaceous, 14=Salt Sutures, 15=Homogeneous Salt, 17=Heterogeneous Salt. From Fehler and Keliher (2011).

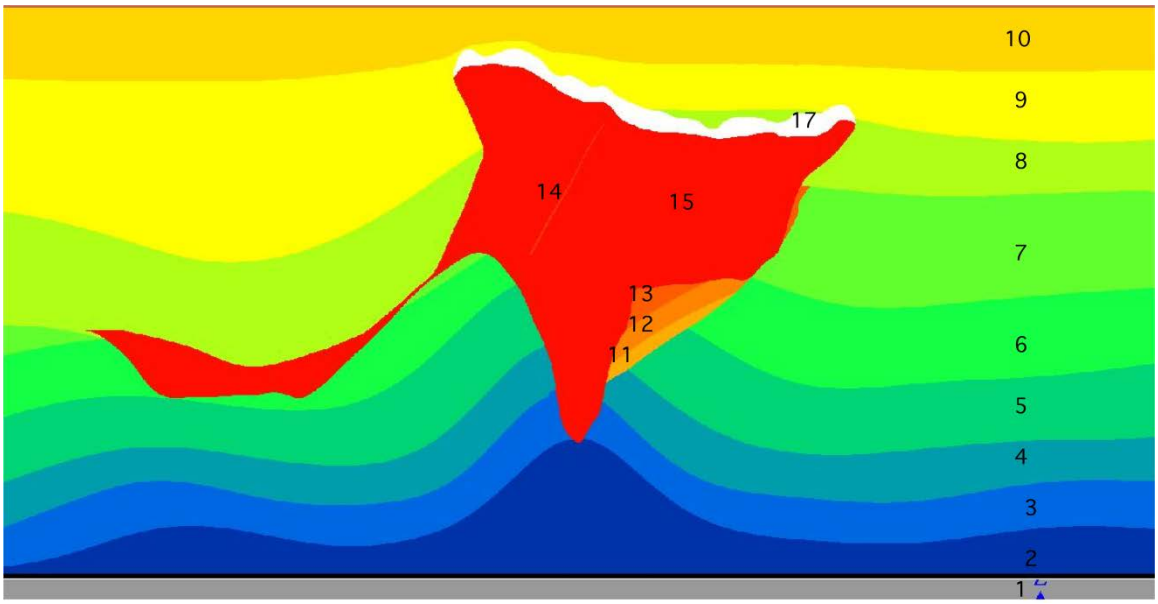

Figure 1-5. Middle Miocene sheet turbidite vshale, 35 km across. Left: Single stratigraphic slice 20 meters thick. Right: vertical average of vshale over 80 meters constituting one subsheet. From Fehler and Keliher (2011).

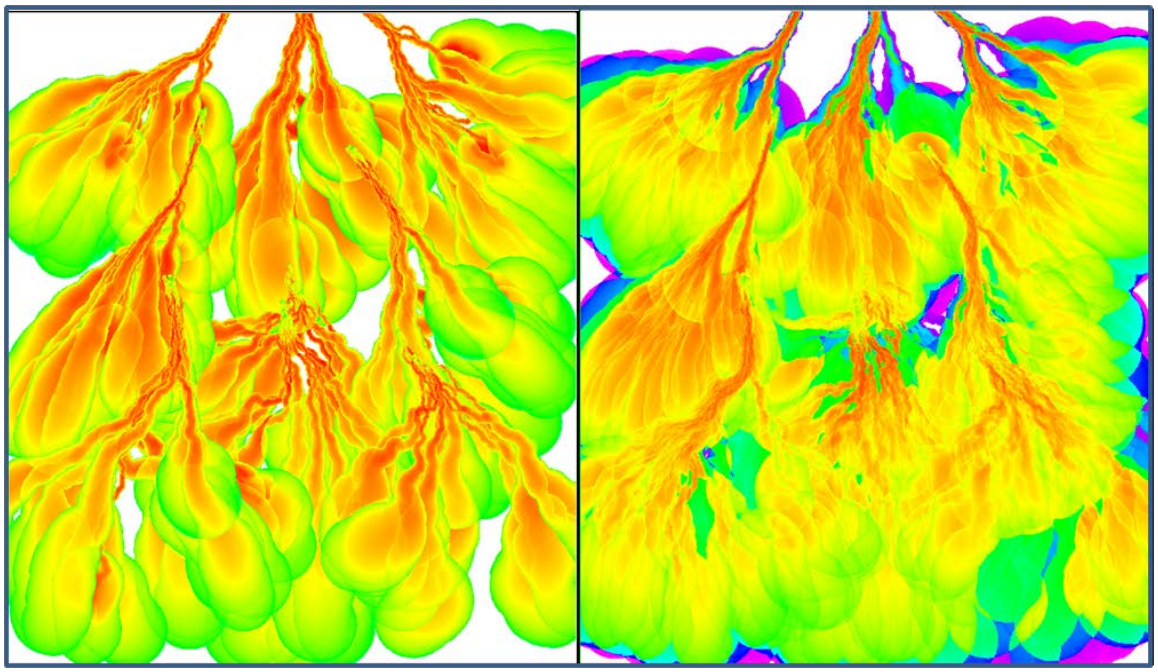

Figure 1-6. Cumulative vertical sum of reservoir thickness. Black=0 m, White=800 m. Note how either salt or the northern model edge truncate the turbidite stems. From Fehler and Keliher (2011).

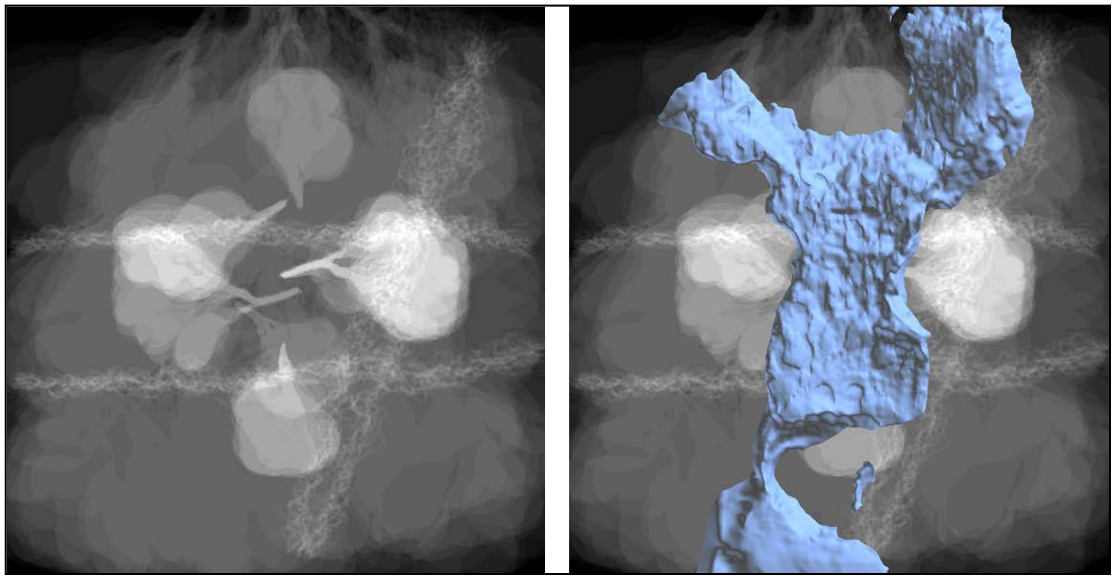

Figure 1-7. A model cross-section of the original S-Velocity model shows considerable variation ranging from 120 m/s – 1500 m/s in the shallow portion of the model. Note a vertical exaggeration of about 5:1 in the figure. Modified from the file Fehler_April_26_MC_reorder.ppt , 2012, in the SEAM online archive.

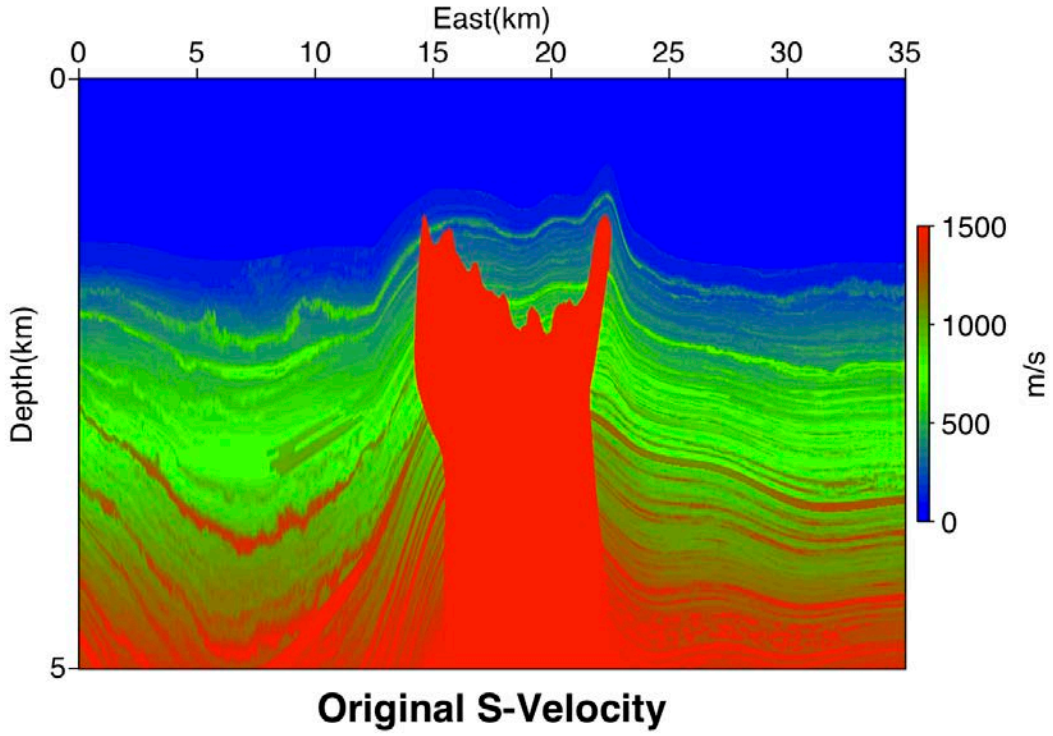

Figure 1-8. Linear adjustment applied to shear velocities ranging from 100 – 800 m/s. Modified from the file Fehler_April_26_MC_reorder.ppt , 2012, in the SEAM online archive.

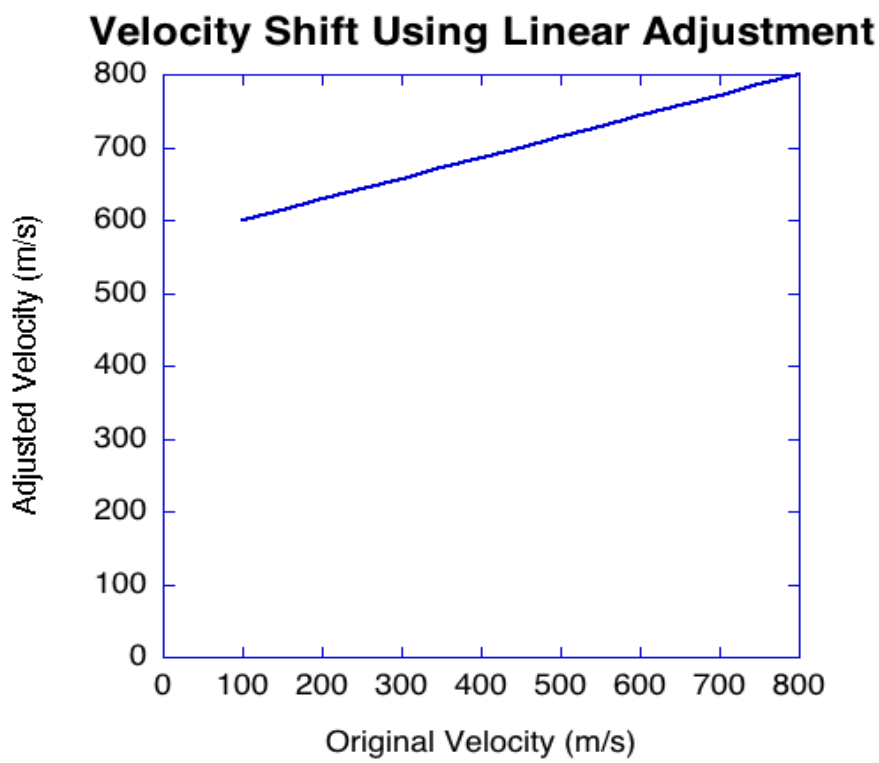

Figure 1-9. Vs model after adjustment of values in Vs model shown in Figure 1-7 within a range of 100 to 800 m/s to be between 600 and 800 m/s using linear scale. Note the vertical exaggeration of about 5:1 in the figure. Compare to the original Vs in Figure 1-6. Modified from the file Fehler_April_26_MC_reorder.ppt , 2012, in the SEAM online archive.

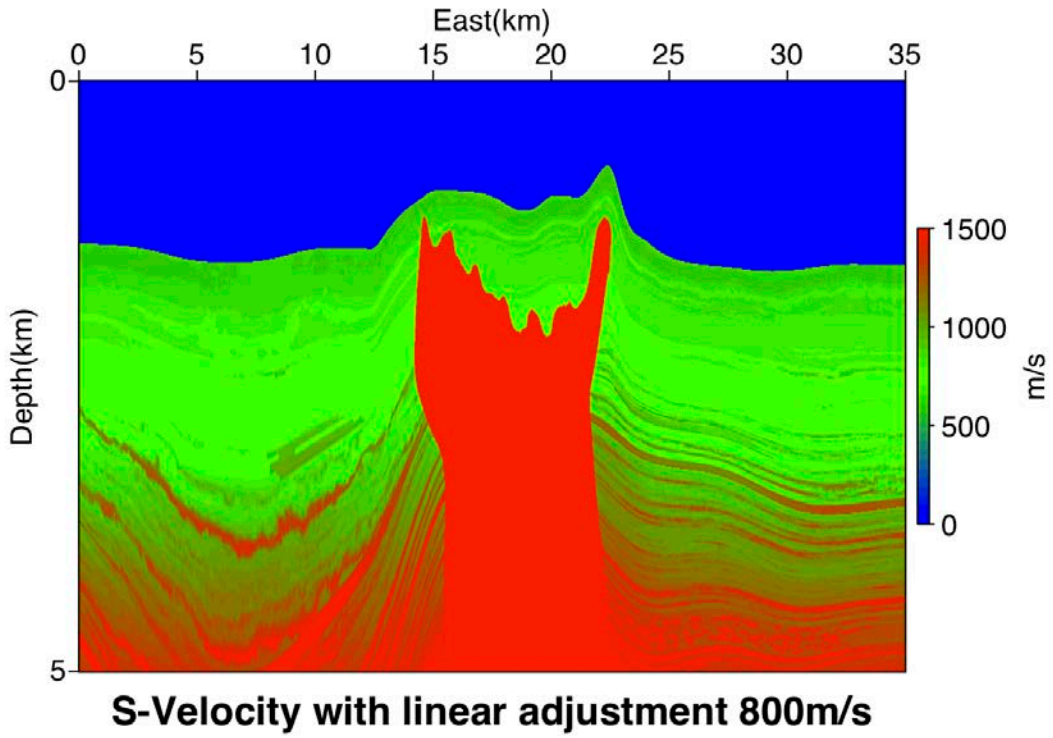

Figure 1-10. A model cross-section of the original Vp/Vs shows considerable variation including very high ratios near the seafloor. Note the vertical exaggeration. Modified from the file Fehler_April_26_MC_reorder.ppt , 2012, in the SEAM online archive.

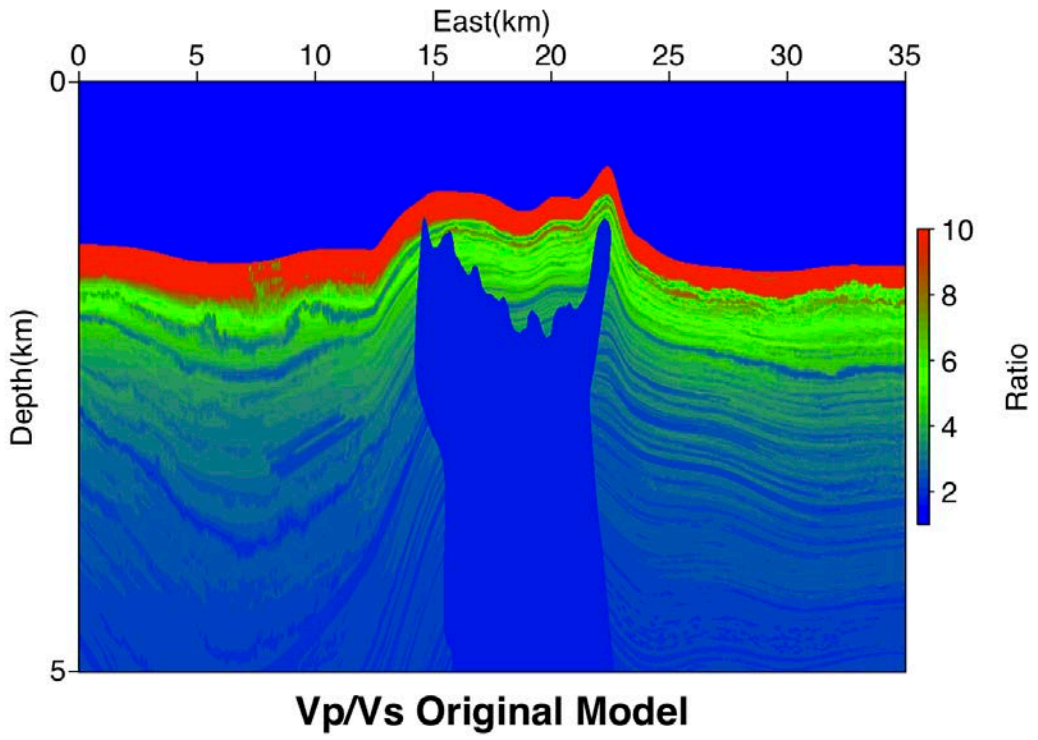

Figure 1-11. A model cross-section of the adjusted Vp/Vs shows reduced variation but as depth increases the Vp/Vs ratio varies less. Note the vertical exaggeration of 5:1 and that the color scale differs from the one used in Figure 1-10. Modified from the file Fehler_April_26_MC_reorder.ppt , 2012, in the SEAM online archive.

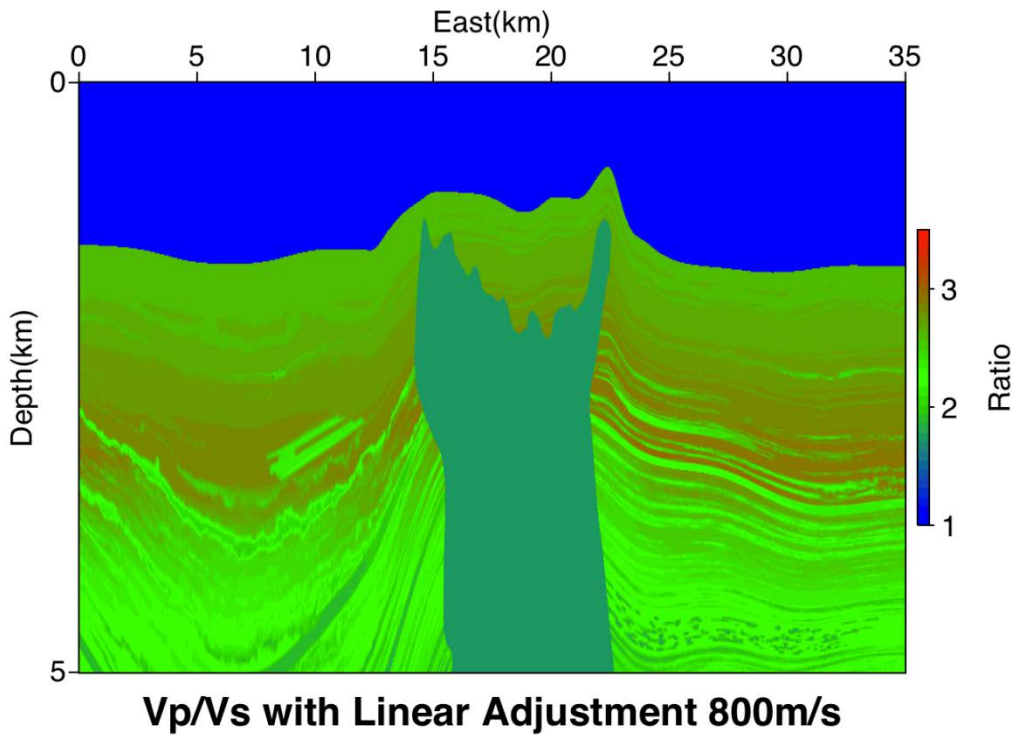

Figure 1-12. SEG logo diffraction test pattern. Blue = no density deviation from the background, green = 0.13 g/cc above background, red = 0.5 g/cc above background. In the model, the logo is aligned east-west and is centered in both X and Y. The east-west distance between the tips of the logo is 30 km, and the north-south distance between tips is 16 km. (Binary pixels file courtesy of Dave Hale.)

NUMERICAL SIMULATION

Numerical Simulation Issues

SEAM chose to specify what the outcome of a simulation should be rather than how the simulation was to be conducted. The reason was that SEAM wanted to allow vendors to develop and use simulation approaches that extend the state-of-the art for simulation of seismic acquisitions in large complex models like the SEAM Phase I model. Our lack of specificity extended to how the source was inserted into the simulation scheme. SEAM chose to specify what a far-field source pulse should look like rather than specify the time-history of the source. Similarly, the trace amplitudes were specified to be scaled to a given surface trace amplitude at a given offset (990 m) in a half space water model. All other traces were to be scaled relative to this given amplitude.

Trace amplitude scaling and source characteristics are described in detail in the SEAM Phase I report (Fehler and Keliher, 2011). Figure 2-1 shows the far-field source pulse shape that was specified by SEAM. The pulse shape was not changed for different simulations. The pulse shape is defined to be the required shape at far offset in a full space water model. The vendor was to insert a source time-history into their simulation code to yield the required far-field pulse shape. A digital version of this pulse is included with the digital media accompanying Fehler and Keliher (2011).

All simulations were conducted using various approaches for finite differencing of the wave equation. The approach for the AUS simulations is described in the SEAM Phase I report. The approaches used by Advanced Geophysical Technologies (AGT) for the TTI and elastic simulations is described in the reports on those simulations that were provided to SEAM by AGT and retained in the SEAM community documents of the SEG website.

AUS Simulations

Since we desired to collect data that were similar to the data that were previously simulated on the model with a free surface, we used the same source time history as was used for the free-surface simulations. We desired to match the source 15 m depth used in the free-surface simulations. To take account of the near-source and near-receiver surface reflections in the free-surface simulations that effectively modify the spectrum of the recorded data, we followed a recommendation of the simulation vendor, Tierra Geophysics, now Landmark. The approach was to use two identical and simultaneous sources for each shot, one located 15 m below the sea surface and one 15 m above the sea surface. The source above the sea surface had the opposite polarity of the source below the surface. Similarly, the wavefield was recorded at 15 m above and 15 m below the sea surface and the difference of the wavefields at the two locations

became the trace for the 15 m receiver depth. An absorbing boundary was placed above the model at a sufficient distance to avoid interference with the source and receivers placed 15 m above the sea surface. The result is a data set that has no free surface multiples and has reflections scaled identically to those of the simulations conducted with a free surface. The only arrival that is not scaled correctly is the direct arrival through the water, which has twice the amplitude on the AUS data set compared with that on the free surface data set. Thus, gathers obtained by subtracting those simulated with the two different upper surface boundary conditions provide a data set containing only phases that result from waves that interact with the free upper surface. Figure 2-2 shows an example of a gather that was simulated with a free-surface boundary condition, one that was calculated using the AUS boundary condition, and the difference of the two. The AUS gather is free of any waves that are generated by reflections from the free surface and the Difference gather contains only the waves that result from interaction of the wavefield with the free surface.

TTI Simulations

TTI simulations were conducted by AGT using a high-order finite difference code. This was the first simulation conducted for SEAM by AGT. AGT provided a detailed report that summarized their simulation approach and their internal QC. Information in that report will not be repeated here as the report is available on the SEAM Phase I RPSEA website. A comparison between a TTI simulation and one conducted by Tierra Geophysics on the isotropic acoustic model is shown in Figure 2-3. This figure also shows the Absorbing Upper Surface and Elastic simulation results for the same shot. When evaluating the traces near the source, it is clear that the source insertion approach used by AGT differs substantially from that used by Tierra. Never the less, the far-field traces are nearly identical.

Elastic Simulations

The elastic simulations were conducted by AGT using a high order finite difference code. AGT provided a detailed report describing their simulation approach. They also describe their approach for insertion of the source. The QC section describes troubling issues of the stair-stepping of the seafloor and the uncertainty of the seafloor receiver positions relative to the seafloor.

Source insertion in an elastic model when given the form of a far-field pulse proved problematic since the elastic wave equation requires the integration of the far-field pulse to derive the desired source time history. Since our desired far-field pulse is always positive, the integral of the pulse is nonzero and integrating it leaves a large DC value at the end of the source pulse. The report by AGT (retained in SEAM community documents) describes their approach for dealing with this troubling issue.

Figure 2-3 shows common shot gathers from the four simulations for a common source position for all simulations. Note that elastic shot numbering scheme does not align with that for the other simulations. Overlaying the panels in the plot allows one to visualize the similarities and differences of the different paramaterizations of the model.

Figures

Figure 2-1. Far-field source characteristics. The source used for all SEAM Phase I seismic simulations was identical. Reproduced from Fehler and Keliher (2011).

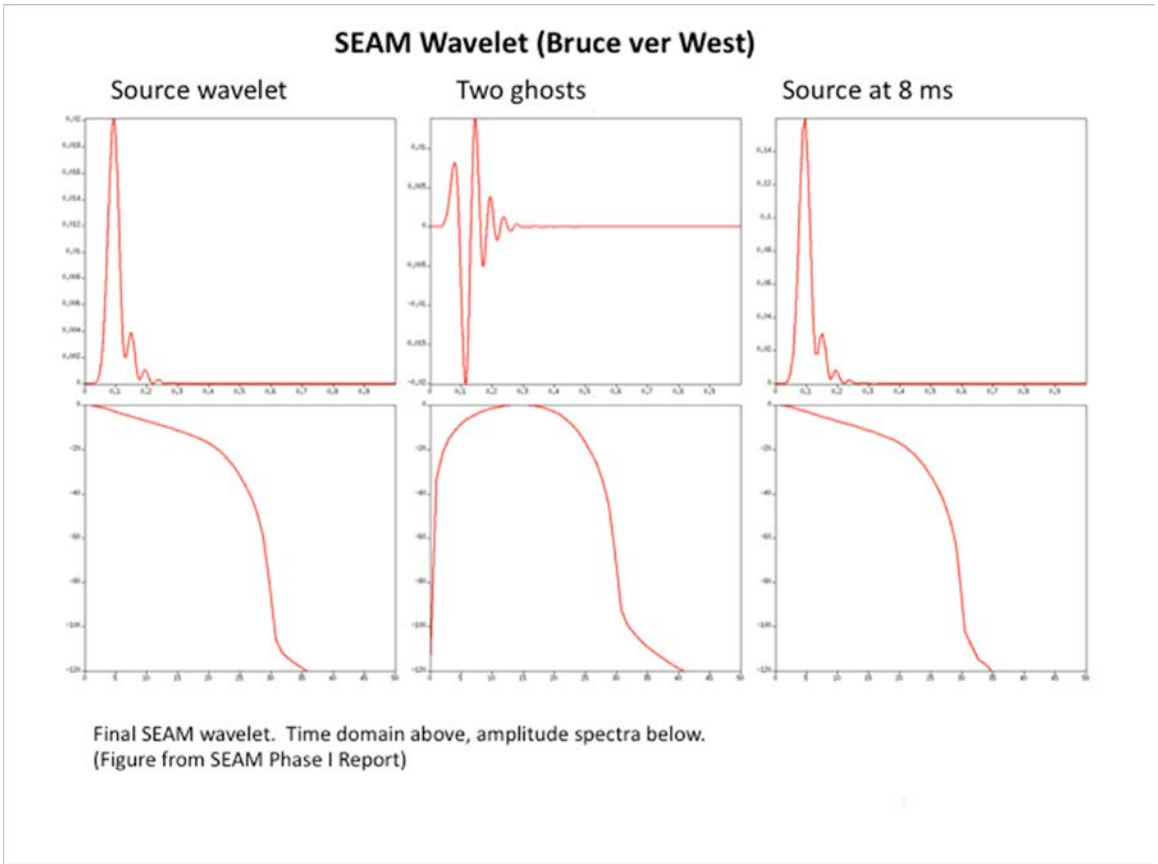

Figure 2-2. Common-shot gather from shots simulated with a free upper surface (left), an absorbing upper surface (right), and the difference of the two (bottom).

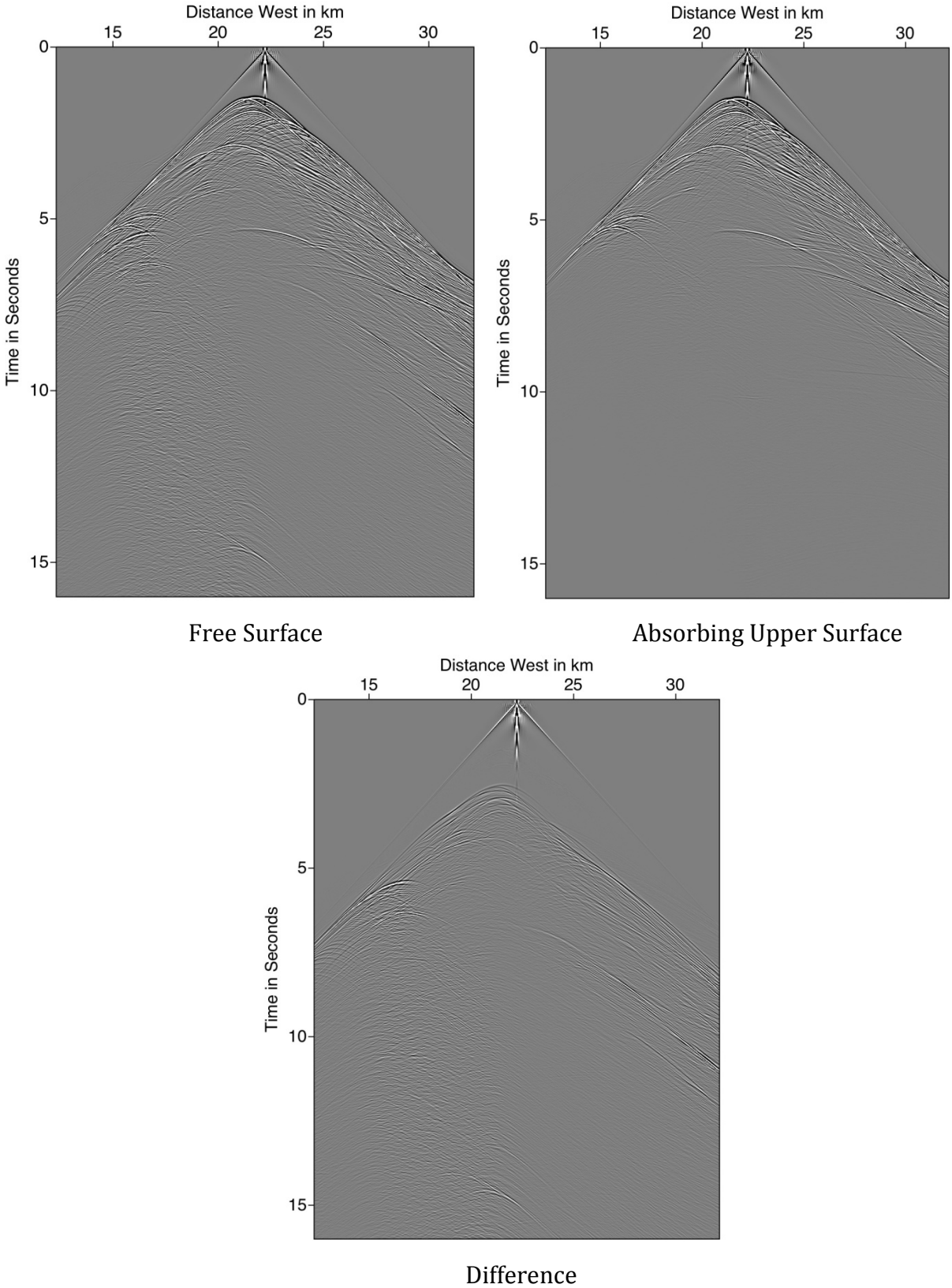

Figure 2-3. Common shot East-West gathers through the source for a common shot location but with different simulation approaches. Approaches are labeled in the panel identifiers. Shot is 12873 in the acoustic model. The elastic numbering scheme does not align with that used for the other simulations so shot 409 in the elastic simulation is at almost the same location as is shot 12873 in the other simulations.

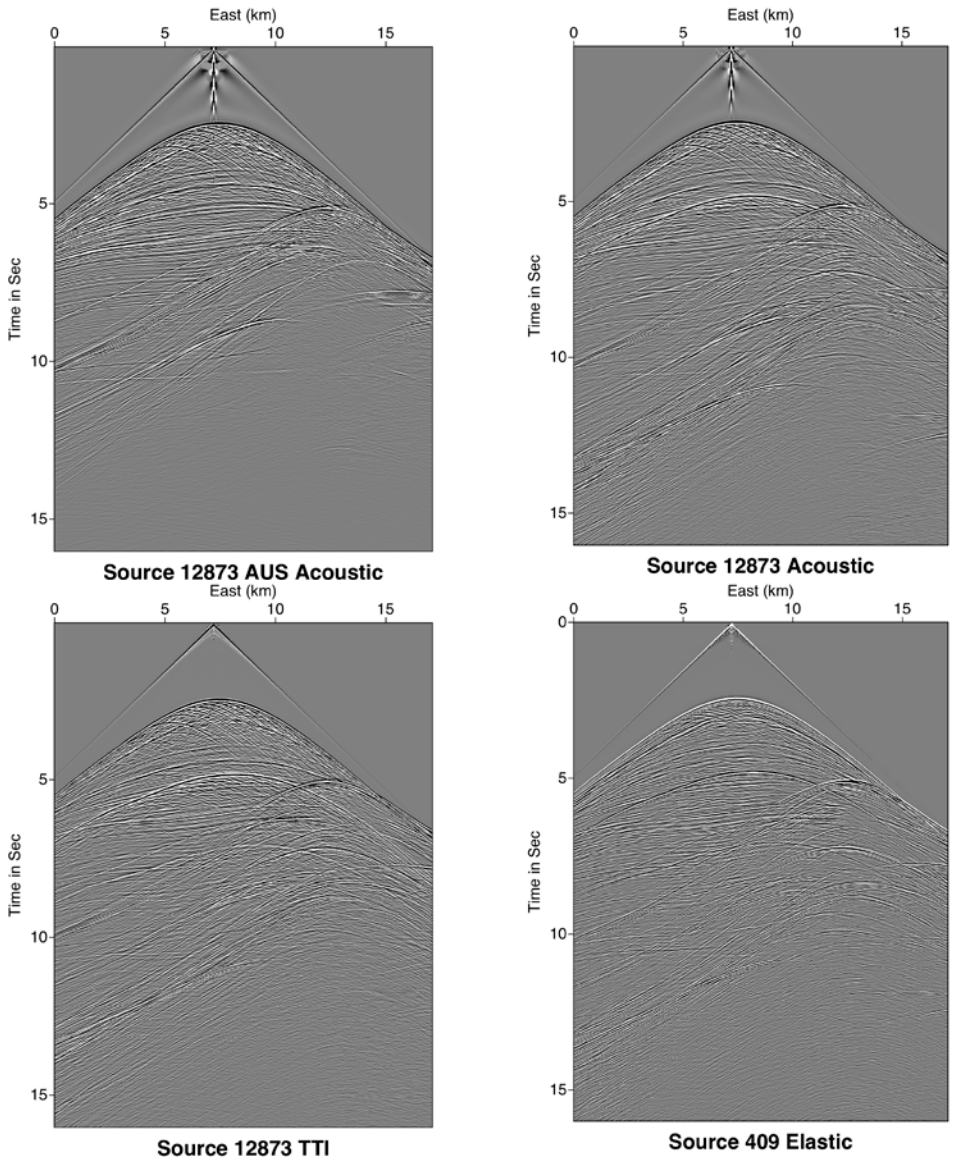

SEISMIC ACQUISITION

Acquisition was designed to provide data sets to meet the project objectives including those of testing and comparing acquisition design geometries, developing and testing processing methods, and evaluating imaging algorithms. As with field acquisition, there are economic and practical (operational) limitations together with the geophysical considerations that influence the parameters including spatial sample intervals in both source and receiver domains, record length, time sample interval, source to receiver offsets, simulation aperture, area of simulation, and bandwidth. Ray trace, 2D acoustic, and limited 3D modeling were carried out to establish some of the geophysical parameters and to understand the time and cost implications for the project. The acquisition and simulation specifications changed over time as more details were developed by the technical committees, more knowledge was gained about the capabilities and limitations of numerical modeling and data storage and through discussions with the simulation vendors once they were under contract, and finally approved by the SEAM Management Committee. In addition the needs varied for the different models and data sets.

The acquisition parameters for the acoustic and TTI simulations are listed below and Figure 3-1 illustrates the shot-receiver patch geometry. Shot and receiver location and numbering conventions are defined in Appendix B of this report.

Source: explosive	depth 15 m Max frequency 30 Hz
Surface Receiver grid	Shallow (streamer) pressure at 15 m (9 Line NS acoustic Data Set is dual sensor at 15 and 17m)
Receiver grid interval	30 m
Grid size	19.8 km EW by 19.8 km NS or up to the model boundary
Number of receivers	up to 436,921 traces per shot (661 EW by 661 NS)
Grid location	Grid moves with the shots at center of the grid
Offset range	0 to +/- 9900 m
Simulation grid	centered on shot except near model boundaries
Simulation Grid size	29.9 km EW by 29.9 km NS
Record length	16.0 seconds
Sample interval	0.008 seconds/sample

Data types simulated under the RPSEA funding portion of SEAM Phase I include acoustic absorbing upper surface (AUS), non-seismic (gravity, CSEM, MT, see non-seismic section), acoustic TTI, and elastic. Acquisition geometry and location of each data set is described below. Acoustic free surface data were simulated previously and reported on in Fehler and Keliher (2011). Acquisition designs used for non-seismic simulations are described in separate sections of this report.

The full data volumes are available. However, smaller data sets (Classic Data Sets) were either simulated directly or created by decimation of the total data volumes to create more manageable sizes to emulate present day acquisitions like Narrow Azimuth and Wide Azimuth geometries.

Simulations Conducted Prior to the Beginning of the SEAM Phase I RPSEA Project

Acquisition parameters for the classic data sets are fully defined in the following sections and summarized in tables. For reference to the original SEAM acoustic free surface data, the parameters of each classic data set developed prior to the start of the SEAM Phase I RPSEA project are shown in Table 1-1 (updated from Fehler and Keliher, 2011). Volumes given are estimated volumes of uncompressed data. These classic data sets are designed to be easily accessible, compact, and complete, so they become standards for analysis by many investigators allowing for a wide range of investigations including:

- wide azimuth acquisition and processing tests and development
- wide vs. narrow azimuth comparisons
- surface vs sea floor data comparisons
- imaging algorithms
- surface, interbed, and diffracted multiple attenuation
- velocity and reservoir property inversion
- general processing and imaging with quality numerical data
- teaching with manageable data volumes

The first three classic data sets in Table 1-1 contain all originally acquired receiver traces.

*9 NS lines with pressure at 15 and 17 m

*9 NS lines with pressure at 15 and 17 m with absorbing upper surface

*2793 Sparse 3D shot coverage with 600 m shot spacing

Two-component data were included for the 9 NS line data sets in light of the new "Geostreamer" and over-under technology. The second component desired is vertical velocity. The simulation vendor planned to calculate vertical velocity from the difference in pressures measured on a grid at two closely-spaced depths. It was decided to output the pressure values at two depths since pressure is the most basic form of simulated data and hence might have additional value compared to having the resulting velocity estimation. Users can calculate velocities from the stored pressure data at two

depths. Some participants expressed concerns about the two receivers only being 2 m apart.

All other classic data sets are extracted from the full survey, compiled, and recompressed. All classic data sets will be made available from the data storage facility as separate distributions.

The classic data set geometries resulted from discussions within the Acquisition Design Committee and the Management Committee as a whole on whether these data sets should represent only achievable streamer geometries (i.e., no split spreads), on the difference between WATS and WAZ acquisition geometries in current use, or on interleaving streamer acquisition in opposing directions as in WAZ so as to achieve the benefit of directional illumination without resorting to split spreads. Consensus developed that the classic data sets should be realistic, should allow simulation of WAZ geometry, and should be no larger than 5 TB each.

Table 3-1. Classic Data Set Geometries for acoustic and acoustic absorbing upper surface simulations conducted prior to the start of the SEAM Phase I RPSEA project. The two 9 NS line 2-C data sets have receivers at 15 and 17 m depths recorded as separate shots; all other data sets have receivers at only 15 m depth with free surface upper boundary. Data volume listed includes both receivers and assumes all shots have the maximum number of traces. Actual volume will be about 13% less. Data volume is listed as uncompressed but without trace headers. Headers add another 3% to the volume; compression ratio for the trace data is about 8:1. Traces/shot listed is a maximum; shots near boundaries have fewer traces. (Table modified from Fehler and Keliher, 2011).

Classic Data Sets	#Sail Lines	#Shots / Line	# Shots	Shot Spacing X	Shot Spacing Y	X-start	X-end	Y-start	Y-end
9 NS lines 2-C	9	267	2403	150	150	16825	18025	50	39950
9 NS lines 2-C AUS	9	267	2403	150	150	16825	18025	50	39950
2793 sparse shots	49	57	2793	600	600	3025	31825	3050	36650
WAZ NS push-pull	49	228	11172	600	150	3025	31825	3050	37100
WAZ EW push-pull	57	196	11172	150	600	3025	32275	3050	36650
NAZ NS push-pull	49	228	11172	600	150	3025	31825	3050	37100
NAZ EW push-pull	57	196	11172	150	600	3025	32275	3050	36650

Classic Data Sets	# Cable	Cable Space	Cross-line Offset Min	Cross-line Offset Max	GRP	Inline Offsets Min Offset	Inline Offsets Max Offset	Traces/ Shot	Data Vol TB
9 NS lines 2-C	661	30	-9900	9900	30	-9900	9900	436921	*16.8
9 NS lines 2-C AUS	661	30	-9900	9900	30	-9900	9900	436921	*16.8
2793 sparse shots	661	30	-9900	9900	30	-9900	9900	436921	9.8
WAZ NS push-pull	70	120	-4140	4140	30	-9900	9900	46270	4.1
WAZ EW push-pull	70	120	-4140	4140	30	-9900	9900	46270	4.1
NAZ NS push-pull	20	60	-570	570	30	-9900	9900	13220	1.2
NAZ EW push-pull	20	60	-570	570	30	-9900	9900	13220	1.2

Acoustic Absorbing Upper Surface Data

Limited simulations had been conducted using the AUS condition prior to the start of the SEAM Phase I RPSEA project. However, additional simulations were desired to make a more complete data set. Acoustic data with an absorbing upper surface were simulated using the isotropic earth model to provide test data without surface multiples. Processing of this data can be compared to the free surface data to evaluate effectiveness of multiple attenuation and to evaluate other processing and imaging methods without multiple interference. Even with the additional simulations conducted by SEAM Phase I RPSEA, there are considerably fewer shots simulated with an AUS than with a free surface. Classic data sets include

Surface 2793 shot set,
Acoustic 9 North-South Line Classic Data Set,
28 East-West Lines Data Set,
Limited NAZ (Narrow Azimuth) Classic Data Set, and
Limited WAZ (Wide Azimuth) Classic Data Set.
(For this simulation, only 3822 of the 11172 shots comprising the complete WAZ and NAZ classic data sets were simulated.)

Table3-2. Acoustic Absorbing Upper Surface Classic Data Sets Geometries

				Shot Spacing					
Classic Data Sets	#Sail Lines	#Shots /Line	# Shots	X	Y	X-Start	X-End	Y-Start	Y-End
9 NS lines	9	267	2403	150	150	16825	18025	50	39950
2793 sparse shot	49	57	2793	600	600	3025	31825	3050	36650
28 EW Lines	28	234	6552	150	150	25	34975	21800	25850
WAZ EW push-pull	7	196	1372	150	600	3025	32275	21800	25850
	50	49	2450	600	600	3025	31825	3050	36650
NAZ EW push-pull	7	196	1372	150	600	3025	32275	21800	25850
	50	49	2450	600	600	3025	31825	3050	36650

			Cross-line Offset			Inline Offsets			
Classic Data Sets	# Cable	Cable Spacing	Min	Max	Group Interval	Min Offset	Max Offset	Traces / Shot	Data Vol GB
9 NS lines	661	30	-9900	9900	30	-9900	9900	436921	1462
2793 sparse shots	661	30	-9900	9900	30	-9900	9900	436921	733
28 EW Lines	661	30	-9900	9900	30	-9900	9900	436921	1640
WAZ EW push-pull	70	120	-4140	4140	30	-9900	9900	46270	175
NAZ EW push-pull	20	60	-570	570	30	-9900	9900	13220	75

Acoustic Absorbing Upper-Surface 2,793 shot Classic Data Set

This is a sparse-shot data set that can be used for testing imaging algorithms and some data acquisition geometries. The shots are on a 600 m grid over most of the model with each shot in the center of a recording patch of up to 19.8 km x 19.8 km as shown in Figure 3-1. Up to 436,921 receivers are spaced on a 30 m x 30 m grid. In-line and cross-line offset ranges are equal at +/- 9,900 m yielding full azimuth data that can be decimated for comparing azimuthal and dip effects. The absorbing upper surface provides water bottom multiple free data for testing without interference from multiples and for comparison to imaging results that includes free-surface multiples. This data set provides a good comparison with the 2793-shot Free-surface, TTI, and elastic data sets. Additional specific information on all the AUS data sets including shot interval, sail-line interval, number of streamers, location on the model, and offsets are shown in Table 3-2 along with the same information for all AUS Classic Data Sets.

Acoustic AUS 9 North-South Line Classic Data Set

There are nine shot lines, or sail lines, shot in a north-south direction across the center of the model with receivers at both 15 and 17 m depth recording pressure. Two depths make simulation of dual sensor streamer technology possible. Vertical particle velocity may be obtained by taking the difference in pressure at two depths. The 150 m shot spacing makes this data set a 1.2 km wide shot swath and a good data set for testing processing methods such as velocity analysis, deconvolution, de-bubble, simultaneous shooting and shot separation. It is also an excellent data set for 2D or narrow azimuth imaging and for teaching and training. There are no free-surface multiples in this data set which makes it useful for testing imaging methods; and for comparison to the corresponding free-surface data set and for the effectiveness of processing and imaging methods in the presence of water bottom multiples.

Acoustic AUS 28 East-West Lines Data Set

There are 28 shot lines, or sail lines, shot in an east-west direction across the model centered at 23900 north with receivers at 15 m depth recording pressure. The 150 m shot spacing makes this data set a 4.05 km wide shot swath and a good data for testing processing methods such as velocity analysis, deconvolution, de-bubble, simultaneous shooting and shot separation. It is also an excellent data set for 2D or narrow azimuth imaging and for teaching and training. There are no free-surface multiples in this data set which makes it useful for testing imaging methods; and for comparison to the corresponding free-surface data set and for the effectiveness of processing and imaging methods in the presence of water bottom multiples. In addition to crossing the salt body and both flanks, this swath crosses a thick sequence of stacked reservoirs. See Figure 3-2. Note that shots that comprise the 2793 shot classic data set and fall within the simulation region used for the 28 EW line classic data set are only included in the 2793 shot data set. Thus, there are some missing shots in the 28 EW lines classic data set.

Acoustic AUS NAZ (Narrow Azimuth) Classic Data Set

Narrow Azimuth data sets from the 28 EW line and 2793-shot Acoustic Absorbing Upper Surface data sets, simulating typical wide-tow single vessel acquisition, are available in an East-West orientation. Data are collected along the shot lines in both directions from the source which in total provides data acquired in two narrow azimuths. Acquisition geometry is 20 x 19,800 m long streamers (30 m group interval) with a streamer separation of 60 m, shot point interval of 150 m, and sail line interval of 600 m. Outside the area of the 28 EW Line data set, the shot point interval is 600 m inline. This is a good minimal NAZ data set for testing and training without water bottom multiples that can be compared to the Acoustic Free-surface NAZ data processing and imaging. The NAZ geometry is illustrated in Figure 3-3.

Note that this data set is not identical to the one collected with a free upper surface. For the Absorbing Upper Surface Acoustic (AUS) simulation, only the NAZEW classic data set is available. In addition, fewer shots are included in the AUS NAZEW classic data set than in the free surface NAZEW classic data set. The AUS NAZEW classic data set is a subset of the one collected with a free upper surface.

Acoustic AUS WAZ (Wide Azimuth) Classic Data Set

This Wide Azimuth classic data set simulates wide azimuth-long offset acquisition in an EW sail-line orientation. This data set was constructed from the 28 EW line and 2793-shot Acoustic Absorbing Upper Surface data sets. This allows for testing acquisition geometry width and orientation, processing techniques, and imaging algorithms. In addition, shots can be summed together to simulate and test simultaneous shooting schemes. Each shot is recorded by 70 x 19,800 m streamers with a streamer separation of 120 m, shot point interval of 150 m, and sail line interval of 600 m. The geometry is push-pull so there are streamers on both sides of the shot. The WAZ geometry is illustrated in Figure 3-4.

Note that this data set is not identical to the one collected with a free upper surface. For the Absorbing Upper Surface Acoustic (AUS) simulation, only the WAZEW classic data set is available. In addition, fewer shots are included in the AUS WAZEW classic data set. The AUS WAZEW classic data set is a subset of the one collected with a free upper surface.

Tilted Transverse Isotropy

Acoustic data were simulated with a free surface using the acoustic TTI earth model to provide anisotropic test data. The same acquisition parameters were used as for the AUS data set and are shown in Figure 3-1. However, more East-West shot lines were simulated over a larger area of the model, additional shots were added to extend WAZEW, WAZNS, NAZEW, and NAZNS data sets so they would be identical to the acoustic free surface data Classic Data Sets, and four 4 component VSPs were recorded. Shot locations are shown in Figure 3-6. This data were designed to test and develop processing and imaging methods for TTI data and compare the effects of anisotropy on the results obtained using the isotropic case. The push-pull geometry for both NAZ and WAZ, and the full azimuth 109 line swath provide data for testing a variety of acquisition geometries. Practical considerations of geophysical objectives, time, cost, and data volumes limited the total data volume simulated to be less than the acoustic free-surface, but enough data are provided to meet the objectives.

Specific information on all the TTI data sets including shot interval, sail-line interval, number of streamers, location on the model, and offsets are shown in Table 3-3. To

address specific geophysical tests and analyses, the following Classic Data Sets were generated and described in the following sections.

TTI 109 EW Line swath
Surface 2793 shot set,
NAZ (Narrow Azimuth) Classic Data Set,
WAZ (Wide Azimuth) Classic Data Set
VSP Classic Data Set

The acquisition parameters for the acoustic TTI simulations are listed below and Figure 3-1 illustrates the shot-receiver patch geometry.

Source:	depth 15 m	Max frequency 30 Hz (see Simulation section for characteristics)
Surface Receiver grid		
Shallow (streamer)	pressure at 15 m	
Receiver grid interval	30 m	
Grid size	19.8 km EW by 19.8 km NS	
Number of receivers	up to 436,921 traces per shot (661 EW by 661 NS)	
Grid location	Grid moves with the shots at center of the grid	
Offset range	0 to +/- 9900 m	
Simulation grid	centered on shot	
Grid size	29.9 km EW by 29.9 km NS	
Record length	16.0 seconds	
Sample interval	0.008 seconds/sample	

TTI 109 EW Line swath

These data are an expansion to the north and south from the 28 EW lines acquired with the Absorbing Upper Surface (AUS) data set. This provides a significantly wider area and aperture for 3D imaging testing. This swath of lines is centered on North 23900 which is the east-west line that the 4 VSPs are located on. The acquisition parameters are listed and the area is illustrated in Figure 3-5.

Source:	depth 15 m	Max frequency 30 Hz
Source grid		
SP interval	150 m	
Grid size	33.2 km EW by 16.2 km NS	
Number of sail lines	109	
Number of SPs	24,307	
Grid location	East	900 to 34100 m
	North	15800 m to 32000 m
Surface Receiver grid		
Shallow (streamer)	pressure at 15 m depth	

	Receiver grid interval	30 m
	Grid size	19.8 km EW by 19.8 km NS
	Number of receivers	up to 436,921 traces per shot (661 EW by 661 NS)
	Grid location	Grid moves with the shots at center of the grid
	Offset range	0 to +/- 9900 m
VSP s	(Four)	4 Components –vertical, EW, NS, Pressure
	Depth range	1,000 m to 7990 m
	Receiver interval	15 m
	Locations	1. East 10075 m North 23900 m
		2. East 12025 m North 23900 m
		3. East 15025 m North 23900 m
		4. East 27025 m North 23900 m

Simulation grid	centered shot
Grid size	29.9 km EW by 29.9 km NS
Grid location	moves with shot
Record length	16.0 seconds
Sample interval	0.008 seconds/sample

Table 3-3. TTI Classic Data Set Geometries

				Shot Spacing					
Classic Data Sets	#Sail Lines	#Shots /Line	# Shots	X	Y	X-Start	X-End	Y-Start	Y-End
2793 sparse shot	49	57	2793	600	600	3025	31825	3050	36650
109 EW lines	109	234	25506	150	150	25	34975	15800	32000
VSP 4-C	34	34	1156	600	600	varies with the VSP location			
WAZ EW and NS	57	196	11172	150	600	3025	32275	3050	36650
NAZ EW and NS	57	196	11172	150	600	3025	32275	3050	36650

			Cross-line Offset			Inline Offsets			
Classic Data Sets	# Cable	Cable Spacing	Min	Max	Group Interval	Min Offset	Max Offset	Traces / Shot	Data Vol GB
2793 sparse shots	661	30	-9900	9900	30	-9900	9900	436921	927
109 EW lines	661	30	-9900	9900	30	-9900	9900	436921	
VSP 4-C	1		-9900	9900	15	-9900	9900	1864	896
WAZ EW and NS	70	120	-4140	4140	30	-9900	9900	46270	964
NAZ EW and NS	20	60	-570	570	30	-9900	9900	13220	336

Acoustic TTI 2793-shot Classic Data Set

This is a sparse-shot data set that can be used for testing imaging algorithms and some data acquisition geometries. In addition, in conjunction with the Acoustic 2793 shot Classic Data Sets, effects of TTI anisotropy can be compared to isotropic data. The shots are on a 600 m grid over most of the model with each shot in the center of a recording patch of 19.8 km x 19.8 km. Up to 436,921 receivers are spaced on a 30 m x 30 m grid. In-line and cross-line offset ranges are equal at +/- 9,900 m yielding full azimuth data that can be decimated for comparing azimuthal and dip effects. The free-surface provides realistic water column multiples. 4C VSP data are also included from 4 well locations for each shot (VSP data were acquired only for wells within the surface recording aperture of the shots). VSP data are 4-component, pressure plus 3 components of particle acceleration, at 15 m depth intervals between depths of 1000 and 7,990 m.

Acoustic TTI – NAZ Classic Data Set

Narrow Azimuth data sets, simulating typical wide-tow single vessel acquisition, are available in both East-West and North-South orientation. Data are recorded along streamers placed both in front of and behind shots along the tow direction which in total provides data acquired in four narrow azimuths. Acquisition geometry is 20 x 19,800 m streamers (30 m group interval) with a streamer separation of 60 m, shot point interval of 150 m, and sail line interval of 600 m. This free-surface data set is ideal for testing NAZ processing and imaging, and comparing the effects of TTI versus isotropic imaging methods and the impact TTI has on the data compared to the isotropic data set.

The shot and trace acquisition geometry for the TTI NAZ classic data set is identical to those used for the free surface acoustic NAZ classic data set and is illustrated in Figure 3-3. The area and shot lines are shown in Figure 3-6 along with the 109 line swath and the VSPs. The shots shown in Figure 3-6 includes all additional shots required to make the NAZEW acquisition identical to that of the free-surface acoustic NAZEW acquisition were acquired.

Acoustic TTI – WAZ Classic Data Set

This Wide Azimuth classic data set simulates full azimuth-full offset acquisition in both a NS and EW orientation. This allows for testing acquisition geometry width and orientation, processing techniques, and imaging algorithms. In addition, shots can be summed together to simulate and test simultaneous shooting schemes and the data used to test and compare the effects of TTI versus isotropic imaging methods and the impact TTI has on the data compared to the isotropic data set. Each shot is recorded by 70 x 9,900 m streamers placed both in front of and behind shots along the sail direction

with a streamer separation of 120 m, shot point interval of 150 m, and sail line interval of 600 m.

The shot and trace acquisition geometry for the TTI WAZ classic data set is identical to those used for the free surface acoustic WAZ classic data set illustrated in Figure 3-4.

Acoustic TTI – VSP Classic Data Set

Four VSP wells located on the EW line at 23900 north on the model. Four components were recorded; pressure, vertical acceleration, EW acceleration, and NS acceleration. One of the wells is through the salt overhang, penetrates some reservoirs, and re-enters the salt root. This is a very realistic scenario for Gulf of Mexico wells. The other three wells are outboard of the salt and penetrate reservoirs. VSP data were collected for any shot simulated during the TTI acquisition for which a given well fell within the surface trace acquisition grid of the shot. Source to well offsets range from +/- 9,900 m in both EW and NS directions from the well. Receiver depths ranged between 1,000 and 7,990 m with a 15 m spacing. The VSP parameters are shown in Table 3-4 and the locations in Figures 3-7 and 3-8.

The locations are:	1.	East 10075 m	North	23900 m
	2.	East 12025 m	North	23900 m
	3.	East 15025 m	North	23900 m
	4.	East 27025 m	North	23900 m

Table 3-4. TTI VSP Classic Data Set Geometries

VSP data - TTI Model											
	Well X	Well Y	# Sail Lines	# Shots /Line	Total Shots	Shot Interval		X-Start	X-End	Y-Start	Y-End
						X	Y				
VSP 1	10075	23900	29	33	957	600	600	3025	19825	14250	33450
VSP 2	12025	23900	32	33	1056	600	600	3025	21625	14250	33450
VSP 3	15025	23900	33	33	1089	600	600	5425	24625	14250	33450
VSP 4	27025	23900	25	33	825	600	600	17425	31825	14250	33450

VSP Data - TTI Model											
	Well X	Well Y	Depth Interval		Cross-line Offset		Inline Offset		Group Interval	Traces /Shot	Data Vol GB
			Min	Max	Min(E)	Max(W)	Min(S)	Max(N)			
VSP 1	10075	23900	1000	7990	-7050	9750	-9650	9550	15	1864	218
VSP 2	12025	23900	1000	7990	-9000	9600	-9650	9550	15	1864	240
VSP 3	15025	23900	1000	7990	-9600	9600	-9650	9550	15	1864	248
VSP 4	27025	23900	1000	7990	-9600	4800	-9650	9550	15	1864	188

Elastic Data

The elastic model was constructed with realistic shear wave velocities of as low as 120 m/s near the seafloor. The near-seafloor portion of S-wave model was modified for use in the simulation to limit the minimum Vs to 600 m/s as described in the Model Section of this report. Thus, there are two versions of the S-wave velocity model. Some additional acquisition modeling was conducted to assist with the design of the parameters for elastic simulation including shear waves. Spatial sample intervals, simulation aperture, maximum travel time, and maximum offsets needed to be estimated to account for the S-wave velocities. The acquisition design was evaluated by assuming that recorded S-waves had converted from P to S waves at the image point.

3D ray-tracing and illumination analysis were the primary tools for acquisition design. In addition, some limited Finite Difference modeling was run to verify results and look for model gridding effects. Early discussions included determining what shear modes were of most interest and should drive the selection of acquisition parameters. There is significant P wave energy converted to S modes at all salt-sediment interfaces, but the shear velocity in salt is similar to the sediment P velocity so longer travel times would not likely be needed for these modes. Conversion of down-going P to S at the seafloor

and reflected upward as Shear would require the longest travel times but may not be the most significant modes for exploration purposes. The decision was made to model and record with parameters designed for shear waves that are converted from down-going P at the target horizons at depth which would also provide adequate simulation time and offset for salt-sediment interface converted waves.

Four shot points were used to estimate travel time needed and are shown in Figure 3-9. Illumination analysis displays agreed with these travel time estimates and indicated the longest offset needed was 11.3 km for the target horizons in dipping areas. The maximum observed travel times of the PS converted waves to the seafloor nodes from two selected target horizons were 14 seconds. This time and the maximum observed offset from modeling were considered minimums, so the record length was extended to 16 seconds and the simulation area to 22.5 km east-west and 18.0 km north-south.

The elastic modeling is computer time intensive and costly. The project timeline and budget would not allow acquiring surface and seafloor data over the entire model similar to the acoustic free surface SEAM data set. So the objectives were carefully evaluated to ensure the design of a survey compatible with the project goals. Three major topic areas were considered; acquisition, processing, and imaging applications. One of the key criteria was acquiring enough data over a large enough area for adequate testing and comparison of the images generated with various acquisition designs, processing flows, and imaging methods. The 2793 shot set was repeated for imaging comparison to all the acoustic data sets. For the denser survey the area selected was determined to provide enough area for imaging some of the reservoirs both outboard and under the salt wing.

Elastic data were simulated with a free surface using the elastic earth model with modified shallow shear wave velocity (see the Model Section of this report), to provide elastic test data at both the surface and seafloor. The acquisition parameters are different from those used for the acoustic modeling due to geophysical and operational considerations without degrading the data quality. These data were designed to test and develop processing and imaging methods for elastic data and test various acquisition geometries including streamers and seafloor nodes. Practical considerations of geophysical objectives, time, cost, and data volumes limited the total number of shots simulated to be less than for the acoustic free-surface simulation, but enough data were provided to meet the objectives. As with the acoustic data sets the entire data volume is available as well as Classic Data Sets which provide more manageable data volumes with acquisition geometries similar to common field practice today. There is also a small high resolution seafloor data set suitable for studying Scholte waves and other near seafloor phenomena.

The parameters of the entire elastic data set are listed below. Additional specific information on all the elastic classic data sets including shot interval, sail-line interval, number of streamers, location on the model, and offsets are shown in Table 3-5. To

address specific geophysical tests and analyses, the following Classic Data Sets were generated and described in the following sections:

Surface 2793 shot set,
NAZ (Narrow Azimuth) Classic Data Set, and
WAZ (Wide Azimuth) Classic Data Set
VSP Classic Data Set
Seafloor Classic Data Set
1600 shot Classic Data Set

The elastic simulation consisted of three somewhat independent sets of data. They are (1) 2793-shot data set, (3) data set for shots located in a 15 km by 8 km box on the Western half of the model, and (3) a 1600 shot set of tight source and receiver spacing (10 m for each). The acquisition parameters for the 15 km by 8 km grid of sources are listed below and Figure 3-10 illustrates the shot-receiver patch geometry and Figure 3-11 the area in relation to the stacked subsurface reservoirs.

Acquisition parameters –Elastic 15 km by 8 km grid shot set

Source grid		centered on East 11200 m, North 23900 m
	SP interval	100 m
	Grid size	15 km EW by 8 km NS
	Number of SPs	12,231 (151 EW by 81 NS)
	Grid location	East 3700 to 18700 m
		North 19900 to 27900 m
	Depth	15 m
	Bandwidth	1 – 30 Hz
Surface Receiver grid		
	Shallow (streamer)	pressure at 15 m depth
	Receiver grid interval	25 m
	Grid size	22.5 km EW by 18 km NS
	Number of receivers	649,621 traces per shot (901 EW by 721 NS)
	Grid location	East 0 to 22500 m
		North 14900 to 32900 m
		fixed location for all shots
Sea floor Receiver grid		
		4 Components – vertical, EW, NS (all accelerations), and Pressure
	Node interval	100 m
	Grid size	22.5 km EW by 18 km NS
	Number of receivers	40,680 (226 EW by 181 NS)

Number of traces / shot	162,720 (4 components x 40,680)	
Grid location	East	0 – 22500 m
	North	14900 to 32900 m
	Fixed location for all shots	
Depth	sea floor	
Simulation area	same as receiver grid	
size	22.5 km EW by 18 km NS	
location	East	0 – 22500 m
	North	14900 to 32900 m
VSP s (Four)	4 Components – vertical, EW, NS, Pressure	
Depth range	1000 to 7990 m	
Receiver interval	15 m	
Locations	1. East 10075 m	North 23900 m
	2. East 12025 m	North 23900 m
	3. East 15025 m	North 23900 m
	5. East 15025 m	North 22900 m*
Record length	16.0 seconds	
Sample interval	0.008 seconds/sample	

* Note that wells 1 – 3 are at the same locations as wells 1-3 in the TTI simulation. Well 4 in the TTI simulation is located outside of the simulation grid for the elastic 15 by 8 km acquisition grid so no data were collected from this well for that acquisition. Data were acquired from well 4 for elastic shots in the 2793-shot set when the well was located within the acquisition grid for a given shot. Well 5 is a new well used for the elastic acquisition.

Elastic 2793-shot Classic Data Set

This sparse shot data set can be used for testing imaging algorithms, and comparing imaging results from streamer and seafloor nodal data. Unlike the acoustic 2793 sparse shot data sets, the elastic receiver patch is 22.5 km EW and 18.0 km NS. EW source-receiver offsets range between +/ - 11,250 m and NS source –receiver offsets range between +/- 9,000 m for both surface and seafloor receiver. The shot is located 50 m west of the center of the receiver patch. Four component VSP data were also recorded in up to five vertical wells when the shots were within the simulation box range of each well providing source offsets to each VSP of +/- 11,250 m EW and +/- 9,000 m NS. This data set is meant to be similar to those collected for other seismic acquisitions (e.g. acoustic free surface, acoustic absorbing upper surface, acoustic TTI). While the acquisition of the elastic simulation is similar, it is not identical. Shot locations for the elastic simulations are offset 25 m West and 50 m South of those used for the acoustic simulations. Trace geometry for the elastic simulation differs from that for

the acoustic simulations. Data acquisition parameters and locations are listed in Table 4.

Five VSPs were simulated and recorded four components; pressure, vertical acceleration, EW acceleration, and NS acceleration. Two of the wells are through the salt overhang, penetrate some reservoirs, and re-enter the salt root. This is a very realistic scenario for Gulf of Mexico wells. Three of the wells are outboard of the salt and penetrate reservoirs. The VSP parameters are shown in Table 6 and the locations of wells 1, 2, 3, and 5 are in Figure 3-12 and Figure 3-13. The location of well 4 is shown in Figure 3-7.

The VSP locations are:

1. East 10075 m North 23900 m
2. East 12025 m North 23900 m
3. East 15025 m North 23900 m
4. East 27025 m North 23900 m
5. East 15025 m North 22900 m

Table 3-5. Elastic Classic Data Set Geometries

				Shot Spacing					
Classic Data Sets	#Sail Lines	#Shots /Line	# Shots	X	Y	X-Start	X-End	Y-Start	Y-End
2793 sparse shot	49	57	2793	600	600	3050	31850	3000	36600
1600 shot	40	40	1600	10	10	7300	7690	23700	24100
Seafloor nodes 4C	81	151	12231	100	100	3700	18700	19900	27900
VSP 4-C	31	38	1178	600	600	varies with the VSP location.see Table 3-6			
WAZ EW push-pull	17	151	2567	100	500	3700	18700	19900	27900
NAZ EW push-pull	57	151	2567	100	500	3700	18700	19900	27900

			Cross-Line Offset			Inline Offsets			
Classic Data Sets	# Cable	Cable Spacing	Min	Max	Group Interval	Min Offset	Max Offset	Traces / Shot	Data Vol GB
2793 shot-surface rcvrs	661	25	-9900	9900	25	-9900	9900	436921	4129
2793 shot - seafloor	226	100	-12200	12300	100	-9000	9000	163624	
1600 shot	201	10	-1000	1000	10	-500	1500	161604	1023
Seafloor nodes 4-C	46	400			400			10488	0.96
VSP 4-C	1		-9000	9000	15	-11250	11250	1864	
WAZ EW push-pull	85	100	-4200	4200	25	-10000	10000	68085	1.4
NAZ EW push-pull	25	50	-600	600	25	-10000	10000	16021	0.34

Table 3-6. Elastic VSP Classic Data Set Geometries for 2793-shot classic data set.

VSP Data - Elastic 4C											
	Well X	Well Y	# Sail Lines	# Shots /Line	Total Shots	Shot interval X	Shot interval Y	X-Start	X-End	Y-Start	Y-End
VSP 1	10075	23900	29	32	928	600	600	3050	19850	14800	33400
VSP 2	12025	23900	32	32	1024	600	600	3050	21650	14800	33400
VSP 3	15025	23900	33	32	1056	600	600	5450	24650	14800	33400
VSP 4	27025	23900	25	32	800	600	600	17425	31850	14800	33400
VSP 5	15025	22900	33	34	1122	600	600	5450	24650	13000	32800

VSP Data - Elastic 4C											
	Well X	Well Y	Depth Interval Min	Depth Interval Max	Cross-line Offset Min(E)	Cross-line Offset Max(W)	Inline Offset Min(S)	Inline Offset Max(N)	Group Interval	Traces /Shot	Data Vol GB
VSP 1	10075	23900	1000	7990	-7050	9775	-9100	9500	15	1864	138
VSP 2	12025	23900	1000	7990	-8975	9625	-9100	9500	15	1864	153
VSP 3	15025	23900	1000	7990	-9575	9625	-9100	9500	15	1864	157
VSP 4	27025	23900	1000	7990	-9575	4825	-9100	9500	15	1864	120
VSP 5	15025	22900	1000	7990	-9575	9625	-9900	9900	15	1864	168

Elastic NAZEW Classic Data Set from the 100 m shot grid

This Narrow Azimuth data set, simulates typical wide-tow single vessel acquisition, is available in an East-West orientation, in a push-pull streamer simulation which provides data acquired in two reciprocal narrow azimuths. Acquisition geometry is 25 x 10,000 m streamers (25 m group interval) with a streamer separation of 50 m, shot point interval of 100 m, and sail line interval of 500. Data along two streamers, each extending 10,000 m from the shot along the sail line direction are recorded. The geometry is illustrated in Figure 3-14 and the comparison with parameters for the acoustic NAZ Classic Data sets are shown in Figure 3-15.

Elastic WAZEW Classic Data Set from the 100 m shot grid

The Wide Azimuth data set simulates wide azimuth-long offset acquisition in a push-pull mode providing data in both an east and west shooting orientation. This allows for testing some acquisition geometries, processing techniques, and imaging algorithms. In addition, shots can be summed together to simulate and test simultaneous shooting schemes. Each shot is recorded by 85 x 10,000 m streamers (25 m group interval) with a streamer separation of 100 m, shot point interval of 100 m, and sail line interval of 500 m. Data along two streamers, each extending 10,000 m from the shot along the sail line direction are recorded, one east of the shot and one west. The geometry is illustrated in Figure 3-16. The comparison with acquisition parameters of the acoustic WAZ data sets are shown in Figure 3-17.

Elastic Seafloor Classic Data Set

This 4 component seafloor data set simulates a more typical node survey with sensors on a 400 m grid. It is comprised only from shots in the 15 by 8 km elastic simulation. It is a more manageable size data set that is useful for testing imaging and processing methods and comparing node to streamer data. This is the same data as the entire elastic seafloor data volume but decimated to a 400 m grid of seafloor nodes and a 100 m grid of shots. These data are not compressed. The parameters and grid location are defined in Table 3-5.

1600 shot tight grid

Noise is a significant issue affecting seismic data recorded on the seafloor. One form of this noise is Scholte waves which can be generated by direct waves from the source and by waves reflected from below. A simulated data set including Scholte waves could be beneficial in understanding the impact on the primary desired signal and the attenuation of the interface waves. Scholte waves are very slow interface modes and acquisition parameters for this shot set were reviewed to ensure adequate recording of them. A small survey was designed specifically to study them based on some detailed evaluation of wave equation modeling by AGT and the Technical Project Manager working with his colleagues at MIT. It was necessary to reduce the model grid size and dramatically reduce the spatial sampling interval. For practical simulation reasons of time and cost, the area of survey was small and record lengths shortened to facilitate the required dense shot and receiver sampling.

The survey area was selected to ensure generation of Scholte waves by changes in bathymetry and near seabed variations and to be located away from salt so there would be minimal impact from salt on the Scholte wave data. There may also be some benefit from integrating VSP data with the tight seafloor grid data, so the receiver grid was located near a VSP location. However, no VSP data were acquired from this simulation.

The minimum near-seafloor S-wave velocity in this model was limited to 600 m/s or greater. The Scholte wave velocity was expected to be less than the minimum S-wave velocity. At 20 Hz, the wavelength would be less than 30 m. To minimize spatial aliasing a shot and receiver sample interval of 10 m was used. The same grid interval was used for both source and receiver to facilitate analyzing the Scholte wave data in both shot and receiver records. Typically seafloor seismic data are acquired on a denser shot than receiver grid and much of the data analysis and processing performed in the receiver record domain to take advantage of the better spatial sampling.

The fixed receiver array consists of a 2000 m by 2000 m grid of four component seafloor nodes at a grid spacing of 10 m. The receiver patch is 201 by 201 receivers for a total of 40,401 receivers (161,604 traces) recorded for each shot. The shots are also spaced at a 10 m interval, but the shot grid is only 390 m by 390 m in dimension for a total of 1600 shots. The shots were recorded on the seafloor only. Figure 3-18 illustrates the location of the shot and receiver patch and their relationship and information is shown in Table 3-5.

Record length was limited to 8.0 seconds to be more consistent with the array aperture and to be compatible with recording mode-converted shear wave reflections to the depth of a shallow reservoir at about 2200 m depth . This record length allows recording of Sv to about 2 Km depth and PSv to about 3 km depth. The time for Scholte waves to cross the receiver array is about 3.0 seconds. The cross section in Figure 3-19 shows the variation in shear velocity and the depth to anomalies and targets beneath the shot and a portion of the receiver spread.

Acquisition parameters - 1600 shot tight grid

Source grid		centered on East 7500 m, North 23900 m
	SP interval	10 m
	Grid size	400 m EW by 400 m NS
	Number of SPs	1600
	Grid location	East 7300 to 7690 m
		North 23700 to 24090
	Depth	15 m
	Bandwidth	1 – 30 Hz
Receiver grid		centered on East 7000 m, North 23900 m
		4 Components – vertical, EW, NS, Pressure
	Node interval	10 m
	Grid size	2000 m EW by 2000 m NS fixed location
	Number of receivers	40,401
	Grid location	East 6000 – 8000 m
		North 22900 – 24900 m
	Depth	sea floor

Simulation grid	centered on receiver grid
Grid size	9000 m EW by 8000 m NS
Grid location	
Record length	8.0 seconds
Sample interval	0.008 seconds/sample

Figures

Figure 3-1. Acoustic, AUS, and TTI simulation recording and simulation patch geometry drawn to scale. The portion of any patch outside the model (shown in gray) is not computed or recorded. Only 22% of shots have a full complement of 436,921 traces. The average number of traces/shot is about 77% of the maximum. (Slide 3 from Classic_Data sets rev 7.ppt by Acquisition Committee).

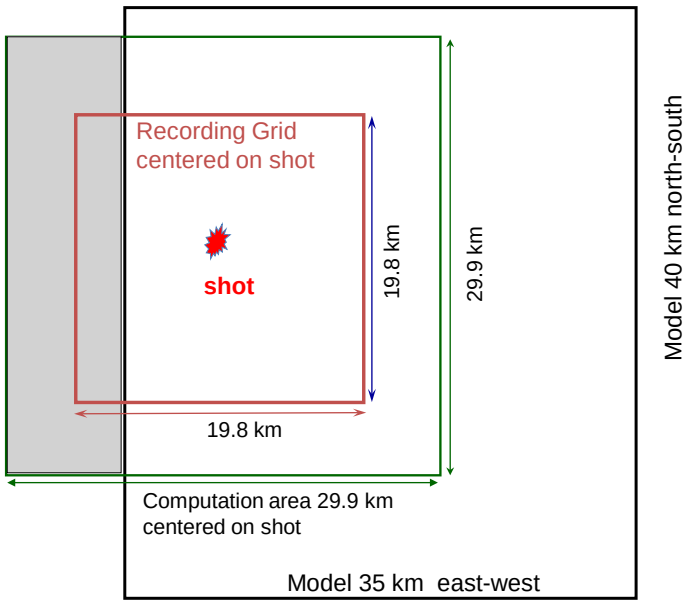

Figure 3-2. Shot locations of the 2,793 shot grid and 28 EW line AUS data sets. The color indicates the stacked thickness of the reservoirs. The 28 EW line data crosses the thickest turbidite and channel sequences.

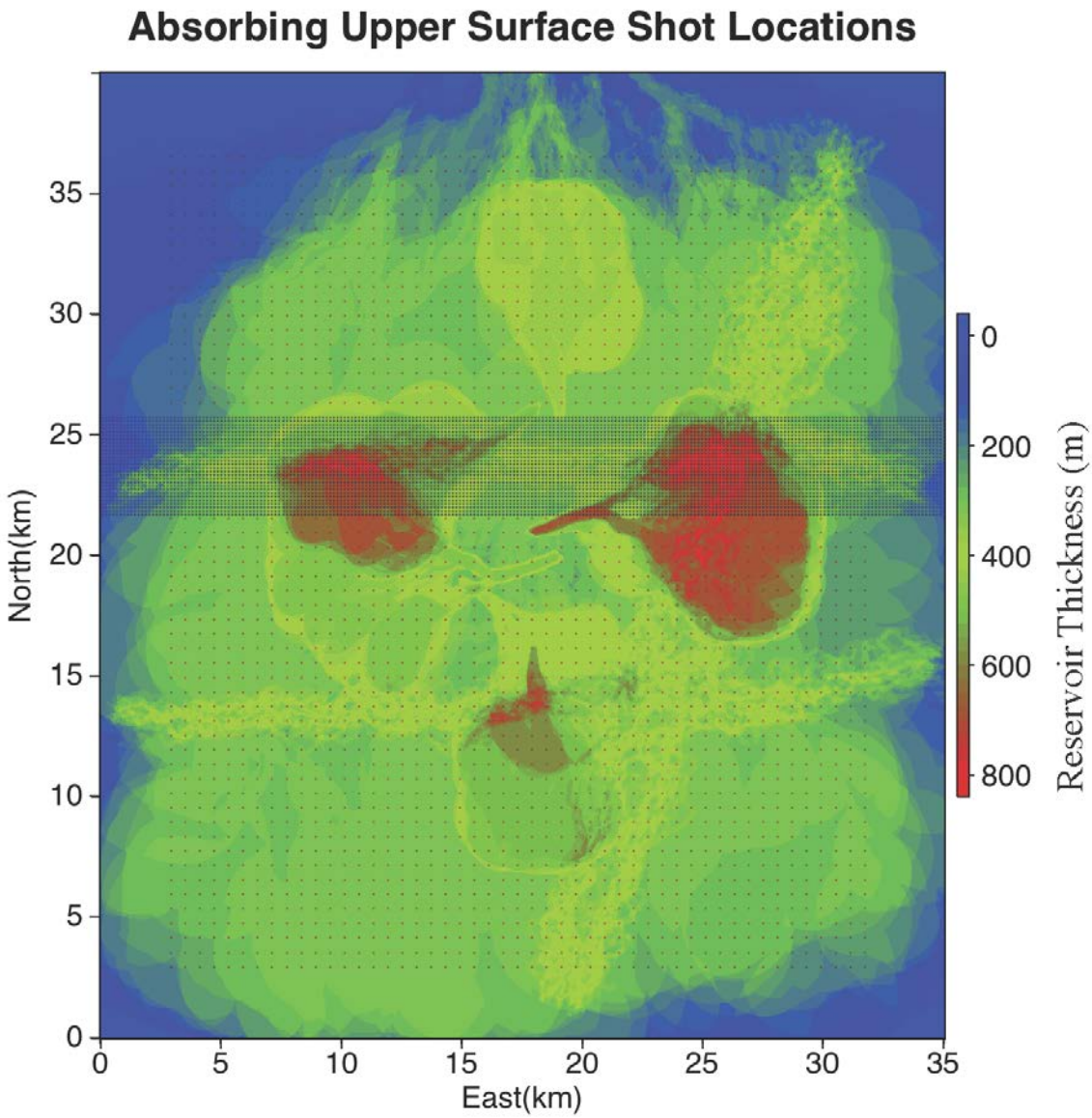

Figure 3-3. AUS NAZ EW source-streamer spread geometry.

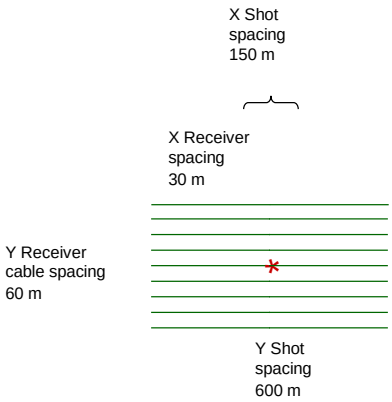

Streamers on both sides of shot

Shots are identical to those for WAZ data set

Shot spacing
Y: 600 m
X: 150 m

Start XY
(3025E, 3050N)
End XY
(31825E,36650N)

Receivers
20 cables
60 m separation
30 m group interval
Spread width 1200m

Figure 3-4. AUS WAZ EW source-streamer spread geometry.

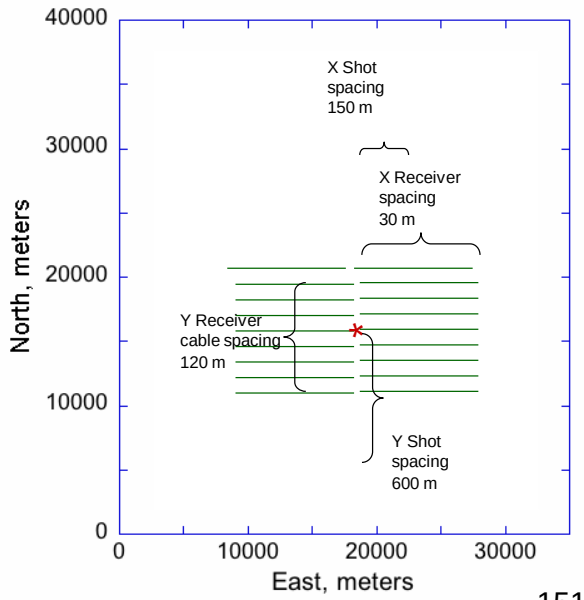

Shot spacing
Y: 600m
X: 150 m

Shot Start XY
(3025E,3050N)
End XY
(31825E,36650N)

Receivers
70 cables
120 m separation
Spread width 8280 m
30 m group interval

Streamers on both sides of shot

151*17 shot grid = 2567 total shots

Figure 3-5. The TTI 2793 shot set (600 m grid of shots) extends over the whole model. The 109 line 150 m shot grid extends east-west across the model between 15800 and 32000 north. This swath is centered on North 23900, the east-west line the VSPs are located on.

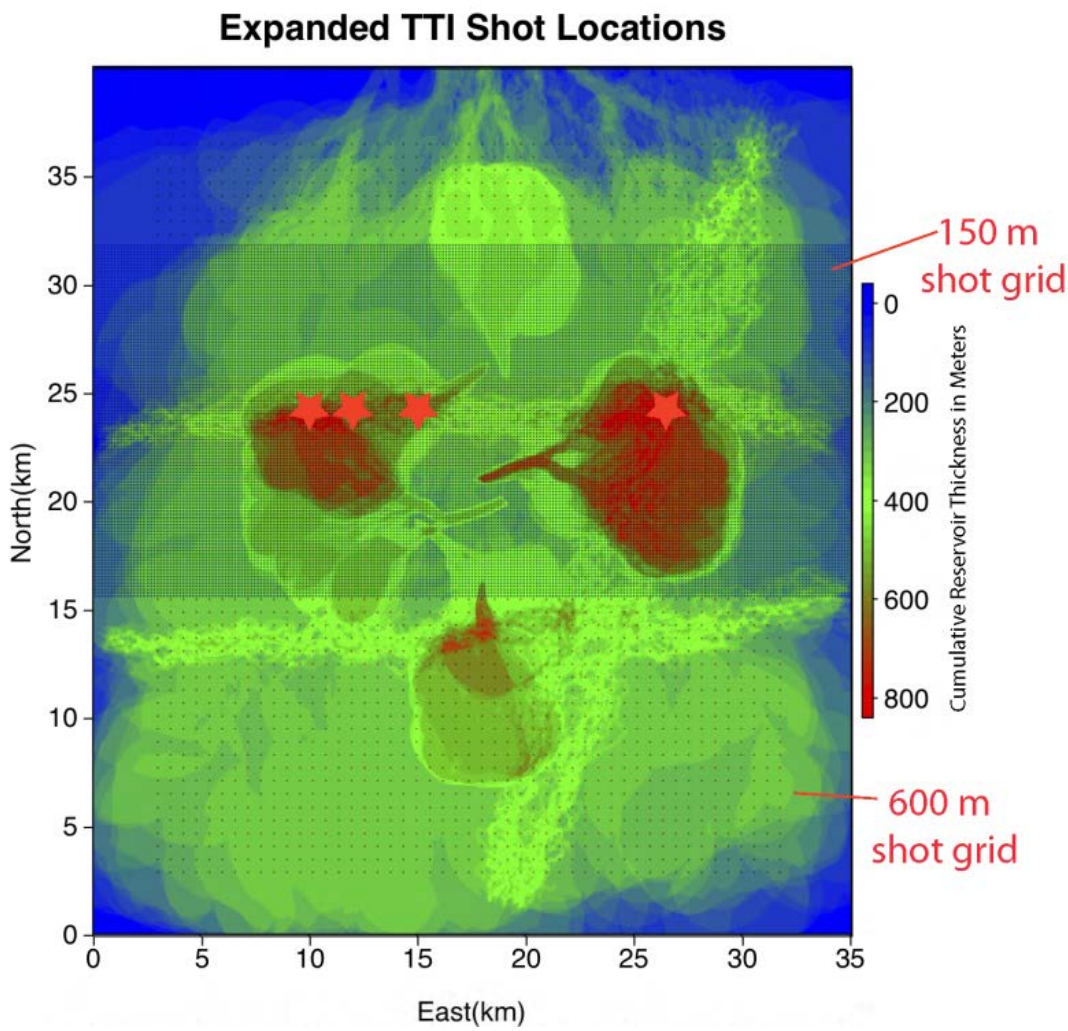

Figure 3-6. The shot lines for the TTI east-west WAZ and NAZ are illustrated relative to the 150 m shot grid and the VSP locations.

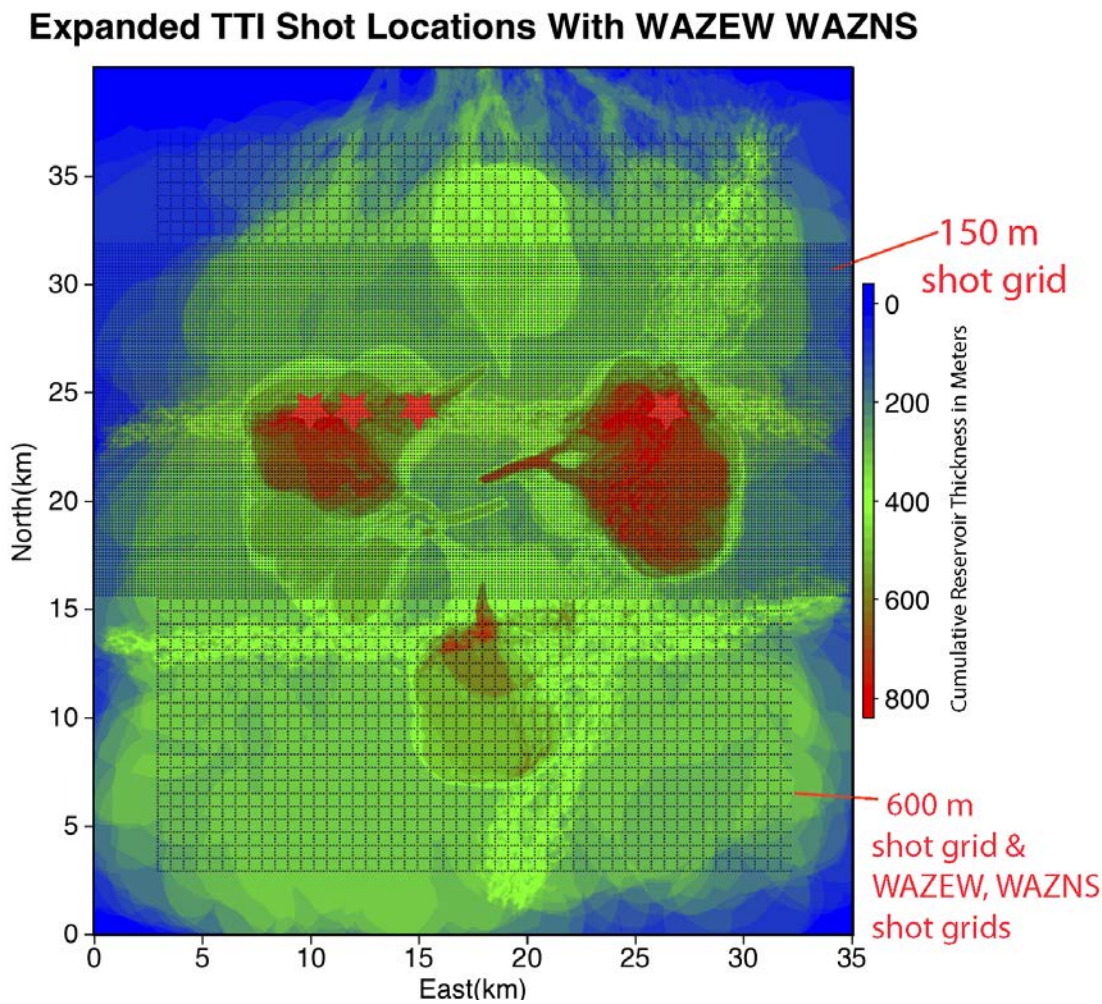

Figure 3-7. The four TTI VSPs are located at north 23900 m in the model where the wells sample three shallow reservoirs away from salt and one through a salt overhang. The receiver depth range is 1000m to 7990m with a sample interval of 15 m.

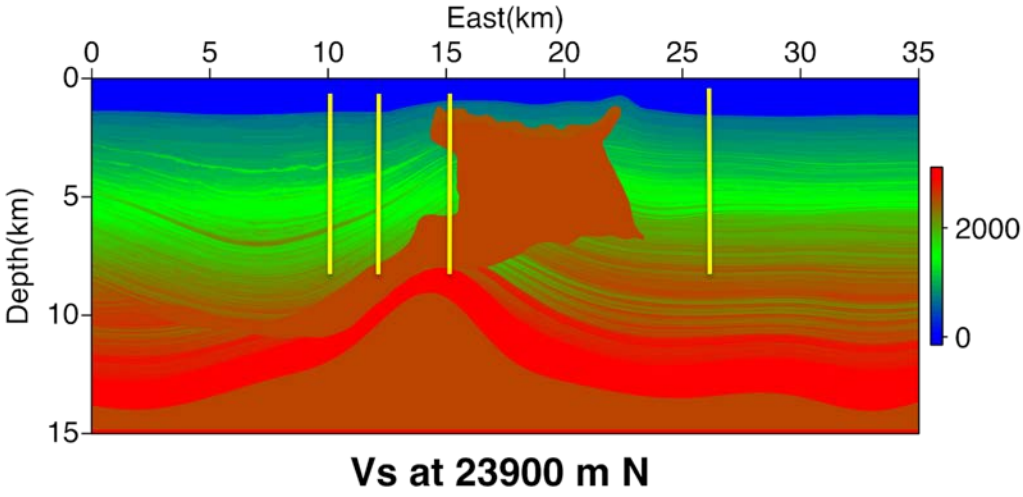

Figure 3-8. TTI VSP Source grid recorded by each well is outlined by the color boxes. The 600 m grid of shots is from the 2793-shot data set.

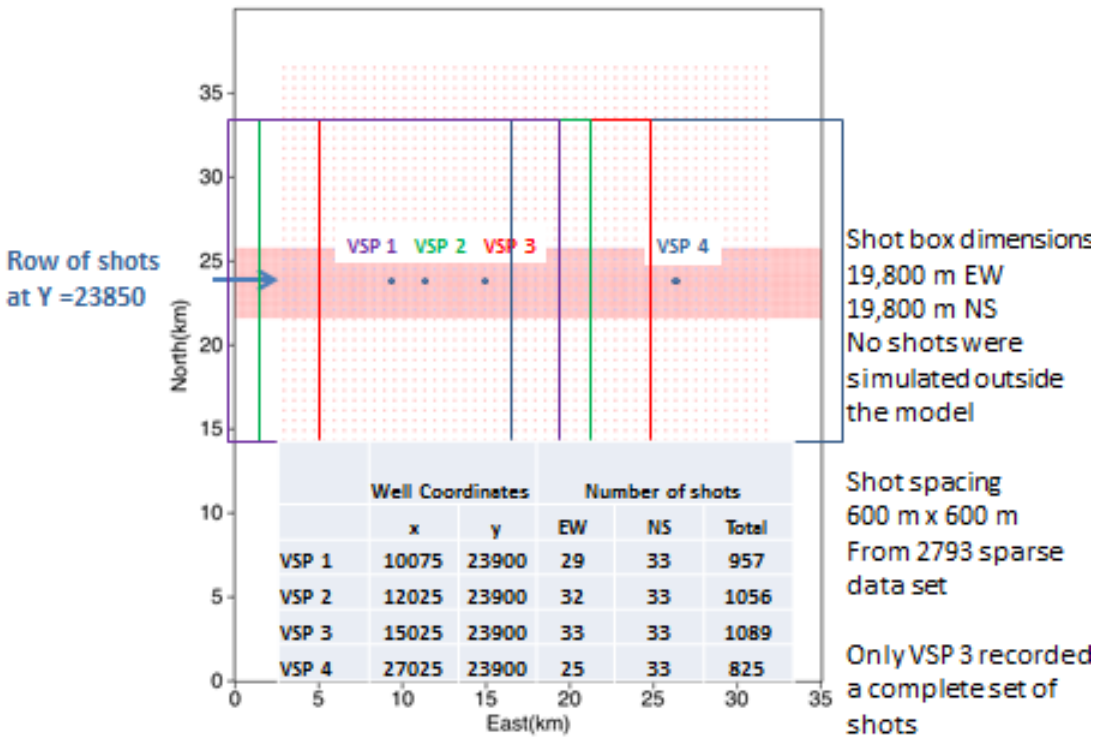

	Well Coordinates		Number of shots		
	x	y	EW	NS	Total
VSP 1	10075	23900	29	33	957
VSP 2	12025	23900	32	33	1056
VSP 3	15025	23900	33	33	1089
VSP 4	27025	23900	25	33	825

Figure 3-9. Ray-tracing indicated a minimum of 14 second seismic records were needed. Sixteen seconds were simulated.

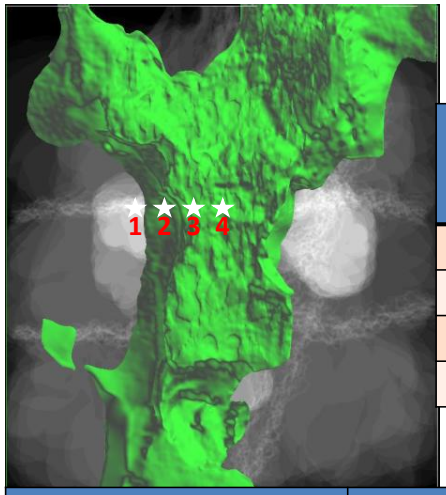

3D Ray-Traced Shot Locations

Shot no	East (x km)	North (y km)
1	10.0	24.0
2	12.5	24.0
3	15.0	24.0
4	17.5	24.0

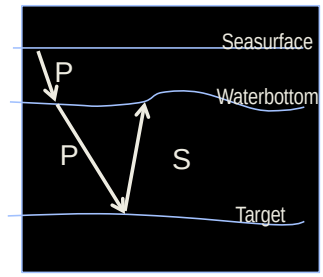

	Shot 1 (outboard of salt)	Shot 2 (inboard of salt)	Shot 3 (inboard of salt)	Shot 4 (inboard of salt)
Plio/mio target (shallow)	12s	11s	14s	4 s
Oligocene target (deep)	14s	No reflection	No reflection	9s

Figure 3-10. Description of the Elastic simulation receiver area and shot patch for the 100 m grid shot set.

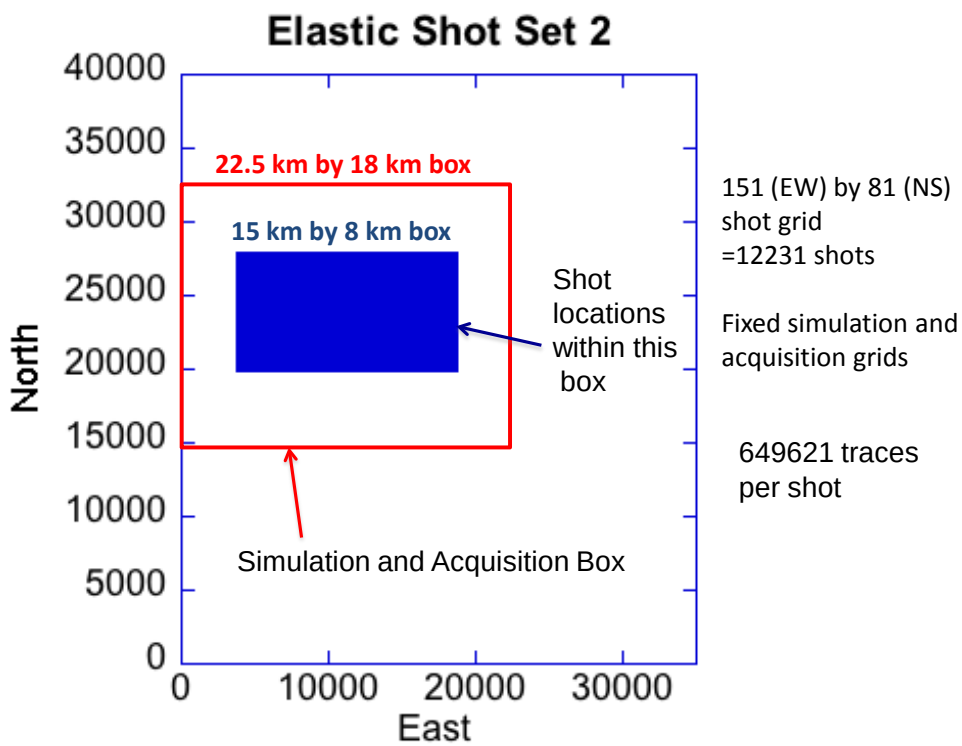

Figure 3-11. Elastic 100 m grid acquisition region. Yellow box shows region containing shots and blue box outlines the simulation and trace acquisition boundary. Overlay on Cumulative Reservoir Thickness map from Joe Stefani.

Shot locations in yellow box, elastics simulation region blue box

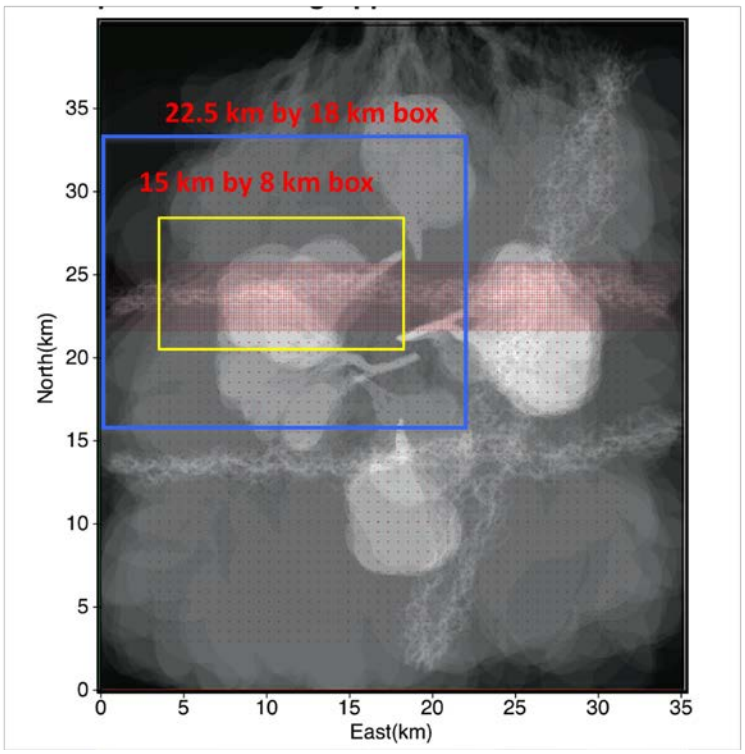

649621 traces per shot

Figure 3-12. The four VSP locations for the elastic simulation are shown. The depth range of receivers is 1000 m – 7990 m at 15 m intervals.

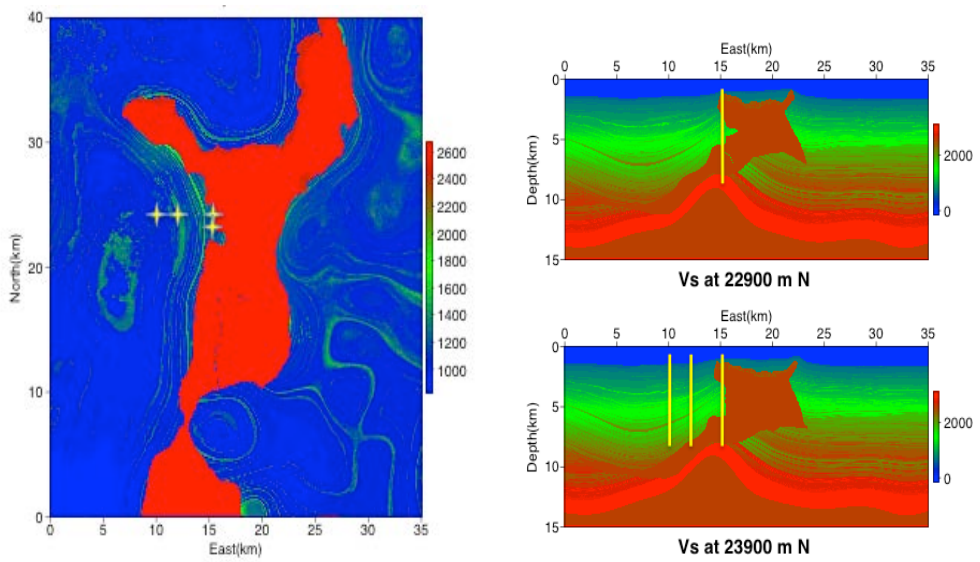

Figure 3-13. Elastic VSP Source grid recorded around each well with the 2793 data set and 600 m shot interval.

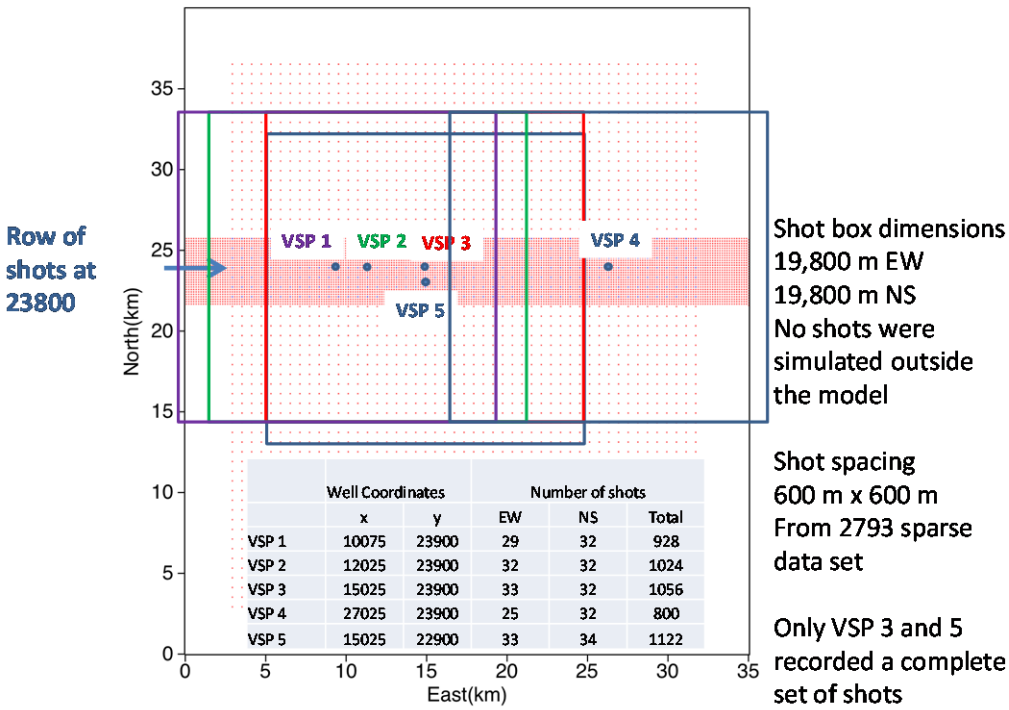

	Well Coordinates		Number of shots		
	x	y	EW	NS	Total
VSP 1	10075	23900	29	32	928
VSP 2	12025	23900	32	32	1024
VSP 3	15025	23900	33	32	1056
VSP 4	27025	23900	25	32	800
VSP 5	15025	22900	33	34	1122

Figure 3-14. Acquisition geometry and location for the Elastic NAZEW Classic Data Set.

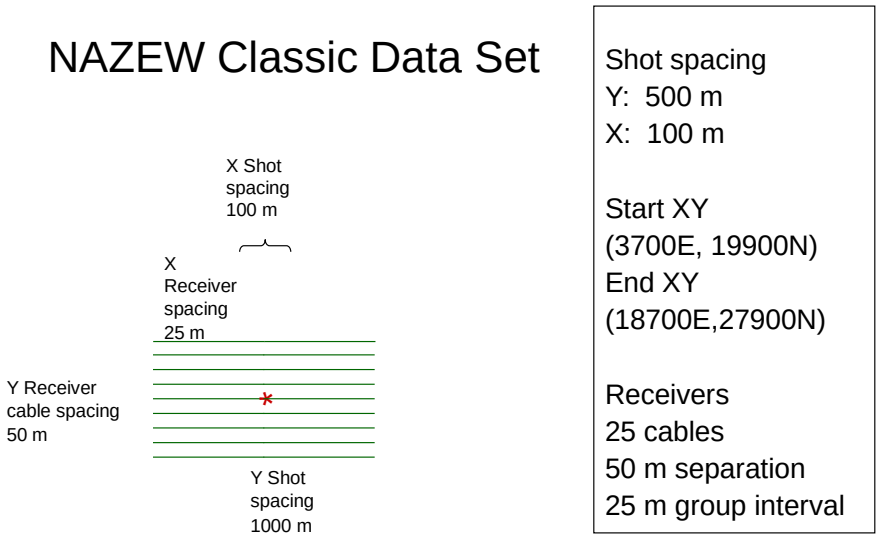

- Streamers on both sides of shot
- Shots are identical to those for WAZ data set
- 2567 total shots

Figure 3-15. Comparison of acquisition geometries for acoustic and elastic East-West narrow azimuth classic data sets. These are push-pull data sets so half the streamer is east of the shot and half is west.

Comparison Acoustic to Elastic NAZEW Classic Data Sets

Parameter	Acoustic	Elastic
Streamer length	19800 m	20000 m
Streamer separation	60 m	50 m
Max Streamer offset NS	570	600
Number of Streamers	20	25
Trace interval	30 m	25 m
Traces per shot in Classic Data Set	13220	20025
Shot Spacing in EW Direction	150 m	100 m
Shot Spacing in NS Direction	1200 m	500
Total shots in NAZEW Classic Data Set	11172	2567
GB per shot (uncompressed)	.11	.16
Size of data set (uncompressed)	1229 GB	411 GB

Figure 3-16. Acquisition geometry and location for the Elastic WAZEW Classic Data Set.

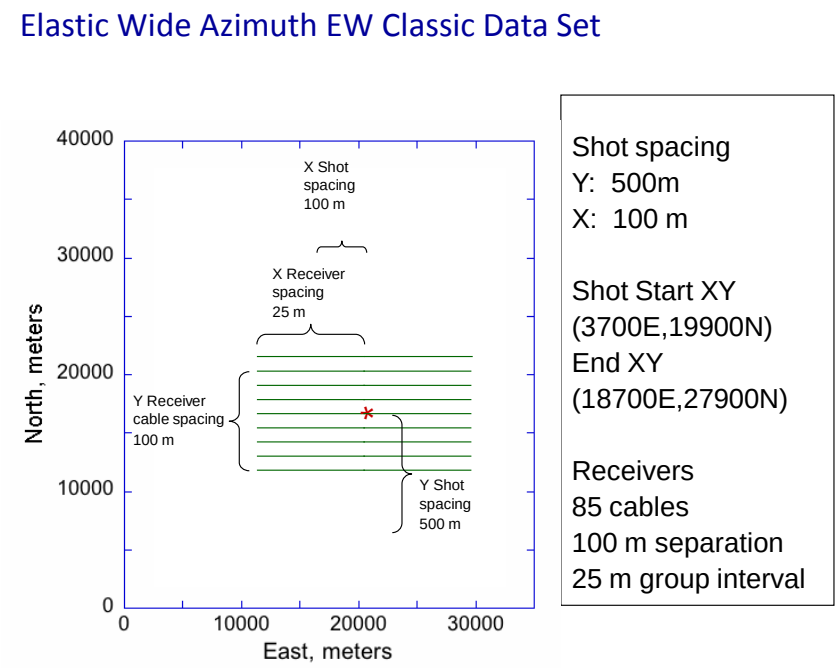

- Streamers on both sides of shot
- 151*17 shot grid = 2567 total shots

Figure 3-17. Comparison of acquisition geometries for acoustic and elastic East-West wide azimuth classic data sets. These are push-pull data sets so half the streamer is east of the shot and half is west**.**

Comparison Acoustic to Elastic WAZEW Classic Data Sets

Parameter	Acoustic	Elastic
Streamer length	19800 m	20000 m
Streamer separation	120 m	100 m
Max Streamer offset NS	4140	4200
Number of Streamers	70	85
Trace interval	30 m	25 m
Traces per shot in Classic Data Set	53970	68085
Shot Spacing in EW Direction	150 m	100 m
Shot Spacing in NS Direction	1200 m	500 m
Total shots in WAZEW Classic Data Set	11172	2567
GB per shot (uncompressed)	.43	.54
Size of data set (uncompressed)	4804 GB	1386 GB

Figure 3-18. Acquisition shot-receiver patch geometry and location on the model for the Elastic 1600 shot Classic Data Set.

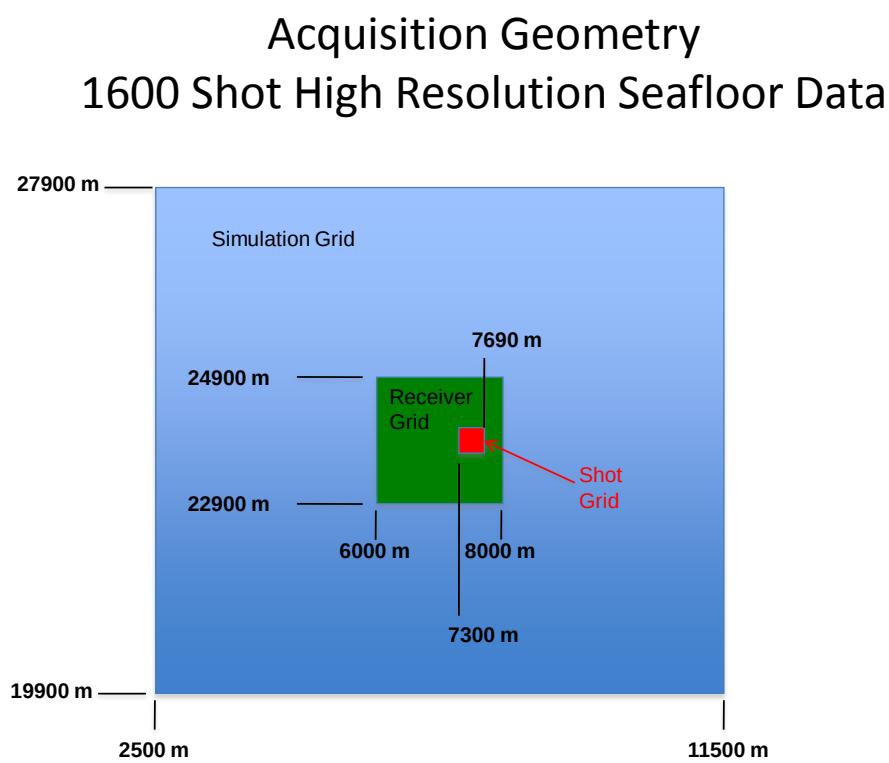

Figure 3-19. Cross-section illustrating the variation of Vs under the 1600 shot, high resolution acquisition spread.

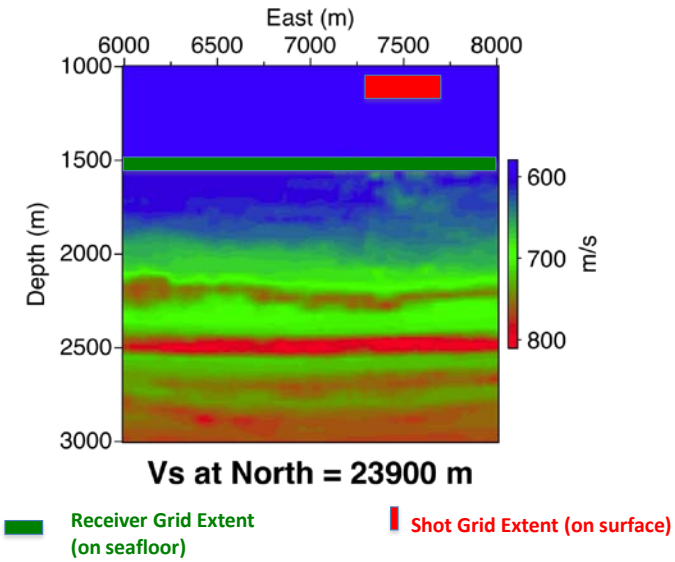

GRAVITY

Gravity is one of the complementary non-seismic data sets (Gravity, CSEM and MT) acquired over the full SEAM model. The data are available in industry standard format that, when combined with the acoustic and elastic seismic and other non-seismic data sets, will enable research into joint inversion methods for enhanced subsurface interpretation of structure, rock and fluid properties. Both the vertical gravity component caused by the density volume and the gravity gradients, or components of the gravity tensor were calculated. Gravity has been commonly used by the industry to model salt geometry either with gravity data alone, or iteratively with seismic depth imaging to optimize the image of the salt body, particularly the base, and the sediment structures below. Gravity gradiometry is a relatively new tool being applied to exploration, and this model and the data simulated from it can be used to help develop and test the application of the technology.

SEAM Gravity Model

INPUT DATA

The SEAM Phase I forward gravity model was calculated from a 40x40x20 (x,y,z) meter size voxet cell density volume (Figure 4-1). The original density model used for acoustic simulations (dx=dy=dz=10m) was resampled to a grid size of 40 m in each horizontal direction and 20 m in depth in order to comply with the software requirement for a file size as well as to make a consistent voxet size of the EM model. The resampling of the density voxet has no measurable impact on the final results. Densities within the model vary from 1.003 g/cm^3 [1] to 3.140 g/cm^3 (density of the SEG logo embossed in the model). All SEAM data are projected and given in Transverse Mercator projection, UTM16N / WGS84, units-meters.

SOFTWARE

The gravity response of the SEAM Phase I density volume was calculated using LCT 3MOD™ (Fugro Gravity and Magnetics) and GM-SYS 3D™ (Geosoft Inc.) software as a verification. Parameters used in the gravity response calculations are the following: smooth 50% extension and extra fine (1/2) layer thickness for LCT 3MOD™, while for the GM-SYS 3D™ a default set of parameters was used. One means of comparative validation is to compare the range of values over the entire model computed for all components of gravity with by the two software packages. The small variations observed in the Table 4-1 suggest that the results from the two systems were similar enough, and data available for delivery was computed with the LCT 3MOD™ software.

[1] There is one additional zero compared with normal salinity sea water density of 1.03; a value of 1.003 was inadvertently used; this has virtually no effect on the modeling results.

GRAVITY CALCULATION

Vertical gravity component (Gz) caused by the density volume and corresponding gravity gradients/components of gravity tensor (Txx, Txy, Txz, Tyy, Tyz and Tzz) were calculated on two levels that mimic marine (0 m elevation) and airborne (150 m elevation) gravity acquisition programs. 150 m is an average airborne acquisition elevation for marine areas such as the offshore Gulf of Mexico. Calculated grids retain the same 40m x 40m cell size as the original data and can be easily resampled to larger cell sizes. Gravity values are given in mGal (milli Gal) while gravity tensor components values are in E (Eötvös) units.

Figure 4-2 illustrates the vector (black) and tensor (blue) components of the gravity field.

In addition to the gravity attraction of the density cube, two types of gravity anomalies were calculated: Free-air and Bouguer. The Free-air anomalies represent calculated gravity attraction of the model with background density of 2.2 g/cm^3. This background density was applied in order to yield calculated response values that resemble anomalous values commonly encountered in exploration geophysics. The chosen background density of 2.2 g/cm^3 represents a mean density value of the entire density model.

Complete Bouguer anomalies were calculated using a Bouguer correction density of 0.997 g/cm^3 (2.000 g/cm^3-1.003 g/cm^3 = 0.997 g/cm^3), and for the control the same anomalies are directly calculated from the model where density of the water layer (1.003 g/cm^3) was replaced with density of 2.0 g/cm^3, which emulates the Bouguer anomaly reduction state.

Figure 4-3 shows a vertical slice through density volume of the SEAM Phase I model.

The computed gravity anomalies are illustrated in figures 4-4 – 4-7 and grid statistics of vertical gravity and gradient values are shown in Tables 4-2 to 4-6.

Calculated grids are stored in the GXF (Grid eXchange File) - an ASCII uncompressed grid format. Detailed description of the GXF format can be found following this link: http://www.geosoft.com/resources/technotes/pdfs/gxfr3d9_1.pdf . The GXF grids can be easily converted into different formats using OasisMontaj Viewer that can be downloaded for free from the website listed below:
http://www.geosoft.com/pinfo/free/montajviewer.asp
Gravity response of the model was calculated by Neda Bundalo (Marathon Oil Company) in October 2009. For any questions regarding calculations please contact Neda Bundalo at nbundalo@marathonoil.com .

ACKNOWLEDGEMENTS

John Bain (Bain Geophysical Services, Inc.), Barry Wiggins, Pat Quist, Dr. Xiong Li (Fugro Gravity and Magnetic Services, Inc.) and Dr. Stuart Hall (University of Houston)

List of Grid Names in the SEAM Gravity Data Set

faa - Free-air anomaly,
Boug – Bouguer anomaly,
Gz – vertical component of gravity,
Txx, Txy, Txz, Tyy, Tyz, Tzz – gravity tensor components (see Figure 4-2),
2pt2 - is listed if background density of 2.2 g/cm^3 was applied,
2pt0 – 2.0 g/cm^3 density for Bouguer correction

<u>Gravity attraction grids on level 0 m</u>:
SEAM_40x40x20_0m_Gz.gxf
SEAM_40x40x20_0m_Txx.gxf
SEAM_40x40x20_0m_Txy.gxf
SEAM_40x40x20_0m_Txz.gxf
SEAM_40x40x20_0m_Tyy.gxf
SEAM_40x40x20_0m_Tyz.gxf
SEAM_40x40x20_0m_Tzz.gxf

<u>Free-air anomaly grids on level 0 m</u>:
SEAM_40x40x20_0m_Gz_2pt2_faa.gxf
SEAM_40x40x20_0m_Txx_2pt2_faa.gxf
SEAM_40x40x20_0m_Txy_2pt2_faa.gxf
SEAM_40x40x20_0m_Txz_2pt2_faa.gxf
SEAM_40x40x20_0m_Tyy_2pt2_faa.gxf
SEAM_40x40x20_0m_Tyz_2pt2_faa.gxf
SEAM_40x40x20_0m_Tzz_2pt2_faa.gxf

<u>Bouguer anomaly grids on level 0 m, Bouguer correction calculated with density of 2.0g/cm^3</u>:
SEAM_40x40x20_0m_Gz_2pt2_Boug_2pt0.gxf
SEAM_40x40x20_0m_Txx_2pt2_ Boug_2pt0.gxf
SEAM_40x40x20_0m_Txy_2pt2_ Boug_2pt0.gxf
SEAM_40x40x20_0m_Txz_2pt2_ Boug_2pt0.gxf
SEAM_40x40x20_0m_Tyy_2pt2_ Boug_2pt0.gxf
SEAM_40x40x20_0m_Tyz_2pt2_ Boug_2pt0.gxf
SEAM_40x40x20_0m_Tzz_2pt2_ Boug_2pt0.gxf

Gravity attraction grids on level 150m above “sea level”:
SEAM_40x40x20_150m_Gz.gxf
SEAM_40x40x20_150m_Txx.gxf
SEAM_40x40x20_150m_Txy.gxf
SEAM_40x40x20_150m_Txz.gxf
SEAM_40x40x20_150m_Tyy.gxf
SEAM_40x40x20_150m_Tyz.gxf
SEAM_40x40x20_150m_Tzz.gxf

Free-air anomaly grids on level 150 m above “sea level”:
SEAM_40x40x20_150m_Gz_2pt2_faa.gxf
SEAM_40x40x20_150m_Txx_2pt2_faa.gxf
SEAM_40x40x20_150m_Txy_2pt2_faa.gxf
SEAM_40x40x20_150m_Txz_2pt2_faa.gxf
SEAM_40x40x20_150m_Tyy_2pt2_faa.gxf
SEAM_40x40x20_150m_Tyz_2pt2_faa.gxf
SEAM_40x40x20_150m_Tzz_2pt2_faa.gxf

Bouguer anomaly grids on level 150 m above “sea level”, Bouguer correction calculated with density of 2.0 g/cm^3:
SEAM_40x40x20_150m_Gz_2pt2_ Boug_2pt0.gxf
SEAM_40x40x20_150m_Txx_2pt2_ Boug_2pt0.gxf
SEAM_40x40x20_150m_Txy_2pt2_ Boug_2pt0.gxf
SEAM_40x40x20_150m_Txz_2pt2_ Boug_2pt0.gxf
SEAM_40x40x20_150m_Tyy_2pt2_ Boug_2pt0.gxf
SEAM_40x40x20_150m_Tyz_2pt2_ Boug_2pt0.gxf
SEAM_40x40x20_150m_Tzz_2pt2_ Boug_2pt0.gxf

Table 4-1. Comparison of range of values computed for components of the gravity gradients as computed using two software packages described in the text.The similarity of the values indicates little difference in the two methods.

Gravity model (LCT)	Gravity model (Geosoft) gradients calculated from vertical component
G_z range = 38.35 mGal,	G_z range = 37.41 mGal,
G_{xx} range = 136.32 E,	G_{xx} range = 135.36 E,
G_{xy} range = 102.86 E,	G_{xy} range = 102.28 E,
G_{xz} range = 165.40 E	G_{xz} range = 165.11 E
G_{yy} range = 118.30 E	G_{yy} range = 115.02 E
G_{xz} range = 148.81 E	G_{xz} range = 148.93 E
G_{zz} range = 182.17 E	G_{zz} range = 181.43 E

GRID STATISTICS

Table 4-2. Range of gravity anomalies and corresponding gradients.

	Gz mGal	Txx E	Txy E	Txz E	Tyy E	Tyz E	Tzz E
FREE-AIR ANOMALIES AT SEA LEVEL	37.65	138.80	104.31	168.57	118.63	151.77	186.31
FREE-AIR ANOMALIES AT 150 m LEVEL	36.08	119.20	92.11	146.67	106.37	131.25	160.73
BOUGUER ANOMALIES AT SEA LEVEL	20.10	21.72	10.64	34.85	15.08	17.96	32.43
BOUGUER ANOMALIES AT 150 m SEA LEVEL	19.67	20.71	9.66	31.72	14.18	16.12	30.46

Table 4-3. Free-air anomalies at 0 m level, background density 2.2 g/cm^3.

	Gz	Txx	Txy	Txz
min	-12.199	-102.574	-60.780	-75.511
max	25.454	36.225	43.529	93.064
mean	6.779	2.735	0.571	2.066
standard deviation	8.32	16.152	9.119	18.357
			Tyy	**Tyz**
min			-86.333	-81.002
max			32.299	70.765
mean			-1.158	-1.389
standard deviation			15.070	17.855
				Tzz
min				-44.716
max				141.596
mean				-1.577
standard deviation				24.944

Table 4-4. Free-air anomalies at 150 m level, background density 2.2 g/cm^3.

	Gz	Txx	Txy	Txz
min	-11.755	-86.286	-53.109	-64.928
max	24.322	32.910	38.997	-81.738
mean	6.802	2.679	-0.558	2.051
standard deviation	8.026	14.840	8.403	16.857
			Tyy	**Tyz**
min			-75.888	-71.566
max			30.487	59.683
mean			-1.184	-1.324
standard deviation			14.043	16.605
				Tzz
min				-41.545
max				119.190
mean				-1.495
standard deviation				22.987

Table 4-5. Bouguer anomalies at 0 m level, Bouguer correction density 2.0 g/cm^3, background density 2.2 g/cm^3.

	Gz	Txx	Txy	Txz
min	64.288	-5.424	-6.459	-13.364
max	84.389	16.301	4.181	21.490
mean	73.908	3.800	-0.384	1.537
standard deviation	4.955	5.260	1.912	7.421
			Tyy	**Tyz**
min			-6.272	-11.577
max			8.808	6.386
mean			0.655	-1.266
standard deviation			2.685	3.067
				Tzz
min				-23.594
max				8.840
mean				-4.455
standard deviation				6.992

Table 4-6. Bouguer anomalies at 150 m level, Bouguer correction density 2.0 g/cm^3, background density 2.2 g/cm^3.

	Gz	Txx	Txy	Txz
min	64.619	-5.078	-5.753	-12.085
max	84.288	15.635	3.904	19.635
mean	73.974	3.750	-0.377	1.522
standard deviation	4.898	5.453	1.829	7.223
			Tyy	**Tyz**
min			-5.824	-10.489
max			8.353	5.632
mean			0.636	-1.245
standard deviation			2.570	2.918
				Tzz
min				-22.554
max				7.909
mean				-4.386
standard deviation				6.757

Figures

Figure 4-1. SEAM Phase I model density cube.

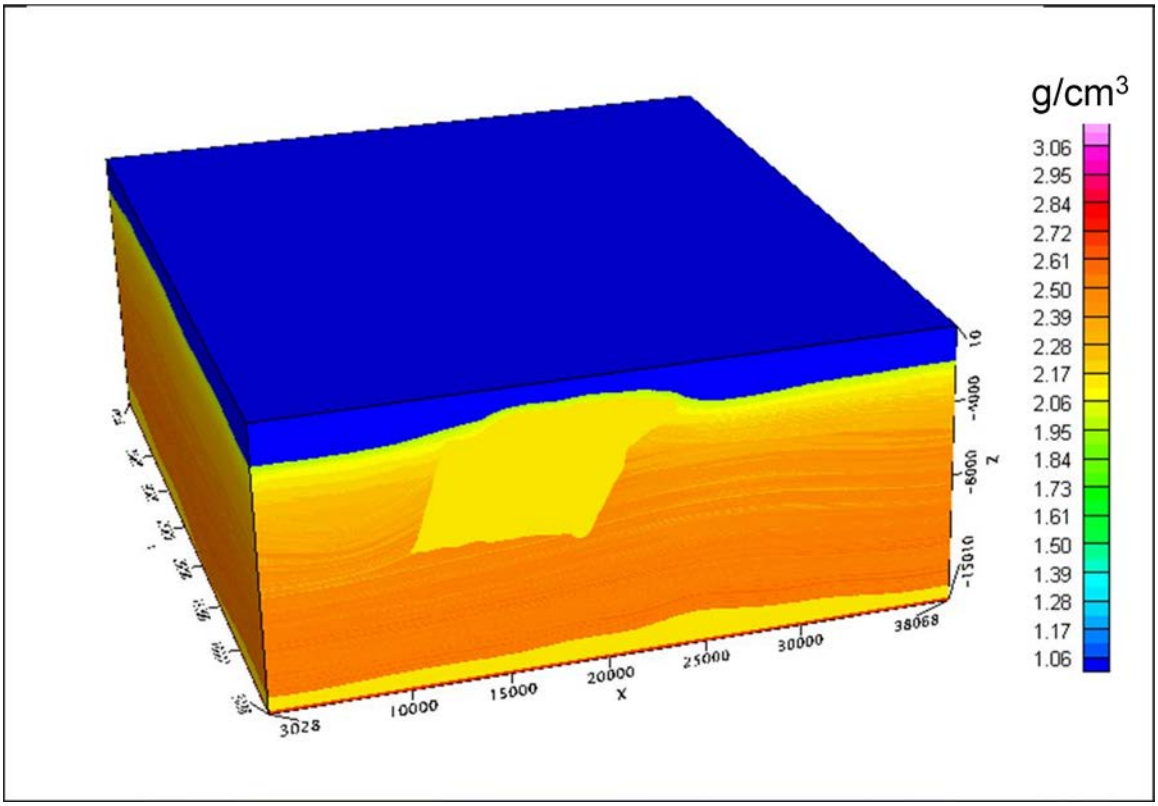

Figure 4-2. Vector (black) and tensor (blue) components of gravity field. (Figure from Neda Bundalo).

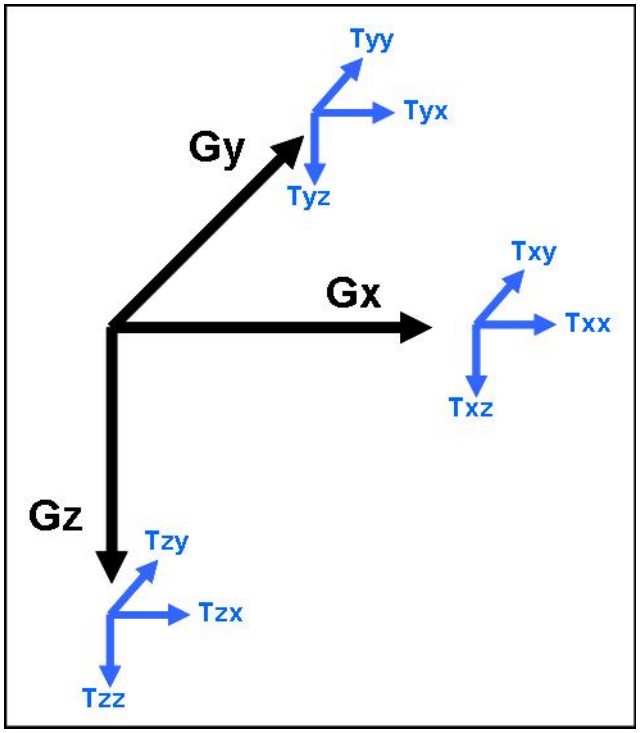

Figure 4-3. Vertical slice through density volume of the SEAM Phase I model.

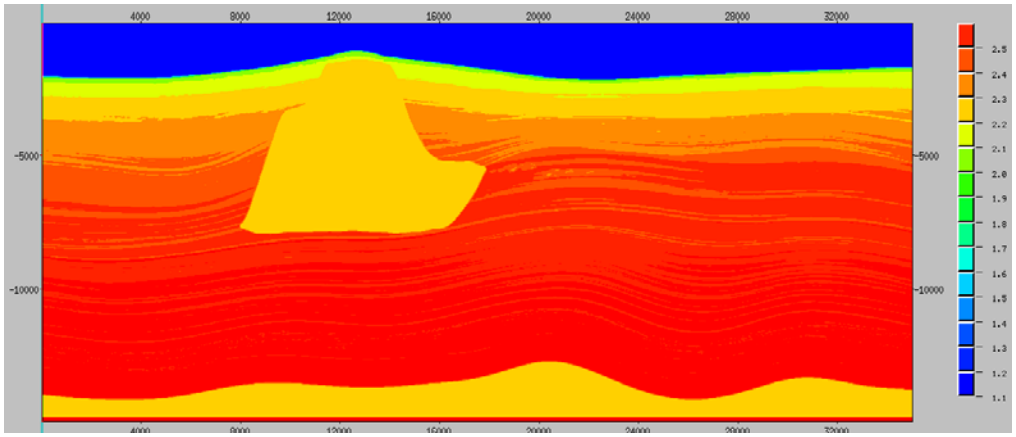

Figure 4-4. Free air anomaly at sea level to simulate ship borne gravity measurement. (Figure from Neda Bundalo.)

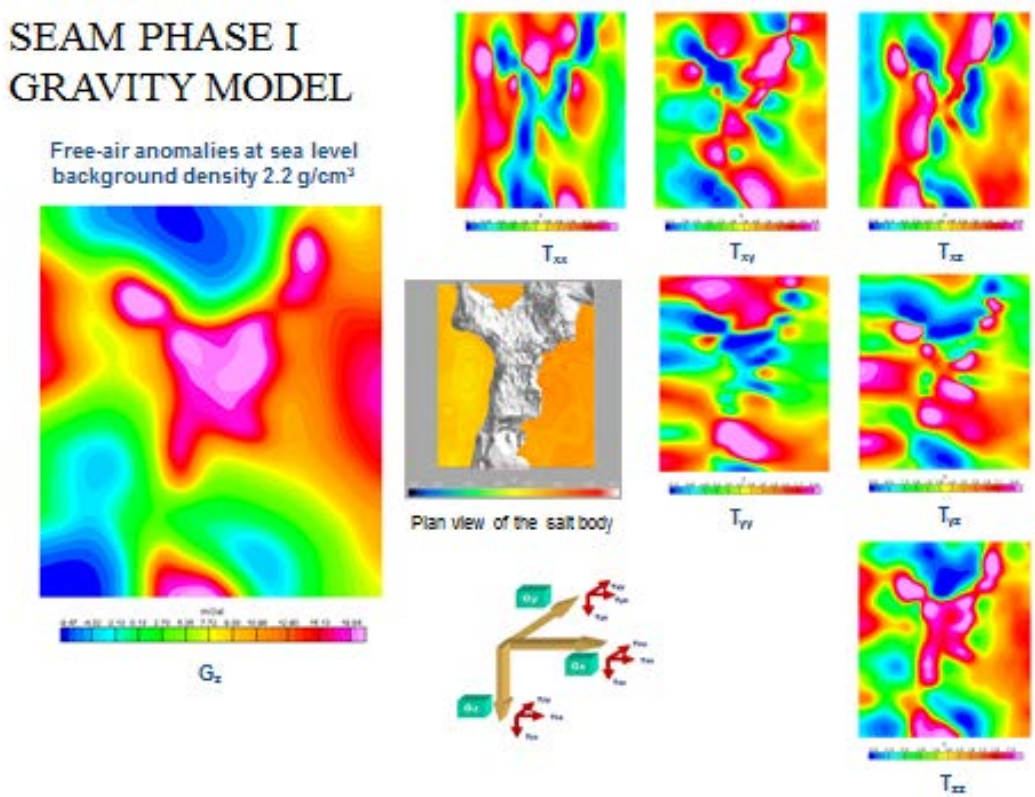

Figure 4-5. Free air anomaly at 150 above the sea surface to simulate airborne gravity. (Figure from Neda Bundalo.)

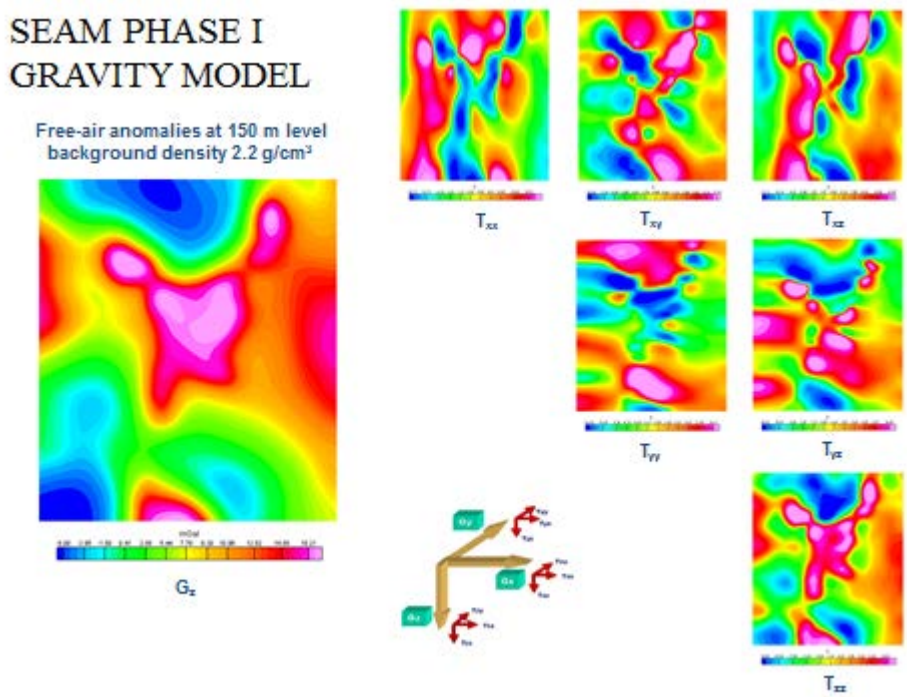

Figure 4-6. Bouguer anomaly at sea level. (Figure from Neda Bundalo.)

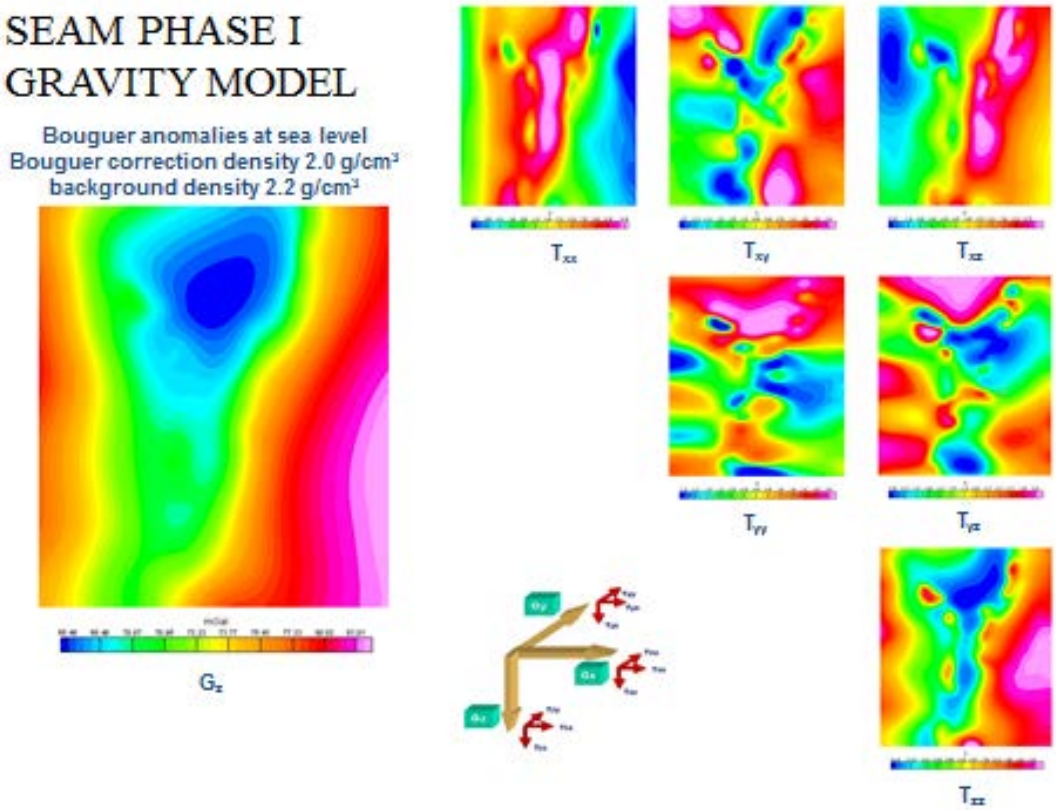

Figure 4-7. Bouguer anomaly at 150 m above sea surface. (Figure from Neda Bundalo.)

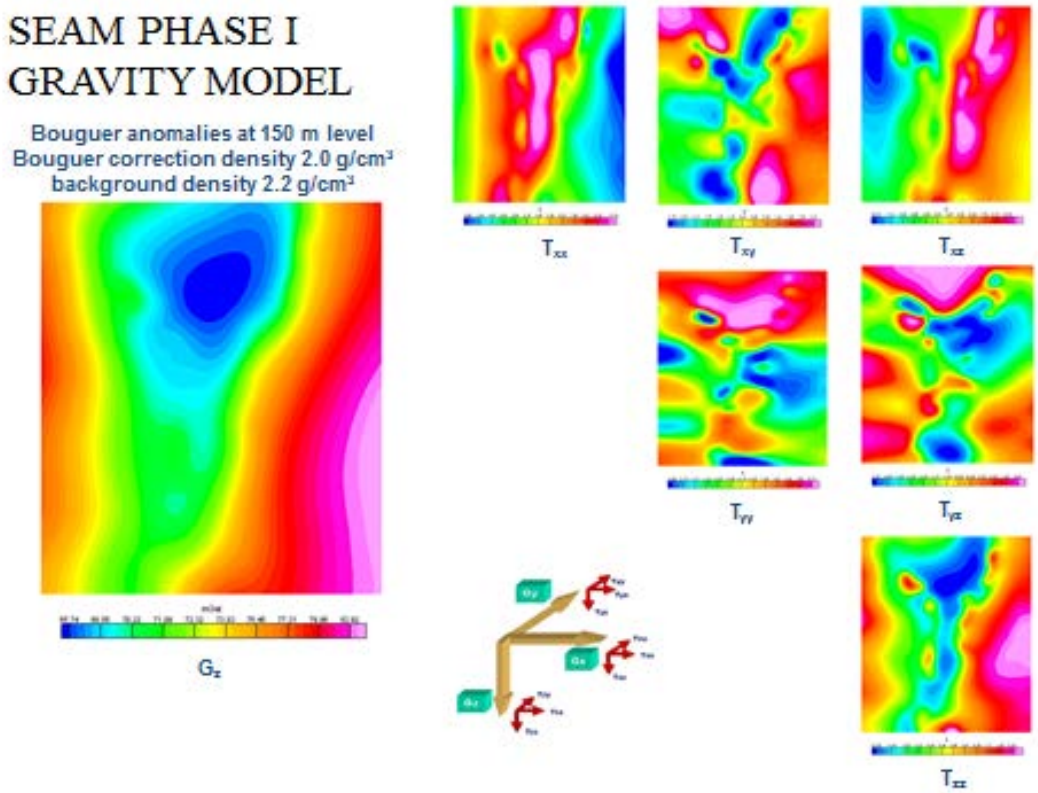

CONTROLLED SOURCE ELECTROMAGNETICS

CSEM data collection and inversion/imaging are of intense interest by companies conducting exploration and reservoir development in marine environments. SEAM's goal in conducting a CSEM simulation on the SEAM Phase I RPSEA model was to provide 3D electromagnetic data that not only mimics current field acquisitions but, in most cases, far exceeds them. The resulting simulation data can be used to validate and ultimately improve 3D EM forward modeling as well as subsurface imaging and characterization methods using electromagnetic data alone or when combined with other types of geophysical data.

The generated 3D CSEM data set for a wide spectrum of frequencies will also be perfectly suitable for testing new integrated interpretation workflows designed for detecting hydrocarbon reservoirs in the presence of complex structural interfaces and bathymetry. Special attention should be given to approaches that overcome the masking effect on the electromagnetic responses from the salt bodies. The large number of receivers in the SEAM data set compared to current field acquisitions allows alternative acquisition geometries to be evaluated and techniques for optimization of CSEM survey design to be tested. Simulations were conducted under contract from SEAM to EMGS.

SEAM Resistivity Model

The SEAM resistivity model has Vertical Transverse Isotropic (VTI) anisotropy in the background, while a large salt body is isotropic and homogeneous with resistivity 100 Ωm. The thickness of the salt is up to 5 km. The model also has 15 anisotropic resistive anomalies (reservoirs). To perform simulations, two separate models containing the horizontal (R_h) and vertical (R_v) resistivities were used. Resistivities in the horizontal model range from 0.3 to 392 Ωm, while resistivities in the vertical model range from 0.3 to 550 Ωm. The background resistivity varies with depth from approximately 0.5 to 4 Ωm, and the maximum value of the anisotropy ratio of the vertical to the horizontal resistivity is approximately 3. The background resistivity is an assumed base level from which all relative EM anomalies are computed. The water is isotropic with resistivity 0.3 Ωm, and the water depth varies in the range 1-2 km.

The SEAM model was initially constructed as a Tilted Transverse Isotropic (TTI) model with bed-parallel and bed-perpendicular values of resistivity. Since it was uncertain as to whether it would currently be possible to simulate using this type of TTI anisotropic resistivity model, it was decided to use a simplified VTI-type model with the geographically-directed vertical and horizontal resistivities that were derived from the bed-normal and bed-parallel models. Details about the use of the petrophysics in the development of the SEAM resistivity model and how the vertical and horizontal resistivity values were

determined from the bed-normal and bed-parallel values are given in the February 2010 TLE SEAM update (Stefani et al. 2010).

Figure 5-1 shows vertical slices through the resistivity model at North = 23.9 km. Plots showing the resistivity models in the bed-normal, bed-perpendicular, vertical, and horizontal directions are shown. The plots have been scaled so that colors are saturated to help emphasize the locations of the reservoirs, which have low resistivity.

CSEM Acquisition Geometry

CSEM Data were simulated for a total of 494 receivers located on the irregular seafloor of the SEAM model. For each receiver, sources were located along 22 tow lines having a spacing of 1000 m. Towlines were located along 11 EW lines and 11 NS lines for each receiver. Each towline had a length of 20 km, extending 10 km away from the receiver or to the edge of the model if the receiver is located less than 10 km from the model boundary. Sources were spaced at 100 m along each towline for a total of 201 source positions along each towline. The source is a 100 m long Horizontal Electrical Dipole (HED), oriented parallel to the towline. Figure 5-2 shows a schematic of the receiver positions and towlines superimposed on a map view of the SEAM model. The model responses (the six electromagnetic field components E_x, E_y, E_z, H_x, H_y, and H_z) for 11 source frequencies of 0.025, 0.05, 0.1, 0.2, 0.4, 0.8, 1.2, 1.6, 2.0, 3.0, and 4.0 Hz were simulated. Figure 5-3 shows the receiver positions and receiver numbering scheme. The CSEM simulation was done for a subset of the receivers used for the MT simulation. The MT receiver numbers are consecutively numbered beginning with receiver 1. The CSEM receiver numbers match those for the MT simulation when they are at an identical position. Figure 5-4 shows the towline numbering scheme.

CSEM Simulation Issues

CSEM data were simulated by EMGS after a competitive bidding process. Part of the bidding process included a technical evaluation of the simulation capability of the vendors who bid to conduct the simulation. The technical evaluation consisted of a qualification procedure that required vendors to provide SEAM with example simulations for 4 towlines for each of two receivers. The vendor simulations were compared against benchmark simulations conducted by one of the SEAM participating companies. The comparison showed that the bidder who was awarded the contract for the simulations had results that were substantially equivalent to those of the SEAM benchmark simulations. It is worth noting that at least one of the other bidder's simulation results were quite different from those of the SEAM benchmark. A thorough analysis about why the vendor results were different convinced us that the comparable simulations of EMGS and the SEAM benchmark were correct.

The receivers were placed on the seafloor. Seafloor was defined as the first depth where resistivity became larger than that of water, or .3 Ohm-m.

EMGS provided SEAM with a detailed report summarizing their simulation procedure and the extensive testing that they conducted on the simulation results prior to final delivery to SEAM. Included is a discussion of how the position of the sources and receiver relative to the seafloor impact the simulation results. The report was included on the DVD along with with the distribution of the CSEM data set.

SEAM conducted Quality Control (QC) evaluations on the data that were delivered by EMGS. Figure 5-5 shows one of the QC plots that compares the EMGS simulation with a simulation conducted by a SEAM participating company. The plot shows amplitude and phase of the data at 2 Hz recorded by one receiver (Rx177) for the East-West towline passing through the source. Note that this receiver is located 5 km from the Western edge of the model so sources were placed a maximum of 5 km to the West of the receiver. The amplitude and phase show excellent agreement except at source offsets greater than about 6 km to the East of the receiver. Here the field has dropped by several orders of magnitude from that near the receiver. Numerical noise probably results in poor data at this offset for this receiver. Data for other field values and at other receivers did not suffer from the degradation at large offsets as is shown in Figure 5-5. Degradation occurs when fields are extremely small, which causes computational round off errors.

CSEM Data

Figure 5-6 shows an example of a small portion of the CSEM data that have resulted from the simulations on the SEAM model. The figure shows plan-view plots of the EW horizontal component of the electric field magnitude (E_x) at various frequencies for East-West source receiver offset of 5 km. The field measured for each source-receiver pair is plotted at the midpoint location between the source and receiver. Included for reference are maps of cumulative reservoir thickness and the vertical resistivity (R_v) model at 2.5 km depth. Cumulative reservoir thickness is the sum of the thickness of all reservoirs located below a given location. Reservoirs are located above and below the salt in addition to locations away from the salt. The red-colored region in the resistivity model shows the horizontal extent of the salt at 2.5 km depth. Visual analysis of the CSEM data shows that high electric field (shown in red) occurs roughly above the outline of the salt body at this depth. Other than the strong field over the salt, one can see a zone of relatively high field east of the salt. This zone of high electric field is most pronounced on the higher-frequency data. This high field region is located over a section of the model having several overlapping hydrocarbon-filled reservoirs at depths less than 5 km. Data from the CSEM simulations may be evaluated separately or combined with analysis of seismic, gravity and MT simulations via modeling- and inversion-based methods.

Data Distribution

Data are distributed as a gzip compressed tar file that contains the results of the CSEM simulation on the SEAM Phase I RPSEA model. Included in the file are the following directories:

Supporting_Documents

Technical specifications for the CSEM simulations as written by SEAM and provided to the CSEM Simulation Vendor EMGS. The following files are included

-FinalContractTechnicalSpecifications.pdf: Specifications for simulation including acquisition geometry and simulation specifications.
- Data_format.pdf: Description of data format
- 2011-04-SeamDepthSensitivityStudy_EMGS.pdf: Report from EMGS about influence of maximum model depth used in simulation on simulation results
- EMGS_SEAM_CSEM_Final_Report_Dec2011_updated.pdf: Final report from EMGS about simulations

Simulation_Data

10,868 files resulting from the simulation. Files are ascii format. File structure is defined in the Technical Specifications document included in the directory Supporting_Documents. Data in a gzipped tar file.

Bathymetry

Bathymetry files generated from model files that give the seafloor depth at grid points. Four files are contained in this directory. The README in the directory explains the four files

Figures

Figure 5-1. SEAM Phase I Resistivity models. Upper two panels show bed-parallel and bed-normal resistivity. Bedding directions change with position. Lower panels show horizontal and vertical resistivities that were derived from bed-normal and bed-parallel resistivities by a simple rotation (described in Fehler and Keliher, 2011). Vertical East-West cross sections though North 23.9 km are shown.

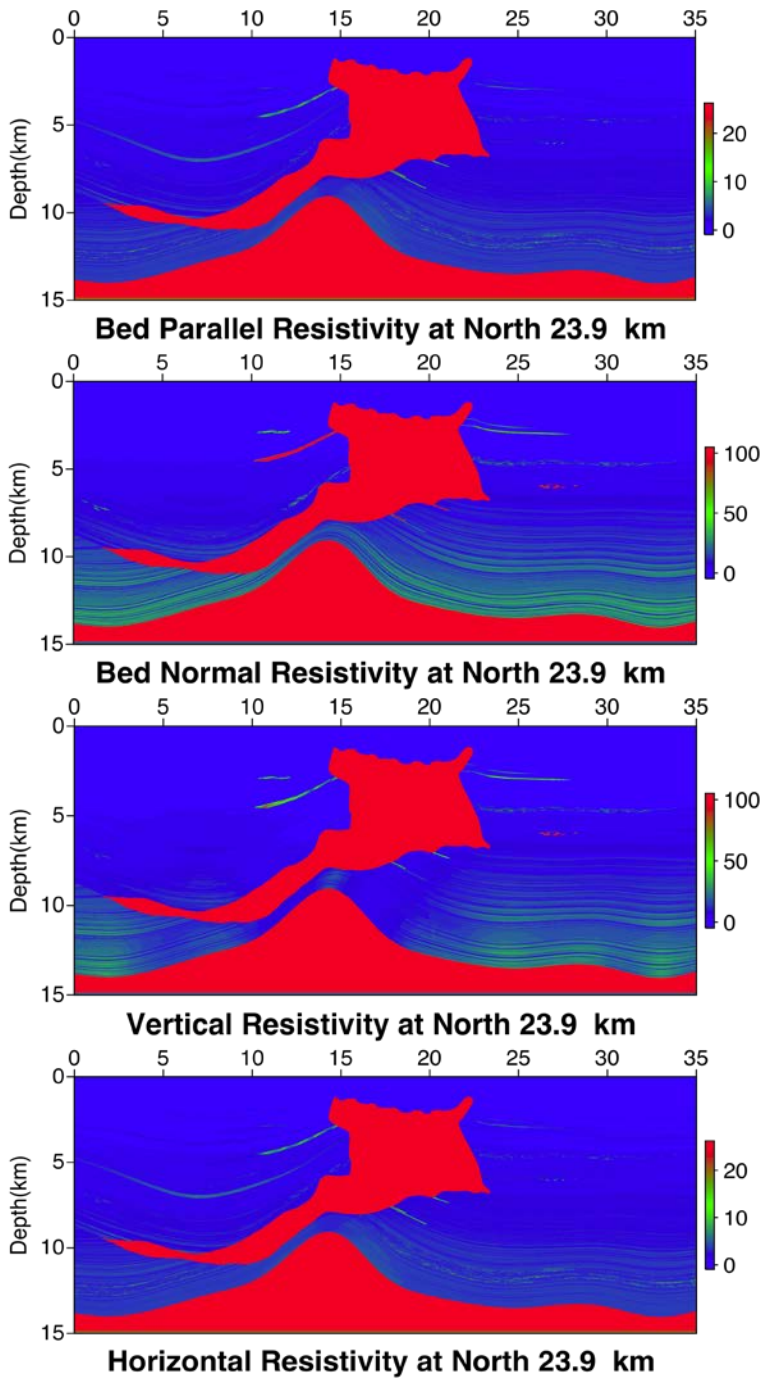

Figure 5-2. CSEM acquisition geometry superimposed on a plan view of the SEAM model. Yellow dots are receiver locations. Green lines are source towlines occupied for the receiver located at East = 11,000 m, North = 26,750 m. Source locations are spaced every 100 m along each towline; the distance between the towlines is 1 km. Synthetic CSEM data were simulated for a total of 494 receivers with 22 towlines for each receiver.

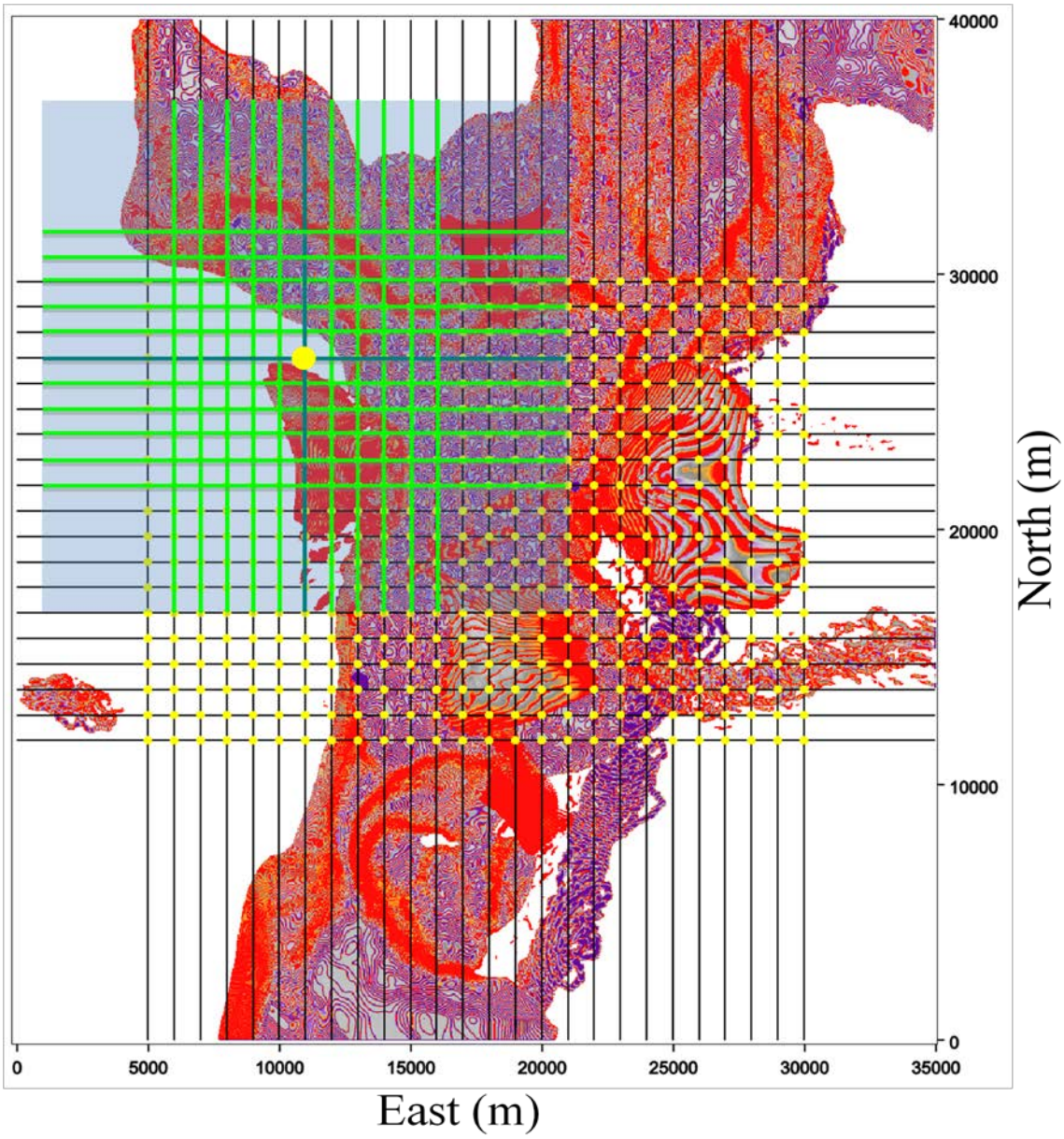

Figure 5-3. Receiver numbering scheme for CSEM simulation. Receivers were placed at 1000 m increments across the center portion of the model. CSEM receivers are a subset of those used for MT simulation. To maintain consistency between CSEM and MT receiver numbering, not all receiver numbers are used for CSEM simulation. Yellow dots show locations of receivers.

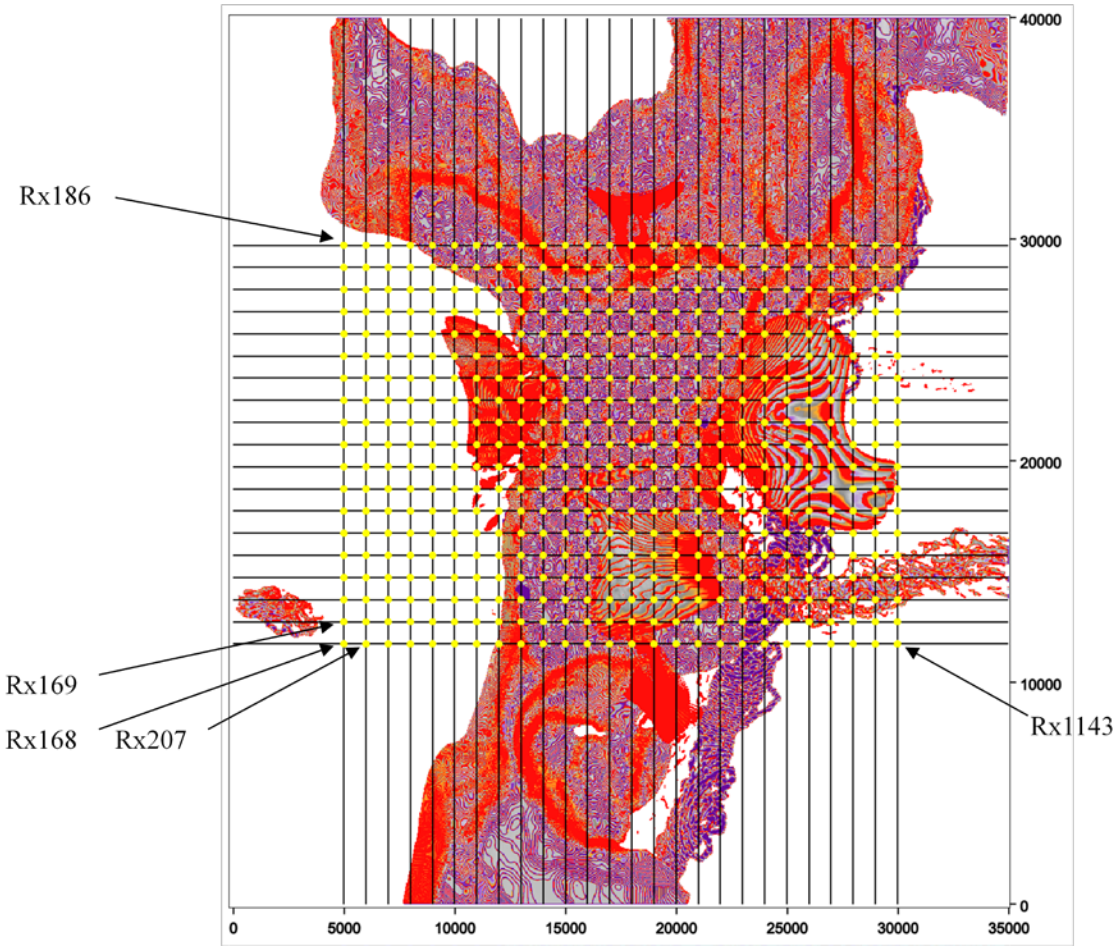

Figure 5-4. CSEM source towline numbering scheme. Towlines for each receiver extend 10 km North, South, East, and West of the receiver position or to the model boundary if the boundary is within 10 km of the receiver. Yellow dots show receivers. Black lines show towlines. Tx001, Tx002, etc. are the towline numbers.

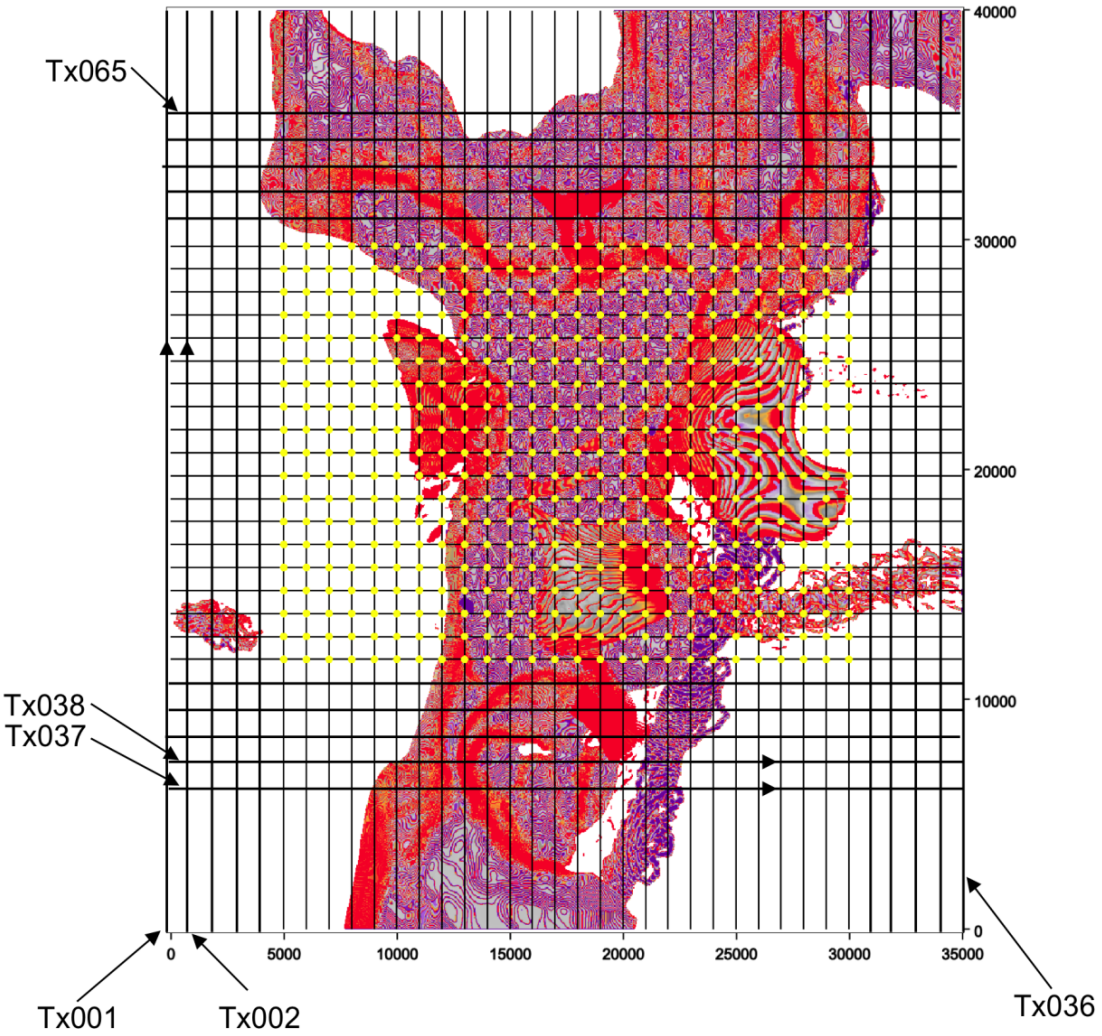

Figure 5-5. Example of the comparison of CSEM simulation data provided by EMGS and by one of the SEAM participating companies. Data for receiver Rx177 are shown for 2 Hz. Sources are located along an East-West line passing through the receiver. Red line shows EMGS result and black line shows benchmark simulation result. Comparison is quite good except at offsets larger than about 6 Km to the East of the receiver where field amplitude is several orders of magnitude smaller than it is near the source. Due to the lower field values, the comparison of phases at this range is not reliable.

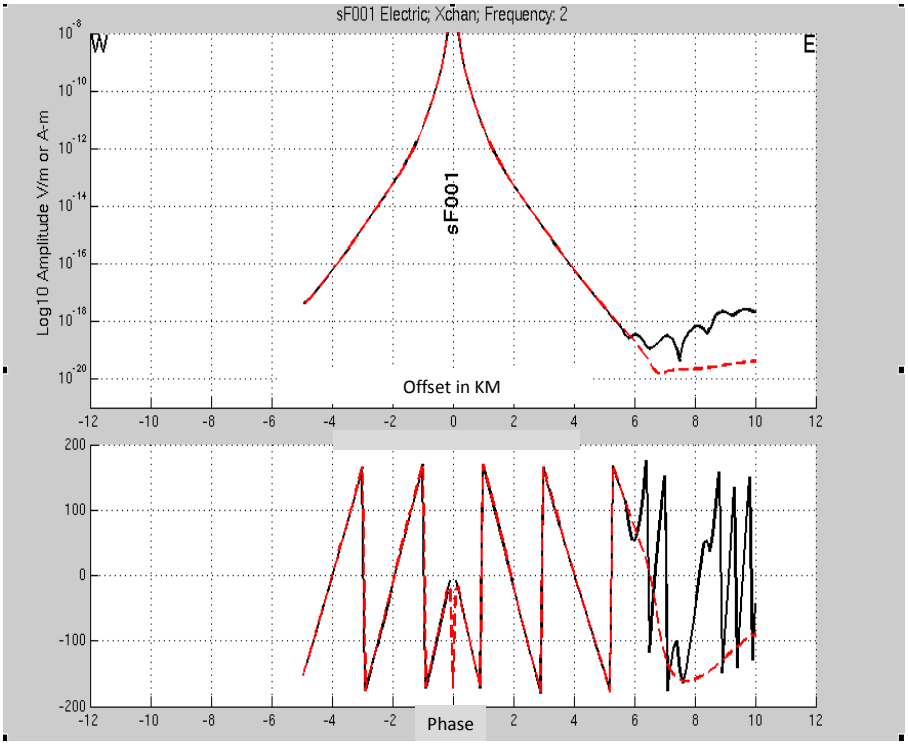

Figure 5-6. Shown are maps of cumulative reservoir thickness and 2.5 km depth vertical resistivity in Ωm for the portion of the model over which CSEM data were simulated. Also shown are maps of Log of the East-West component of horizontal electric field magnitude (E_x in V/m) at 5 km source-receiver offset. Note that log values are all negative so regions with higher field are shown in red. Source is located due West of receiver. Field is plotted at location of midpoint between source and receiver. Results for various frequencies are shown. Note the area of a relatively higher field to the east of the salt body, indicative of resistive hydrocarbon-filled reservoirs.

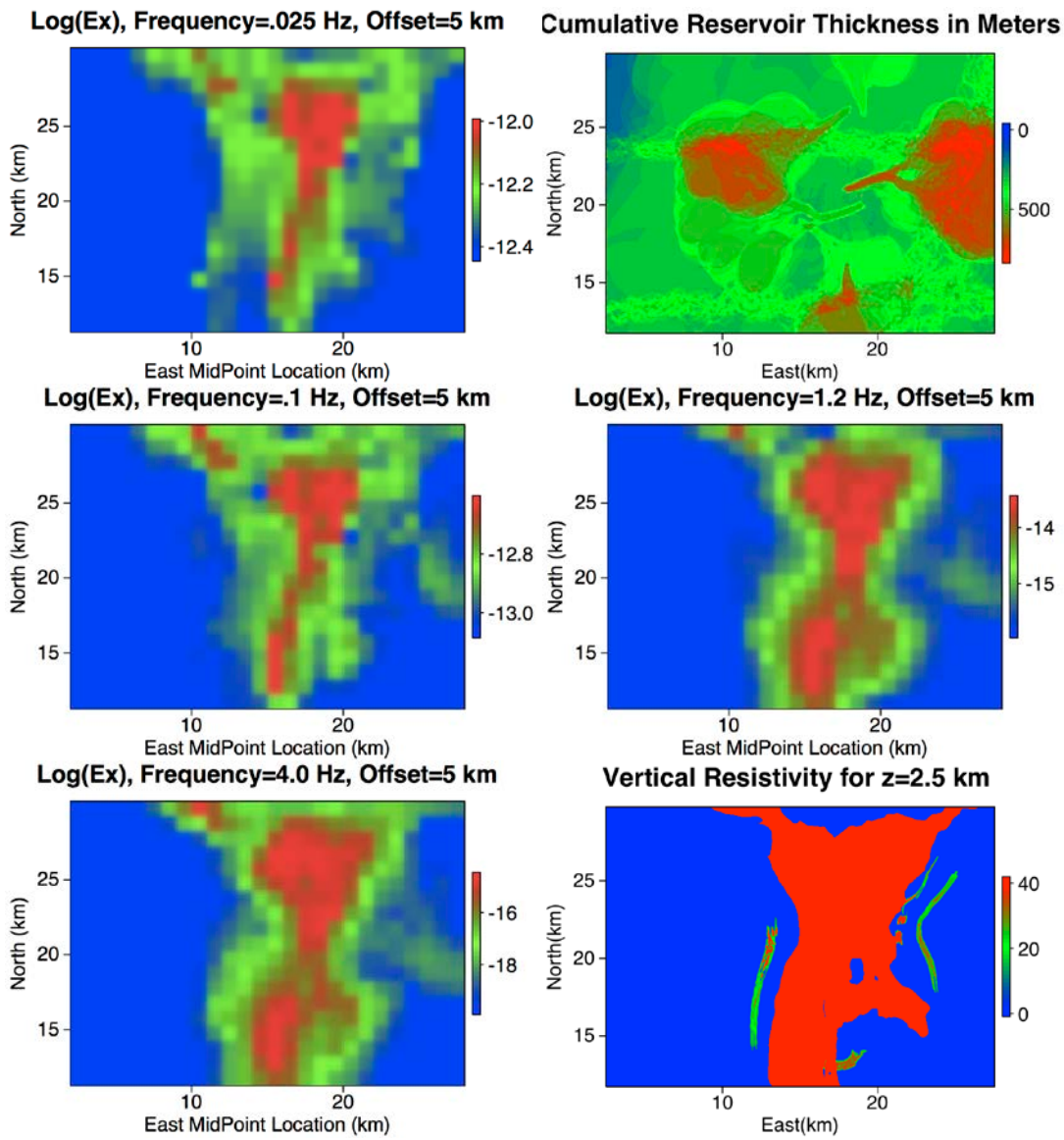

MAGNETOTELLURICS

Magnetotelluric Simulation

Magnetotelluric (MT) data, originating by measuring the natural EM field at the Earth's surface, which is a combination of the field incident on the Earth from space and the response of the Earth's subsurface to that field, have been used alone or in combination with other geophysical data to help constrain subsurface properties. Of particular note have been reports of improvements in the ability to characterize the position and geometry of the base of salt when using MT data in combination with seismic data.

The SEAM Phase I simulation involved calculating the response measured at 1326 locations on a 1 km grid spread across the seafloor of the model. The response at 20 periods ranging from 1 to 1000 seconds was simulated.

The MT response is most strongly influenced by the horizontal component of the Earth's resistivity structure. For this reason, the simulation on the SEAM Earth model used only the horizontal component of resistivity. A vertical cross section through the horizontal resistivity model is shown in the CSEM section.

Since MT is a low-frequency, low spatial resolution method, SEAM provided vendors with a resistivity model that was sampled on a 40 m by 40 m by 20 m (Vertical) interval. This model was obtained by decimating the original 20 m by 20 m by 10 m model. The small model made transfer of the model to vendors more convenient. The range of resistivity values in the horizontal resistivity model is .3 Ohm-m to 392 Ohm-m, with salt having a resistivity of 100 Ohm-m and water having a resistivity of .3 Ohm-m.

Receiver Positions and Numbering

Data for a total of 1326 receivers were simulated. Receiver positions within the simulation grid are shown in Figure 6-1. Receivers are located on a grid with 1000 m spacing in the East and North directions. For the MT simulation, receivers cover most of the model. Receiver numbering is identical to that used for the CSEM simulation. Thus, a receiver at a given location in the CSEM and MT simulations has the same number for both simulations. For MT, receivers extend from 1000 m to 34000 m East and from 750 m to 38750 m North over the model making a 34 by 39 point grid.

Receivers were positioned on the seafloor. An ascii table showing receiver number, receiver position and seafloor depth at the receiver position was provided to vendors with the model disk. Seafloor depth is taken to be the first depth at a given location where resistivity is > .3 Ohm-m (e.g. water resistivity). Since positions of receivers are not located at grid points, depths of receivers are taken at the nearest grid point to the

receiver, which is 10 m North of the receiver position. Figure 6-2 shows a map of seafloor depth.

Data were simulated for the following 20 periods (in seconds):
1000, 700, 500, 350, 250, 180, 125, 90, 60, 45, 30, 20, 15, 10, 8, 6, 4, 3, 2, 1

Output Data

The output of the simulation is the complex impedance Tensor and the Tipper matrix at each seafloor receiver. These relate the magnetic and electric field on the seafloor. The impedance tensor is not necessarily symmetric. The complex Tipper Vector relates the vertical component of magnetic field to the two horizontal components. These were computed following Mackie and Madden, (1993). We now give a description of how these were computed.

For each frequency, two simulations were done, one with an incident E_x and one with an incident E_y from infinity.

Impedances are complex values given by Z_{xx}, Z_{xy}, Z_{yx}, Z_{yy} where from field measurements

$E_x = Z_{xx}*H_x + Z_{xy}*H_y$
$E_y = Z_{yx}*H_x + Z_{yy}*H_y$

Tipper is a complex value given by
$H_z = T_x*H_x + T_y*H_y$

All fields are measured at the receiver.

Z_{xx} Z_{xy}, Z_{yx}, Z_{yy} are components of the complex impedance tensor.

T_x and T_y are elements of the complex Tipper vector

To calculate impedances

Simulation with incident E_x
Measure E_x1, E_y1, H_x1, H_y1, H_z1 at receiver
$E_x1 = Z_{xx}*H_x1 + Z_{xy}*H_y1$
$E_y1 = Z_{yx}*H_x1 + Z_{yy}*H_y1$

Simulation with incident E_y
Measure E_x2, E_y2, H_x2, H_y2, H_z2 at receiver
$E_x2 = Z_{xx}*H_x2 + Z_{xy}*H_y2$

$E_y2 = Z_{yx}*H_x2 + Z_{yy}*H_y2$

This gives 4 equations 4 unknowns
solve for Z_{xx}, Z_{xy}, Z_{yx}, Z_{yy}
note that these are complex values

For Tipper
$H_z1 = T_x*H_x1 + T_y*H_y1$
$Hz2 = T_x*H_x2 + T_y*H_y2$

2 equations, 2 unknowns
solve for T_x and T_y

Output Data Format

Data were output in the MT/EMAP SEG standard. One output file was generated per receiver so a total of 1326 files were generated. The format is described in *The Society of Exploration Geophysicists MT / EMAP Data Interchange Standard www.seg.org/documents/10161/77915/seg_mt_emap_1987.pdf*. The MT/EMAP standard provides a lot of capability for variation. Thus, SEAM provided a description of the data format, which was assumed to conform to the standard. The format is described in an ascii file included with the data distribution.

Simulation Issues

SEAM conducted vendor qualification in a manner consistent with all other simulations. Vendors were asked to provide example simulations that were then compared with a SEAM benchmark simulation conducted by one of the SEAM participating companies. SEAM found excellent agreement between simulations provided by the two vendors that were contracted to conduct the simulations and the SEAM benchmark simulation. Two vendors were selected to conduct the simulation. The reasons for choosing two vendors were (1) the two selected vendors conduct the simulations in very different manners as described below, (2) the cost of the MT simulation was relatively small, (3) having two simulations allowed a comparison of the results from the two vendors as a QC test, and (4) having two vendors allows for a comparison of the methodology for dealing with the boundary conditions at the edge of the SEAM model.

The two vendors selected to conduct the simulations were EMGS and Fugro. Fugro was subsequently bought out by CGG so we will refer to them as CGG in this discussion. EMGS conducts their simulations in the time domain and obtains results in the

frequency domain by Fourier transform. EMGS uses an absorbing boundary condition at the edges of their simulation grid. CGG conducts their simulations in the frequency domain. They extended the SEAM model beyond its boundary to minimize the effects of the boundary on their simulations. Both CGG and EMGS provided complete reports about their simulations. These reports are bundled with the data distributions so we will not provide extensive information from their reports. Both reports describe the simulation methodology, their methods for dealing with the model boundaries, and their methods for conducting QC on the simulation data prior to delivery to SEAM.

Figure 6-3 shows an example of data for one period (20 seconds) calculated by CGG and EMGS. The plots are on identical scales. The comparison between the two results is quite good indicating that even with the differences in computational methodologies and treatment of boundary conditions, the two vendors simulations are very similar. It should be noted that CGG used a coordinate system that is different from that of EMGS. CGG has the x component pointing North and Y pointing East whereas EMGS has x pointing East and Y pointing North. In addition, the results from the two vendors are in different units. To adjust the amplitude of the CGG results to scale like those of EMGS, multiply CGG results by $4*pi*10^{-4.0}$.

Data Distribution

The data distribution containing the MT simulation contains several files. One, EMGS.tar.gz is a gzipped tar file with the results provided by EMGS. Another file, Veritas.tar.gz, is a tar file with the results from the CGG simulations.

CGG included a version of the decimated resistivity model that they used for their simulations. That model is included in the folder containing their simulations.

The tar file named Specifications.tar contains the Technical specifications that were used in the bidding process for the simulations. This document provides information about source configuration, receiver locations, parameter definitions, and data output format.

Note that CGG provided data in two output formats: one conformed to that specified by SEAM, which was meant to mimic MT/EMAP SEG standard format. CGG also provided data in what they consider to be a format that is in closer agreement with the MT/EMAP format.

File model.tar.gz is a gzipped tar directory containing the model and the seafloor depths at each receiver position that was provided to simulation vendors. The model file is binary and the format of the file is contained in a README file within the tar file.

Note that all tar files are compressed with gzip and hence have suffix .gz

Figures

Figure 6-1. MT Receiver numbering. A receiver at a given location in the CSEM simulation has the identical number in the MT simulation.

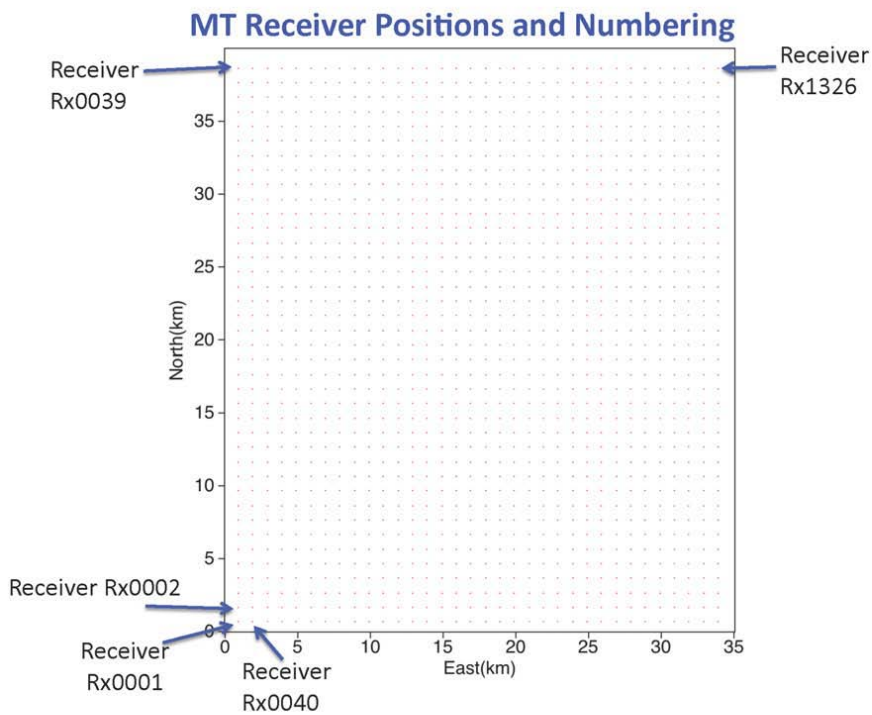

Figure 6-2. Seafloor depth in meters in the SEAM resistivity model.

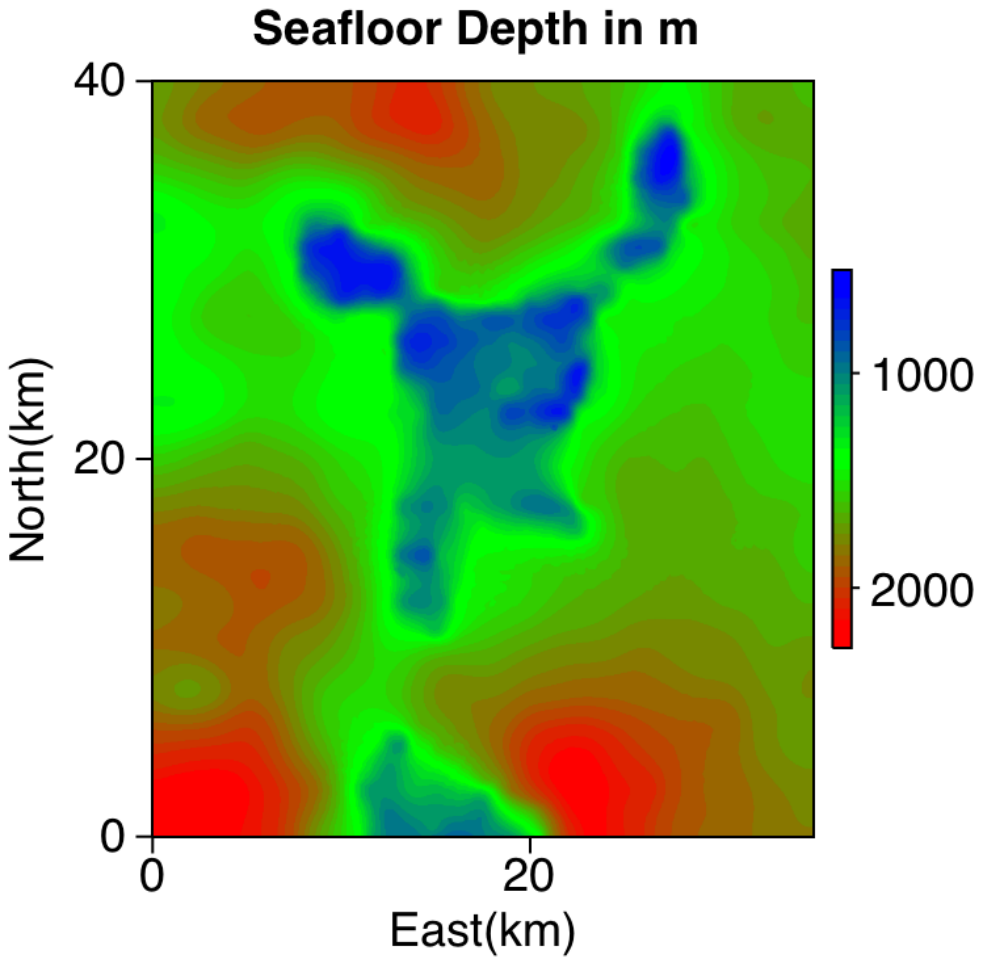

Figure 6-3. Example of MT simulation results. Data from CGG (below) and EMGS (top) are shown. The values of the impedance tensor component Z_{xx} is plotted as a function of position on the SEAM model. CGG data have been rotated and scaled to match the convention used by EMGS.

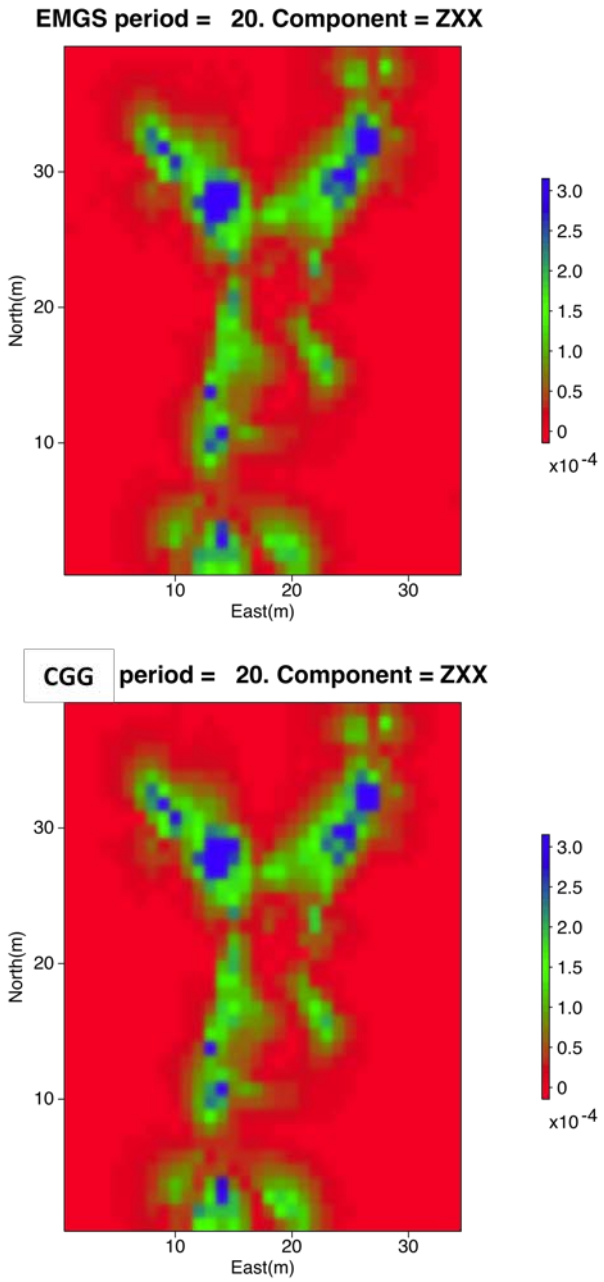

QUALITY CONTROL

QC of Seismic Simulations

This section covers QC of the seismic simulations; e.g. those for the Absorbing Upper Surface (AUS), Tilted Transverse Isotropy (TTI) and Elastic models. QC for non-seismic simulations is discussed in the sections where those simulations are described.

There were four levels of QC implemented to ensure the integrity of the seismic simulations. These were (1) Vendor qualification, (2) QC conducted by the vendor before they delivered data to SEAM, (3) QC conducted by a vendor under contract with SEAM and (4) evaluation of data by the Technical Program manager.

The approach and results for each level of QC evaluation will be described separately. The QC conducted for each simulation benefited from lessons learned from the previous simulations. Thus, the QC on the AUS data benefited from what we learned in the SEAM Phase I acoustic simulations, the QC on the TTI simulations benefited from what was learned from the AUS simulations, etc.

Even with evolving, and hopefully improving, QC procedure, it is not possible to define a comprehensive QC evaluation methodology that catches all possible problems with such a large and complex set of data as those generated during the SEAM project. Decompressed data sizes were on the scale of 10's to 100's of TB so manual evaluation of all data is not feasible. Thus, QC procedures were developed to ensure that the simulations were not contaminated by unexpected numerical noise, that header information was complete and correct, and that shots were at the reported location.

Additional information about QC strategy and procedure is given in the SEAM Phase I Report (Fehler and Keliher, 2010).

Vendor Qualification

Vendor qualification was a required component of each bid package. The qualification procedure was developed by SEAM to allow us to ensure that a vendor's simulation capability could perform well on simple models for which we knew the answer (homogeneous models, layered models, etc), and that vendor simulations on the SEAM model were similar to benchmark simulations available to SEAM. In addition, by asking vendors to perform simulation of one or more shots on the SEAM model, we were confident that bidding vendors had carefully evaluated the challenges involved in conducting simulations on the model before they submitted their bids.

For the AUS simulation, no vendor qualification was conducted because the AUS simulations were an extension of the simulations that were conducted during the SEAM Phase I project and the AUS simulations were conducted by the same vendor as was used for the previous simulations.

For TTI, we were concerned not only with the numerical capability of the vendor but also to confirm that they had correctly interpreted our presentation of the model. We thus asked bidding vendors to provide us their simulations on a homogeneous TTI model that we gridded in a manner identical to the manner that the SEAM TTI model was gridded. We evaluated these simulations not only for dispersion characteristics (e.g. minimal dispersion over the modeled frequency band) and the quality of the non-reflective boundary conditions, but we also evaluated the relative position of the wavefront as a function of time *vs.* what we expected for the model. With this test, we found that one vendor misinterpreted our definition of the axis of symmetry. While this did not disqualify this vendor, it provided us important information for our subsequent discussions with the vendor.

Since SEAM did not have access to a benchmark simulation on the TTI SEAM model, we resorted to comparing the vendor simulations on the SEAM model with those conducted on the isotropic model during SEAM Phase I. Figures 7-1a and 7-1b show East-West shot gathers through the source for shot 12873. Figure 7-1a shows the simulation for the isotropic acoustic model and Figure 7-1b shows the simulation on the TTI model. By overlaying these plots, we were able to determine that a majority, if not all, phases present in the acoustic simulation were present in the TTI simulation. The arrival times for the phases are slightly different as expected and the relative amplitudes are also different.

For the elastic simulations, the vendor qualification involved simulating an elastic layered-medium model in addition to simulating one shot on the SEAM model. We were able to compare the results provided by vendors on the layered medium model with those that the Technical Project Manager obtained by using reflectivity, which is a well-known and mature method for simulating wave propagation in layered elastic media.

Figures 7-2a and 7-2b show example vertical-component acceleration traces in the layered-medium model as simulated by SEAM (labeled Axitra for the name of the public-domain code that was used for the reflectivity simulations) and by the winning simulation vendor Advanced Geophysical Technologies (AGT). Traces from one of the wellbores are plotted. This wellbore is in a region where the water depth is about 1650 m so traces at depths less than 1650 m were recorded in water and those below 1650 m were recorded in the solid earth. The vertical component traces shown in Figure 7-2 show a good comparison between the benchmark reflectivity simulation and the AGT simulation. However, while the East-West component of acceleration, shown in Figures 7-3a and 7-3b compare well at locations away from the seafloor, they do not compare well near the seafloor. This is because the horizontal component of motion changes sign

upon crossing the seafloor-sediment boundary. Slight differences in receiver position relative to this boundary can yield large changes in amplitude. Reflectivity allows the exact positioning of a receiver within a model. With finite difference, the receiver may be located exactly at a boundary or it may be located slightly away from the boundary. In a model with rough seafloor topography, it is impossible to place a receiver exactly on the seafloor in a finite difference simulation using a regular grid. SEAM deemed the uncertainty of the position of the seafloor and VSP receivers relative to the seafloor was a problem that could not be resolved in sufficient time to allow us to conduct production simulations, We thus proceeded with simulations in spite of the potential uncertainty about the location of receivers relative to the seafloor.

To check the quality of vendor simulations on the SEAM elastic model, SEAM contracted with Sandia National Laboratories to conduct benchmark simulations on the SEAM model. Dave Aldridge and Leiph Preston conducted the simulations and provided advice about elastic simulation issues. Sandia is highly respected for their numerical seismic simulation capability. Their code is a low-order finite difference code and thus requires a small model grid spacing to keep numerical dispersion within acceptable limits and to guarantee reliability of the resulting simulations. The comparison between the Sandia simulations and the AGT simulations for the surface pressure records was extremely good. If we had decided to collect only surface seismic data for the elastic model, the AGT simulation would be considered to be acceptable. However, when we compared traces at the seafloor, we noted that, while major characteristics of the simulated traces were correct, there were some notable differences. Figures 7-4a and 7-4b illustrate the differences.

The slow wave found on the Sandia simulation in Figure 7-4a has been identified as a Scholte wave, which is a phase that propagates slowly along the seafloor and whose amplitude decreases exponentially away from the seafloor. Figure 7-4b shows the existence of what appears to be spatially-stationary noise on the AGT vendor qualification simulation. We have attributed this noise to numerical noise that is localized near regions where there are abrupt changes in seafloor topography. The abrupt changes lead to a stair-stepping of the seafloor boundary when the model is gridded. A finite difference simulation using a finite difference code at MIT gave nearly the same spatially varying noise as is present in the AGT simulation. SEAM decided that this noise could not be easily eliminated from the production simulations and decided to proceed even knowing that there would be problems with the seafloor data. While Sandia was able to eliminate this noise in their simulations, their code is far too computationally expensive for it to be used for conducting simulations on more than a handful of shots.

QC Conducted by Simulation Vendors

SEAM required simulation vendors to provide a review plan for their own internal evaluation of data prior to delivery to SEAM. The procedures used for these internal reviews will not be repeated here. The approach used by AGT for both the TTI and Elastic simulations is described in their reports on these two simulations. The approach used for the AUS simulations was similar to that used by AGT.

QC Conducted by a QC Vendor

SEAM contracted with an independent vendor (e.g. not the same one who was selected to conduct the simulations) to conduct a SEAM specified evaluation of all data delivered to SEAM by the simulation vendors. The motivation and main elements of the QC procedure are described in the SEAM Phase I report that is available to the public. Here we provide the procedure used for evaluation of the elastic data set. The QC for the AUS and TTI data sets was similar.

Evaluation Specifications for Near-Surface Trace Data

Decompression

Near-Surface data were provided in compressed format. Surface data had been compressed by the simulation vendor. SEAM provided the compression/decompression algorithm to QC vendor at no charge. The decompression algorithm writes a SEGY file containing surface trace data.

The QC Vendor was to determine reasonable tolerance to use for setting alerts while scanning the data. This was done in consultation with the SEAM Technical Project Manager during the initial phase of the QC evaluation.

Trace Data Evaluation

Read all shot records:

1. Verification of complete file decompression: Record file size (bytes) of decompressed SEGY file and compare with sizes of adjacent shots. Report shots whose file size varies by more than 5% from adjacent shots.
2. Verification of correct amplitudes: Measure amplitude of the traces located at exactly 990 m from the source using the following approach: (a) extract portion of record from .664 to .984 seconds from the beginning of the shot record. This portion contains 41 points and includes the direct wave through the water. (b)

Square the extracted data. (c) Sum the squared data points. (d) Divide by 41. (e) Take the square root. The expected value is 100. Report departures of this value of more than 1%; e.g. the value is < 99 or > 101. This measurement was to be made on up to 4 traces for each shot. The number of traces depends on the location of the shot relative to the model boundary.

3. Verify the Source is correctly located by examination of trace that is located closest to shot or at shot location and checking that first break time is consistent with shot and receiver locations. Confirm the travel-time of the water-bottom reflection pulse for this trace. (A binary file containing water depth *vs.* position on a 20 by 20 m grid that was provided by SEAM.
4. Verify that earliest arrival for all traces delivered for a given shot is on the trace closest to the source.
5. Verify receiver increments and correct receiver locations by examination of trace headers; verify that all traces provided are in agreement with traces required for shot as specified in the acquisition plan.
6. Determine maximum amplitude within shot gather along with trace and sample number where maximum amplitude occurs in shot gather. Store these data. Compare with those stored for other shots (may be done using 2D cross-section contour plots). Note and report anomalous results.
7. Determine amplitude minimum, maximum, and average of the absolute values of the last 125 samples of data in each trace. Store results and compare with other shots. Report anomalous results.
8. Compute midpoint fold distribution. Make a plot showing fold *vs*. midpoint position. Compare with expected results. This plot will be cumulative and include all shots previously analyzed.
9. Collect zero-offset traces from each shot into a separate segy file. Plot representative zero offset gathers and examine for spatial consistency of events.
10. For shots that are replaced to correct issues identified during QC, plot the zero offset trace as part of a gather of zero offset traces of adjacent shots on a scale that allows the continuity of the events in the gather can be compared. Provide plots as part of report.

For each 2 TB Shot Set create a report containing:

a. Map showing locations of shots analyzed
b. Map showing locations of shots and traces for which alerts were identified
c. Description of communications with SEAM Project Manager about alerts and statement of actions taken to correct data that resulted in alerts
d. Identify alerts that require data to be reshot
e. Map showing average amplitudes determined in (7) above for each shot.
f. Cumulative map for all data examined to date.
g. Perform zero-offset migration of all available zero offset traces collected to date as described in #9 above. Include representative plots of these migration results compared with input velocity model.

Evaluation Specifications for VSP Trace Data

VSP data consist of four components of motion for 467 locations along vertical lines representing wells. For each shot, data from each well is provided in a separate segy file. VSP data are not compressed.

QC for VSP data consists of the following:
1. Verify source at correct location by examination of header information about source location.
2. Verify receiver increments, correct locations, and correct components of motion for all receivers based on required VSP receiver geometry for each well and each shot.
3. Verify that data for all wells required for shot are included in delivery. Make a cumulative map for each well of the shot locations for which data have been evaluated.
4. Determine maximum amplitude for each component of motion in each well along with trace and sample number where maximum amplitude occurs for each shot. Store these data. Compare with those stored for other shots. Note and report anomalous results.
5. Determine amplitude minimum, maximum, and average of the absolute values of the last 125 samples of data in each trace. Store results and compare with other shots. Report anomalous results.

VSP Reporting
1. For each well, a map showing cumulative (e.g. current set of shots and previous shots analyzed) locations of all shots recorded.
2. For each well and each component of motion, a map showing the maximum amplitudes for each shot determined in #4 in the VSP Shot Record Verification Process above. Average amplitudes are to be plotted at each shot location for each well.
3. Description of any alerts raised from analysis of VSP data.

Evaluation Specifications for Seafloor Trace Data

Seafloor data consist of four components of motion for up to 42,036 trace locations for each shot. For each shot, data from each component of motion (pressure, Vertical Acceleration, East-West Acceleration, and North-South Acceleration) are provided in a separate segy file. Seafloor data are not compressed.

Seafloor Shot Record Verification Process
1. Verify source at correct located by examination of header information about source location.
2. Verify receiver increments, correct locations, and correct components of motion for all receivers based on required Seafloor receiver geometry for each component of motion and each shot. Verify that all required trace data are present.

3. Determine maximum amplitude for each component of motion along with trace and sample number where maximum amplitude occurs for each shot. Store these data. Compare with those stored for other shots. Note and report anomalous results.
4. Determine amplitude minimum, maximum, and average of the absolute values of the last 125 samples of data in each trace. Store results and compare with other shots. Report anomalous results.

QC Conducted by Technical Project Manager

The Technical Project Manager communicated regularly with both the simulation and QC vendors. Before simulation of each data set was allowed to proceed, the Technical Project Manager was provided example results of simulations for evaluation. The example results were visually inspected by examining representative plots of the trace data. Header values were spot checked for conformity with the SEAM specifications. Finally, scaling of the traces was compared against the proscribed standard.

Once simulation was underway, data were provided to the Technical Project Manager at the same time that they were provided to the QC vendor. The Technical Project Manager examined representative plots of the data and examined header values. He also interacted with the QC vendor to provide an additional evaluation of issues that were identified by the formal QC conducted by the vendor. One lesson learned from the SEAM Phase I simulation was that it is essential for the Technical Project Manager to have a copy of all delivered data so he can make an independent evaluation of issues identified by the QC vendor.

Issues Identified During QC

The main issue that occurred during all the seismic simulations was corrupted data files on the disks delivered to SEAM. We had found this problem during Phase I simulations as well. Beginning with the TTI simulation, AGT recommended that they perform an md5sum on each delivered file and that this be used to check the integrity of the data by subsequent users of the data. Md5sum is an algorithm that produces a digital fingerprint of a file in the form of a string of numerical and alphabetic characters. For example 25e83686e9195b4947b473155289f4e0 is the result provided by the mds5um algorithm for file Elastic_Shot15220.Comp0.SEAFLOOR.sgy. The md5sum value is stored directly in the directory with the data files. Thus running md5sum on a data file will allow all future users of the SEAM seismic data (TTI and elastic) to verify that they have a correct version of the data as provided by AGT. When data files were found to be corrupt on the disk provided to the QC vendor by the Simulation Vendor, the data were replaced with new copies of the data provided by the Simulation Vendor.

Issues with AUS Simulation: Two issues were found with small parts of the AUS data delivery. The first one was corrupt files on the disk delivered to SEAM. These files were

replaced and the replacement data were run through the QC procedure. The second problem had to do with the tolerance of the first break at 990 m. The amplitudes were supposed to be measured using the SEAM standard and the values were to be within 1% of the expected value. For a small number of shots, the values exceeded the 1% threshold by a few hundredths of a percent. Since the AUS simulation was the first one for which we checked these values, we relaxed our threshold for concern to be slightly greater that 1%.

Issues with TTI Simulation: The TTI simulation proceeded quite well. The main QC issues identified were corrupt files and these were replaced by AGT. A small number of shots were found to have numerical instabilities. The instabilities were not observed on the surface traces as the origin of the instabilities was deep in the model and they occurred late in the simulation. Instead, the instabilities were identified on the VSP traces. The instabilities were found to occur at the model boundaries and were considered to have been caused by numerical issues associated with the non-reflective boundary conditions. The shots with these problems were simulated again using a more conservative, but computationally slower version of the non-reflective boundary condition. The instabilities were not observed in the revised simulation data. The revised data replaced data from the initial delivery that had the instability.

Issues with Elastic Simulation: As for other simulations, the main issue identified with the elastic simulation data was corrupt data files. These files were replaced. Another and potentially more serious problem was traced to an undetected hardware problem with the computer used to simulate the elastic data. One of the GPUs employed in the simulation had some problem that resulted in small but detectable noise in the simulation data on a number of traces for a small number of shots. The problem was detected on the VSP traces for the affected shots. Both the simulation vendor (AGT) and the elastic QC vendor (Nanoseis) went to considerable effort to identify which shots were plagued by this problem. The shots identified as bad were replaced.

QC on Classic Data Sets Composed of Selected Traces from Selected Shots

For all seismic simulations, selected traces from selected shots were extracted and used to form WAZ and NAZ classic data sets. Following the procedure used for the SEAM Phase I acoustic simulations, no QC was conducted on the data set extracted from the AUS simulation. This was the chosen approach since the traces had already been evaluated as part of the entire shot set. Unfortunately, the delivery of the Phase I acoustic simulation classic data set was found to be significantly incomplete. Thus, a more rigorous QC was conducted for the AUS, TTI and Elastic WAZ and NAZ classic data sets. For the AUS, this involved a visual inspection of selected trace gathers by the Technical Project Manager and a check on the completeness of the data set by checking to ensure that ***every*** trace from ***every*** shot contributing to the classic data set was correctly included in the data set. For TTI, a similar evaluation was conducted by WesternGeco working under contract to SEAM. WesternGeco also evaluated trace

amplitudes and made near-offset gather plots to ensure that the data were visually correct. For the elastic WAZ and NAZ classic data sets, the evaluation was done by elastic QC vendor Nanoseis. Their procedure was similar to that employed by WesternGeco in their evaluation of the TTI WAZ and NAZ classic data sets.

Figures

Figure 7-1. East-West shot gathers passing through the source position for Shot 12873 in the acoustic simulation (a) and for the TTI simulation (b). Plots like this were used as part of the vendor qualification procedure for the TTI simulation. The plots show remarkable similarity in spite of the simulations having been conducted by independent vendors. Notable differences are slight changes in arrival time and amplitudes of events. The source insertion approach used in the two simulations was quite different and this resulted in differences in the gathers for the first few seconds of the simulation at locations near the source.

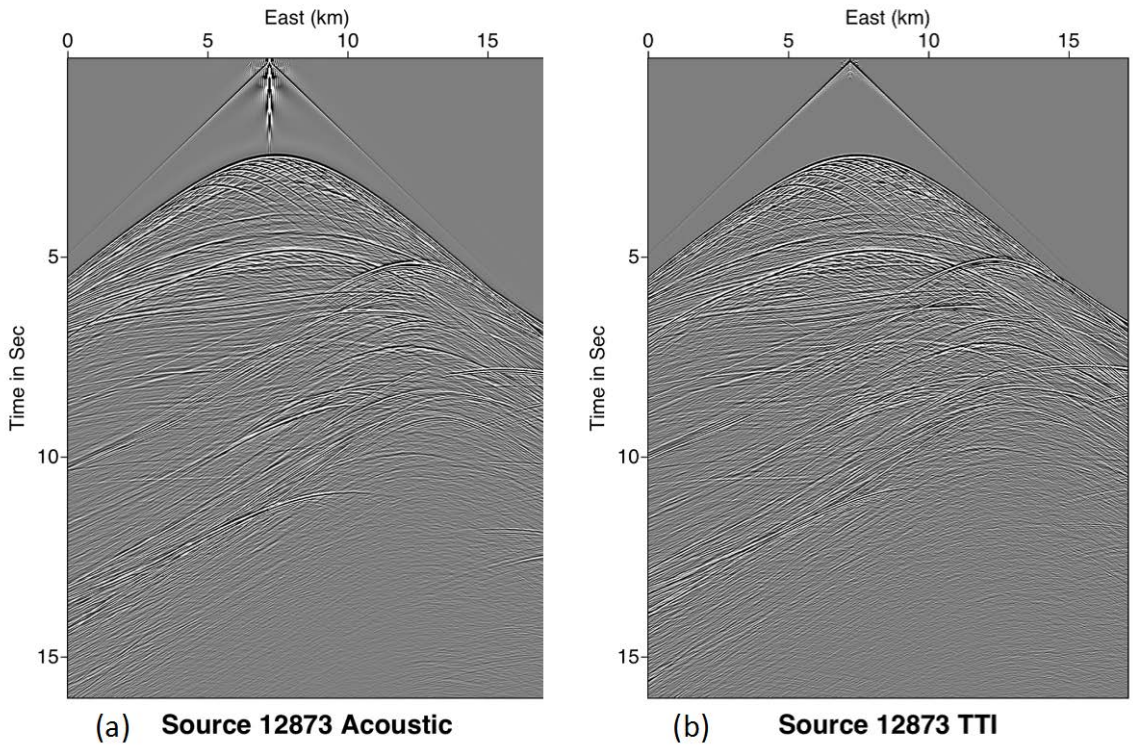

Figure 7-2. Traces resulting from simulations conducted on a layered elastic vendor qualification model using reflectivity (a) and by simulation vendor AGT (b). These traces are for the vertical component of acceleration measured along a vertical line that penetrates the seafloor located at a depth of 1650 m. Receiver depth in meters is given next to the right hand side of each trace.

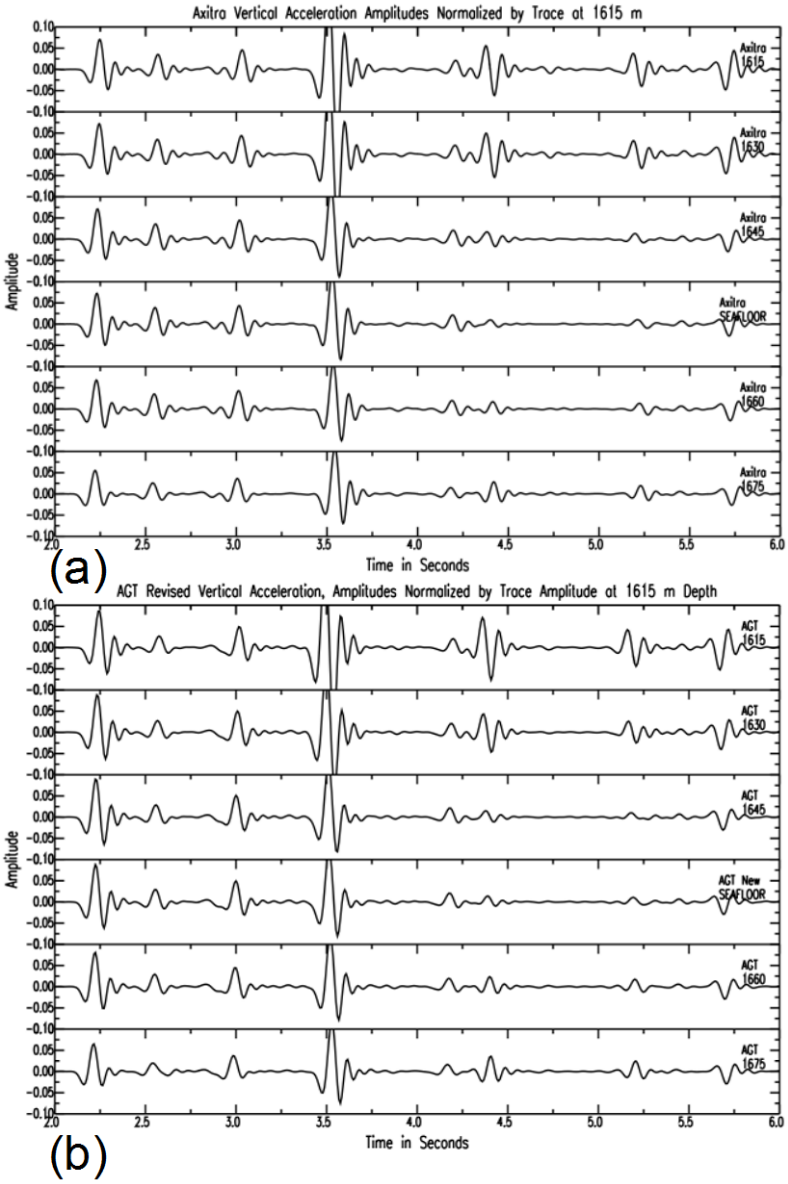

Figure 7-3. Same as Figure 7-2 except that the East-West component of acceleration is plotted.

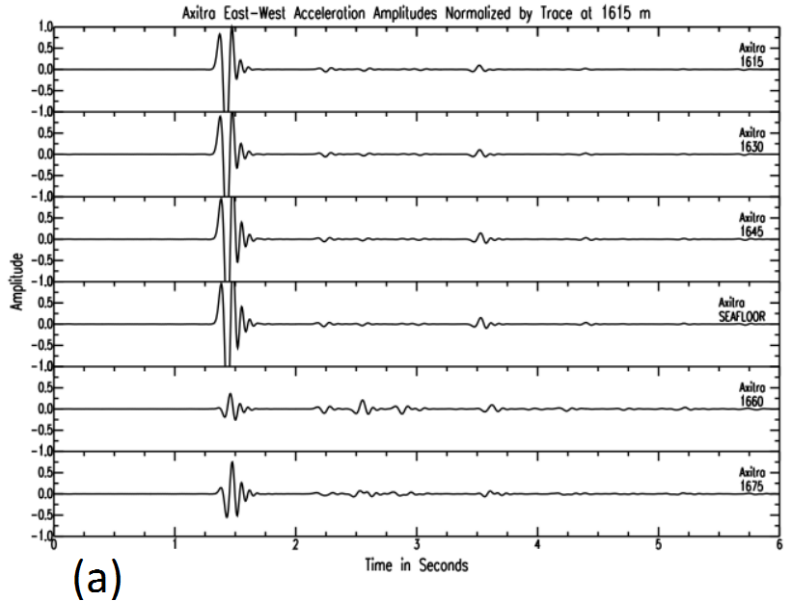

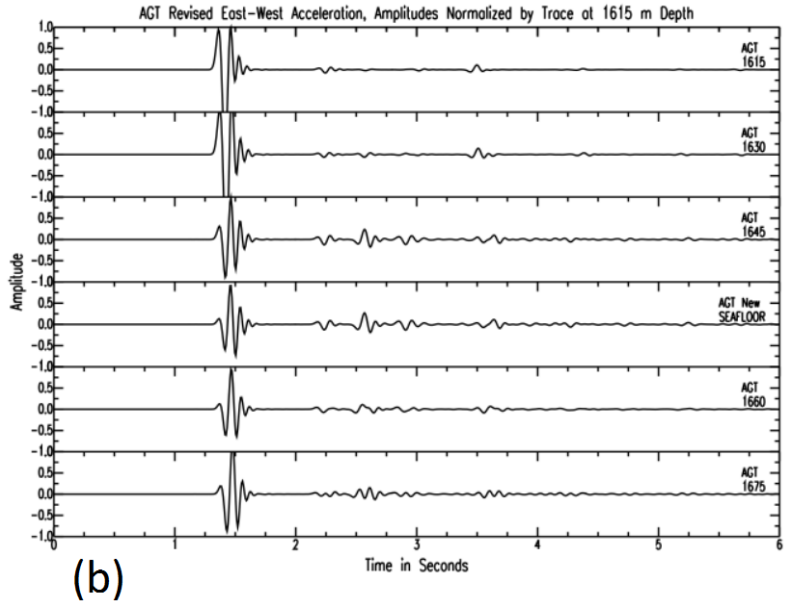

Figure 7-4. East-West gathers for simulation on the seam elastic model conducted by Sandia National Laboratories (a) and AGT (b). The pressure on the seafloor is plotted. The Sandia simulation did not cover as large a portion of the model as did the AGT simulation. Images are scaled so that overlapping portions of the gathers from the two simulations are the same size.

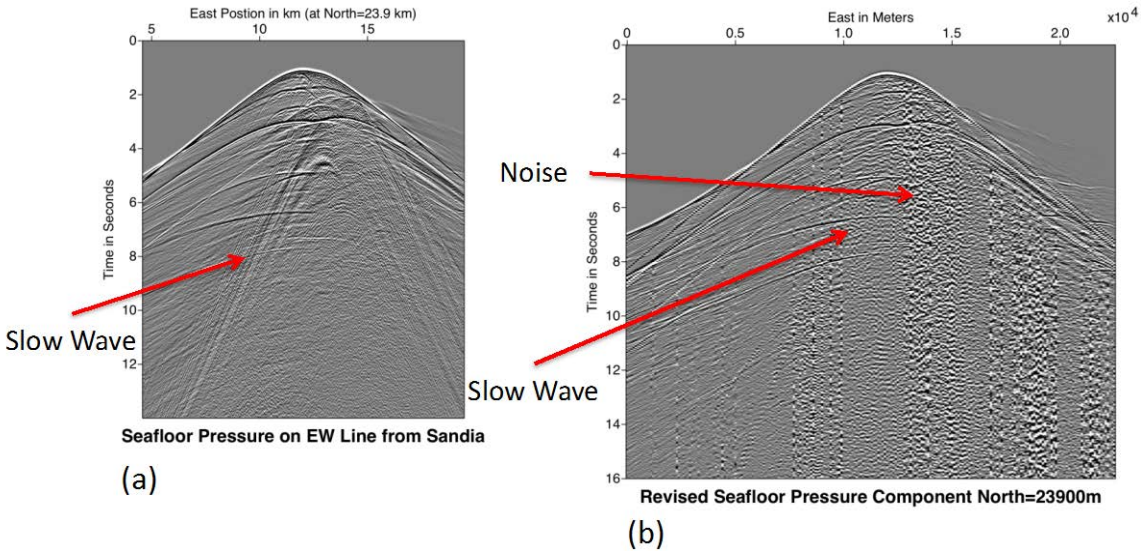

DATA COMPRESSION

The volume of data generated by the SEAM Phase I RPSEA project was substantial. If data had not been compressed, the total data volume would have been between 200 and 300 TB. By current standards, this is a data set that would be expensive and cumbersome to store and distribute. During the SEAM Phase I Project, the decision was made to compress all seismic data. By compressing the data, we were able to reduce the data volume to approximately 20 TB with little loss of data quality. The compression code used in Phase I was provided by Landmark and the decompression code was made available to all SEAM data users free of charge. The SEAM Phase I Report includes a comprehensive evaluation of the compression code and gives examples of how the data are altered by the compression and decompression. The compression is lossy but it was agreed that the quality of the data was not significantly degraded compared to numerical errors in the data introduced during the simulation.

The compression code used in SEAM Phase I compressed shot gathers by a factor ranging from 8:1 to 10:1 depending on the spatial variation in the seismic traces within a shot gather and the number of traces comprising the gather. Less spatial variation leads to a bigger data compression ratio.

For SEAM Phase I RPSEA, it was decided to continue using the compression and decompression algorithms that had been used in Phase I. The decision was also made to compress only the surface traces since the trace spacing was small which meant that the spatial variation in trace character was not large enough to limit compression quality. Initially, using the same decompression code that was used for SEAM Phase I made good sense since the first two seismic simulations conducted by SEAM for the RPSEA-funded project (Absorbing Upper Surface -AUS and Tilted Transverse Isotropy - TTI) had shot and surface receiver geometries that were exact duplicates of those used in SEAM Phase I. For the VSP data collected during the TTI acquisition, the small data volume led us to decide to not compress these data.

The compression ratio on the VSP data would likely not have been large since one component of motion for one shot gather in a given well, which would make a logical set of data to compress, contained only 467 traces compared to more than 400,000 that were collected for most surface trace data sets. The surface-recording data volume for one shot in the TTI simulation was close to 3.5 GB. This would compress to a data volume of about 350 MB. The VSP data volume for one shot recorded in all four VSP wells was approximately 60 MB.

For the elastic simulation, the decision was made to compress only the surface trace data. Seafloor and VSP data were not compressed. Since the elastic acquisition geometry for one shot in the elastic simulation was different than that for previous simulations, SEAM performed tests of the compression code on example elastic data

sets prior to proceeding with compressing the surface trace elastic data. The tests were made to confirm that the decompression code performed well on the elastic data set and that data quality was not significantly degraded.

SEAM also decided to compress the AUS and TTI WAZ and NAZ classic data sets. Before making that decision, tests were performed to investigate the impact of compression on those data.

SEAM decided to not compress the elastic WAZ and NAZ data sets. In fact, the traces in these data sets were extracted from full shot gathers that had never been compressed. This means that compression/decompression has had no impact on these data. There were two reasons that SEAM decided to not compress the elastic WAZ and NAZ classic data sets, which at the outset seems counter to the choice made for the Acoustic, AUS and TTI WAZ and NAZ classic data sets: (1) The elastic WAZ and NAZ classic data sets were constructed from about ¼ the number of shots that were used for the WAZ and NAZ classic data sets for the acoustic and TTI simulations. The small number of shots meant that the uncompressed data volume would be less than those of the other data sets, (2) we wished to keep and distribute some data from the elastic simulation that had never been compressed so that users could compare traces from a given shot recorded at identical positions that had been compressed with these that had never been compressed. Note that all traces in the WAZ and NAZ classic data sets also occur in the full shot gather data sets that were compressed for storage.

Table 8-1 lists the various seismic data sets resulting from the SEAM Phase I RPSEA project, the approximate number of traces in what would be considered to be a logical grouping of data for compression and a column listing whether or not the data were compressed.

All data compression, with the exception of that for the TTI and AUS WAZ and NAZ classic data sets, was conducted by the simulation vendor. Compressed data were therefore delivered to SEAM. The first step in the QC process was for the QC vendor to decompress the data. The reasons for having the simulation vendor compress the data as opposed to having the QC vendor do the compression were (1) to reduce the volume of data that was delivered to SEAM and the QC vendor, and (2) to have the QC process include an evaluation of the successful compression of the data. After the QC vendor completed QC on a set of data, the original compressed files provided by the simulation vendor to the QC vendor were sent to the Data Storage and Distribution Vendor for permanent storage. The compression of the TTI WAZ and NAZ classic data sets was done by the SEAM Phase I Technical Project Manager. The compression of the AUS WAZ and NAZ classic data sets was done by the Data Storage and Distribution Vendor.

Evaluation of Compression of Elastic Data Set

We evaluated data compression for the elastic data set using the vendor qualification data submitted by Advanced Geophysical Technologies (AGT). AGT was the vendor that ultimately won the bid to conduct the simulations. Our main concern in testing the compression algorithm on the elastic data was whether the code that was used for Phase I compression was adaptable to the elastic data that had different trace geometry from the Phase I acoustic simulations. The vendor qualification data were provided to us by AGT gridded on a 15 m square grid for traces and spanning a grid of dimensions of 22,500 m East-West and 18,000 m North-South. This is the geometry that we requested for the vendor qualification. This acquisition differed from the one that was ultimately used for the elastic acquisition only in the trace interval, which was set at 25 m for the production simulations. We tested the compression algorithm on the data as provided by AGT; e.g. on a 15 m group interval. We also decimated the data to a trace spacing of 30 by 30 m and tested the compression algorithm on the decimated data.

Figure 8-1 shows an East-West trace gather that passes 30 m North of the vendor qualification shot point. Trace spacing is 15 m. When the entire shot gather was compressed, the compression ratio was 15:1. This is a much higher ratio than was obtained for the acoustic data sets. The high compression ratio was due to the small trace spacing, which reduced the trace-to-trace variability. Also, the large number of traces – more than 1.8 million gave a large data set for compression. Figure 8-2 shows the gather from Figure 8-1 after the entire shot gather, all 1.8 million traces, had been compressed and decompressed. Figure 8-3 shows the difference between Figure 8-1 and 8-2 but scaled by a factor of 100 to emphasize the differences.

Clearly there are differences. The differences are largest near the major event arrivals and are largely caused by very small phase shifts caused by the compression/decompression algorithms. The phase differences are small but even a very small phase shift leads to a visible difference when traces are subtracted.

Figures 8-4 to 8-6 show the same sequence of images as shown in Figures 8-1 to 8-3 except for the gather after the traces had been decimated to yield a trace spacing of 30 m. In this case, the total number of traces in the shot gather was reduced by a factor of 4 compared to the original data set so there were approximately 450,000 traces that were compressed. The resulting compression ratio was about 9.5:1. The smaller compression ratio is attributed to the smaller number of traces and the increased trace spacing, which meant that there was slightly less similarity between adjacent traces than in the original data set sampled at a 15 m trace interval. Figure 8-6 shows that there are detectable and systematic differences between the original data and the data that have been compressed and then decompressed. The differences are very small as indicated by the need to increase the plot gain by a factor of 100 to show the differences. Figure 8-7 shows the differences plotted on the same scale as the original

data. In this plot, there are no detectable differences except very near the source at the time it was initiated.

Evaluation of Compression of the WAZ and NAZ AUS and TTI Classic Data Sets

The NAZ and WAZ classic data sets for the AUS and TTI simulations were extracted from the full shot gathers while the gathers were being decompressed by the QC vendor during the QC process. Thus, these traces had already been compressed and decompressed one time when they were incorporated into the classic data sets. The decision was made to compress these data again as shot gathers to reduce the volume of data required for storage and distribution. The size of the compressed TTI NAZ and WAZ classic data set volume was approximately 1.4 TB. If the data had not been compressed, the data volume of more than 10 TB would have made the cost of distribution prohibitively expensive.

SEAM evaluated the effects of compression and decompression on the WAZ and NAZ classic data sets for the TTI and AUS simulations. The tests were conducted using AUS data since those data were available first. The main concern with using the compression on the WAZ and NAZ classic data sets was that there were fewer traces for each shot gather and the trace spacing was not uniform. The inline shot spacing for the data sets was 30 m but the cross-line shot spacing was up to 120 m for the WAZ classic data sets. There was concern that the large cross-line spacing might lead to poor performance by the data compression code and result in significant reduction in data quality.

The tests conducted to evaluate compression of the WAZ and NAZ classic data sets were similar to the ones described above that were conducted to test compression of the elastic surface shot gathers. Rather than repeat figures for those tests, we will show the differences in individual traces between those before compression and those after compression and decompression. Figures 8-8 and 8-9 show examples for one trace in an AUS WAZ classic data set. The upper trace in each figure is the trace before it was compressed as part of the classic data set. The middle trace is the result after compression and decompression and the lower trace shows the difference magnified by about 500. Clearly there are differences but the differences are quite small.

A final test on the decompression was to measure the mean energy in the gathers as was done in Fehler and Keliher (2011). For one NAZ shot gather, we measured the mean energy in a shot gather passing through the source. The mean was measured on the data prior to compression and on the data after compression and decompression. The mean energy values were identical to seven significant digits, e.g the precision of the measure. The mean energy of the difference of the gathers was less than 1% of that of the individual gathers.

Use of Decompression Code

Landmark has agreed to allow all users of SEAM data to use the decompression code free of charge. The code is available as a Linux executable. The code is included in a tar gzip file that contains a README. The file name is SEAM_PhaseI_Decompress.tar.gz. To access the code, execute the following Linux commands

```
gunzip SEAM_PhaseI_Decompress.tar.gz
tar -xvf SEAM_PhaseI_Decompress.tar
```

The result will be a directory called SEAM_PhaseI_Decompress that has the following files:

```
README      A file containing instructions for how to use the decompression code
SEAMdecompress.linux64      Linux executable code for decompressing SEAM data
doit.csh            Simple script to run the executable
testdir  directory where decompressed data will reside
```

As an example, the compressed data for surface traces in the elastic simulation for shot 7007 are in a directory called Elastic_Shot7007.sgy.ctk. Within that directory are 4 files as follows:

```
Elastic_Shot7007.sgy.bri
Elastic_Shot7007.sgy.p190
Elastic_Shot7007.sgy.meta
Elastic_Shot7007.sgy.sgh.bz2
```

The first step in decompressing the data is to unzip file Elastic_Shot7007.sgy.sgh.bz2 using bunzip2 as follows:

```
bunzip2 Elastic_Shot7007.sgy.sgh.bz2
```

The result will be a file called Elastic_Shot7007.sgy.sgh

Then the decompression is done using the following command:

```
SEAMdecompress.linux64 input_directory in_filename output_segyfname
```

Where input_directory is the name of the directory containing the four files listed above (note that bunzip2 command must first be executed).

in_filename is the prefix to the filenames in the directory; e.g. in above it is Elastic_Shot7007.sgy

output segyfname is the directory and filename of the output segy file.

Script doit.csh that is included with the executable gives an example of how to run the decompress algorithm.

Table 8-1. Listing of various seismic data sets generated during the SEAM Phase I RPSEA project and whether or not each data set was compressed.

Simulation	Data Set	Approximate Traces per Logical Compressed Data Set	Compressed
AUS	Surface	440,000	Yes
AUS	NAZ Data Set	13,200	Yes
AUS	WAZ Data Set	46,200	Yes
TTI	Surface	440,000	Yes
TTI	VSP	467	No
TTI	NAZ Classic Data Set	13,200	Yes
TTI	WAZ Data Set	46,200	Yes
Elastic	Surface	650,000	Yes
Elastic	Seafloor	42,036	No
Elastic	VSP	467	No
Elastic	NAZ Classic Data Set	20,000	No
Elastic	WAZ Classic Data Sets	68,000	No
Elastic	Seafloor Classic Data Set	2622	No
Elastic	1601 Shot Tight Grid	40,401	No

Figures

Figure 8-1. East-West gather of traces for the elastic vendor qualification shot surface trace data provided by AGT. Gathers are taken 30 m North of the source position. Trace spacing is 15 m.

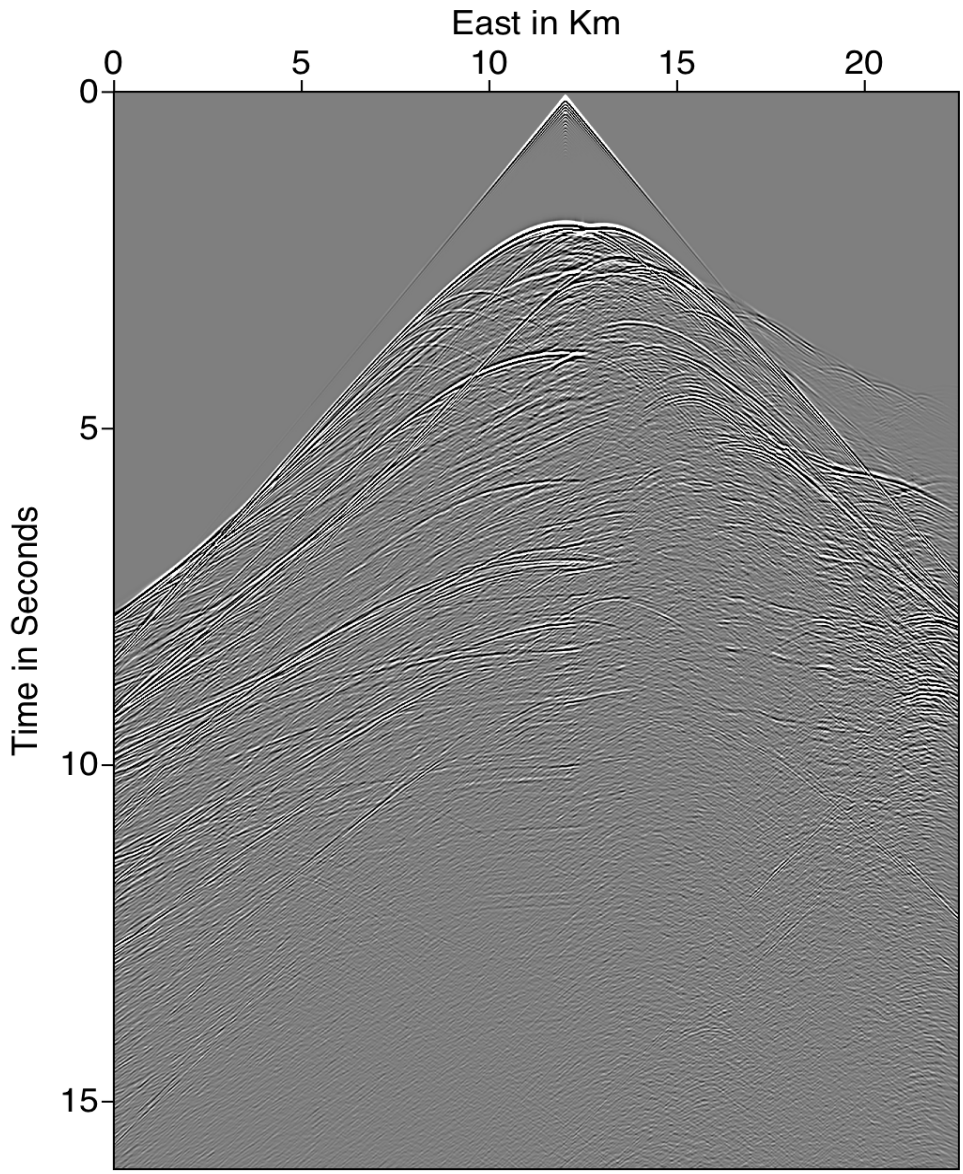

Figure 8-2. Gather from Figure 8-1 after entire shot gather had been compressed and decompressed.

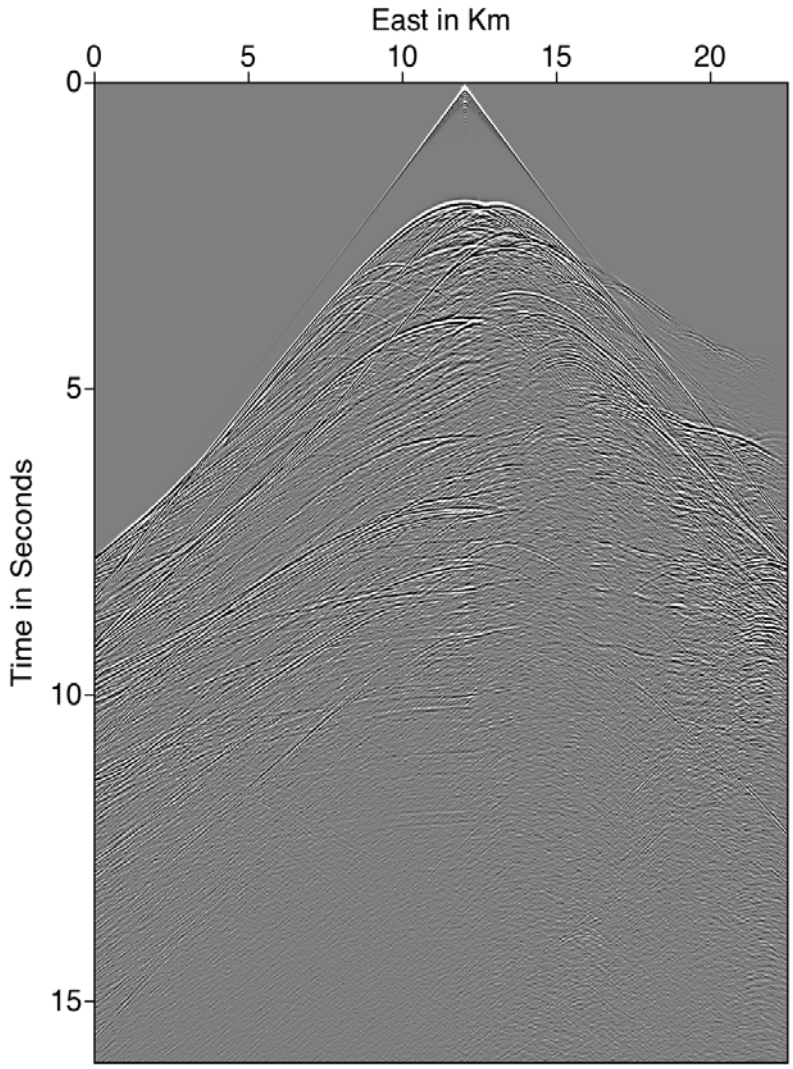

Figure 8-3. Difference of gathers shown in Figures 8-1 and 8-2. Amplitude has been multiplied by 100 to emphasize differences.

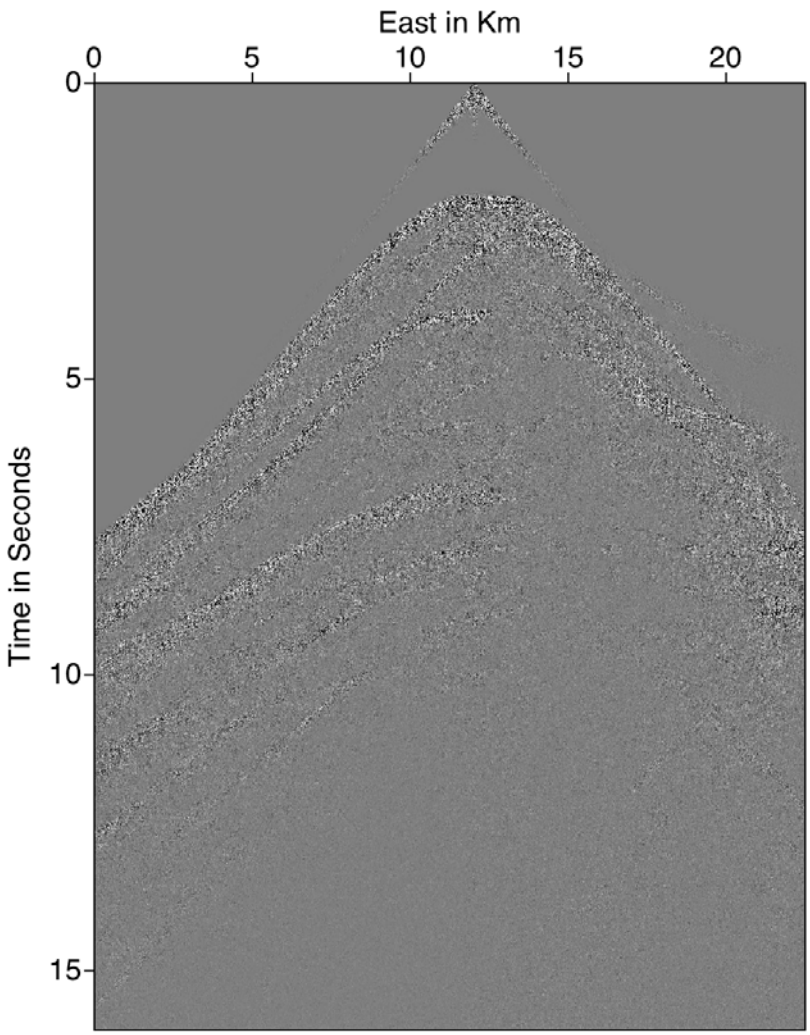

Figure 8-4. East-West gather of traces for the vendor qualification elastic shot surface data provided by AGT. Gathers are taken 30 m North of the source position. Trace spacing is 30 m.

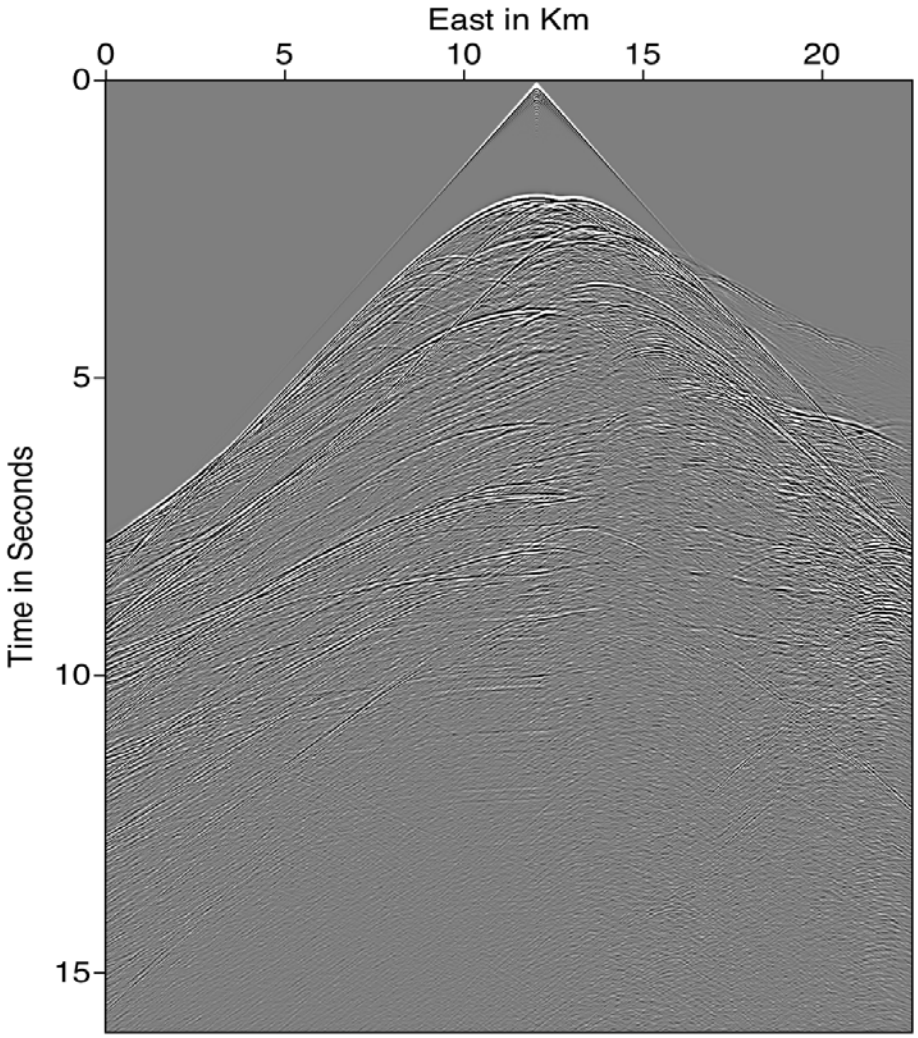

Figure 8-5. Gather from Figure 8-4 after entire shot gather had been compressed and decompressed.

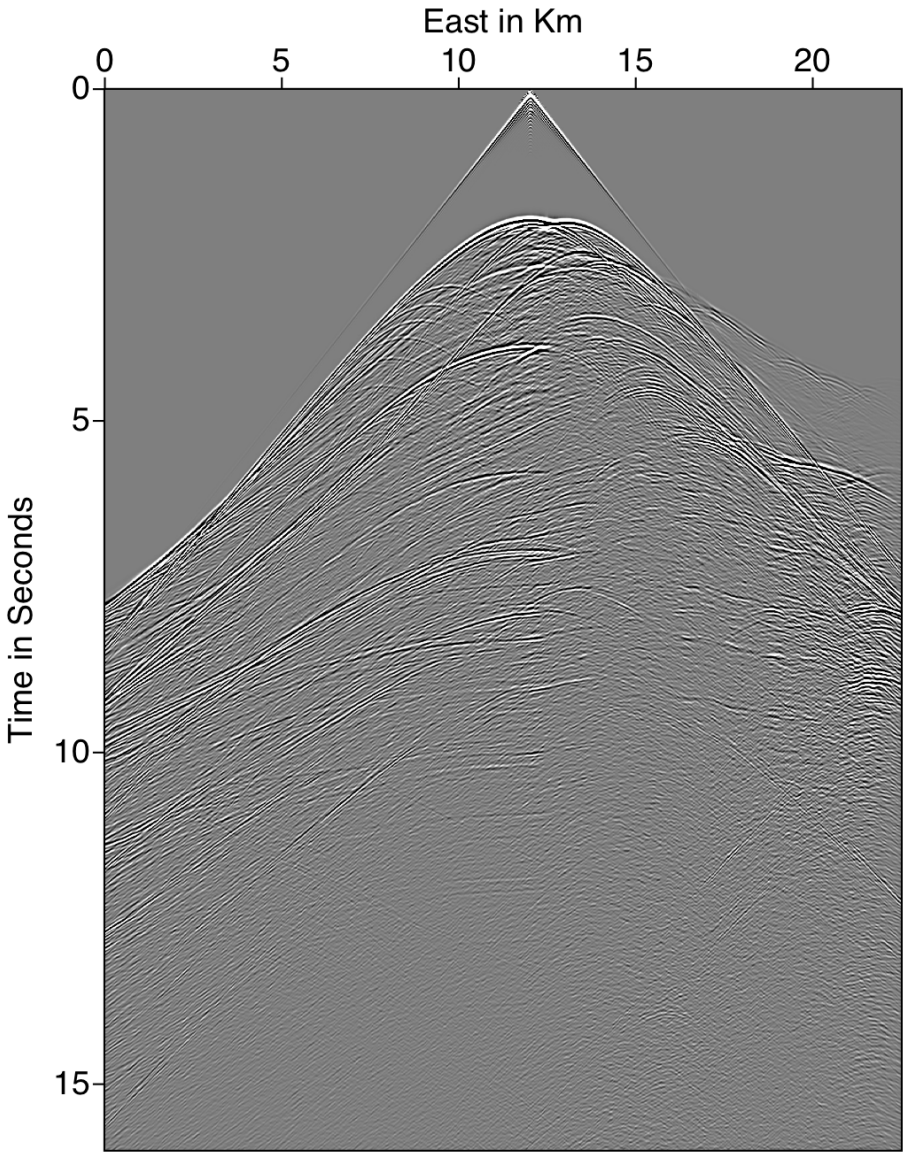

Elastic Vendor Qual After DeCompress 30 m N of Shot 30 m trace sp

Figure 8-6. Difference of gathers shown in Figure 8-4 and 8-5. Amplitude has been multiplied by 100 to emphasize differences.

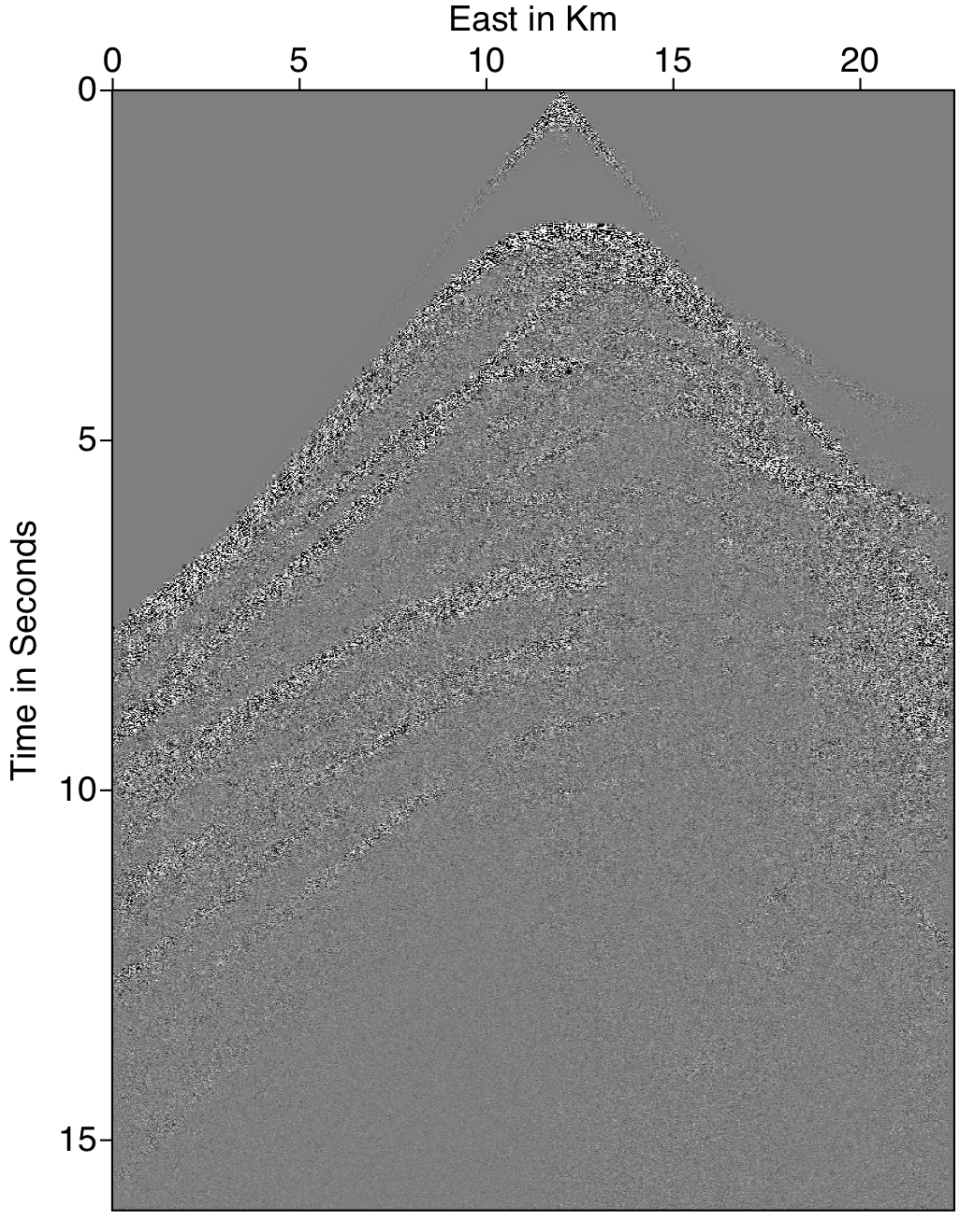

Figure 8-7. Difference of gathers shown in Figure 8-4 and 8-5. Plot is on same scale as Figures 8-4 and 8-5.

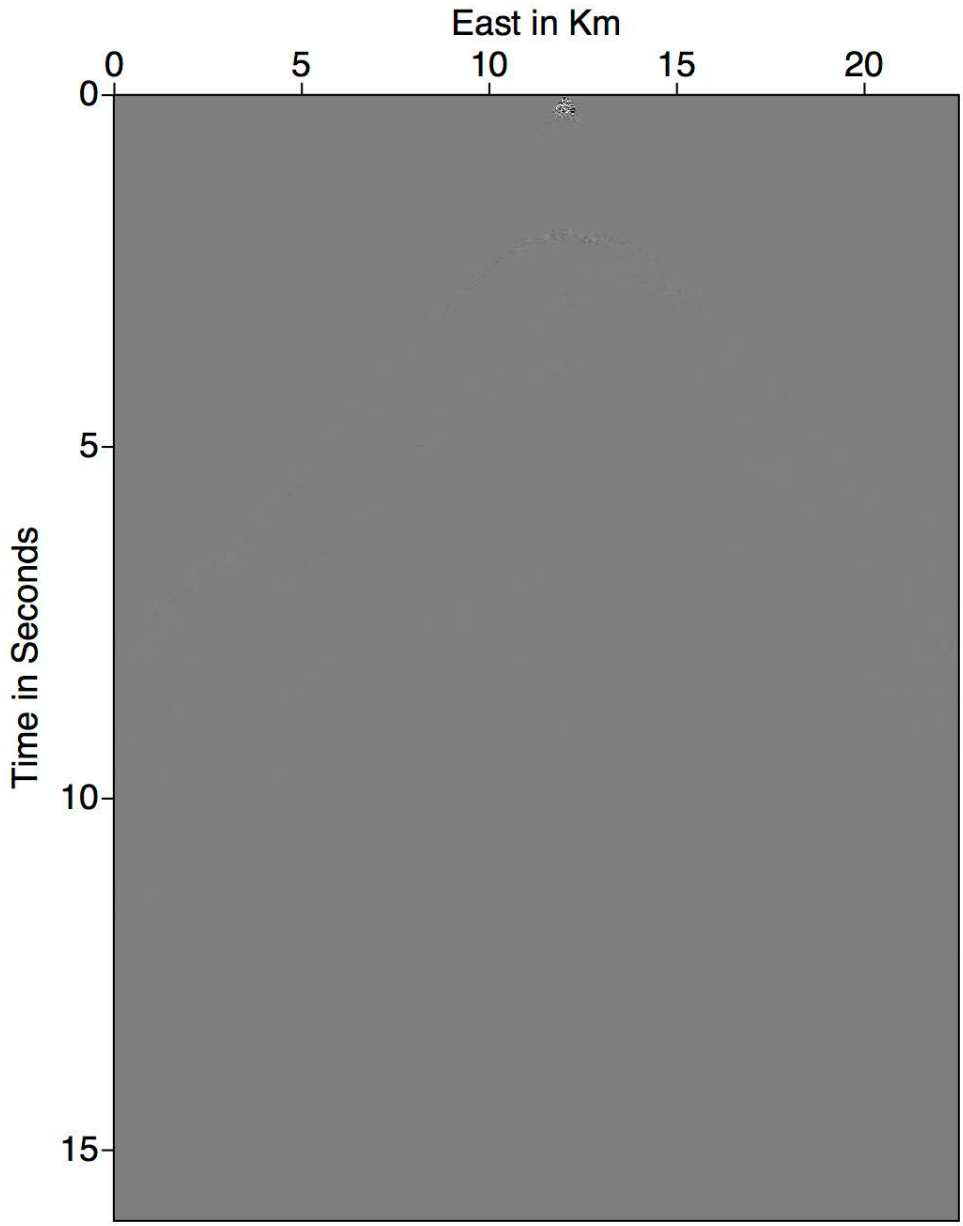

Figure 8-8. Top: Trace from one shot in WAZ data set for AUS simulation that was extracted from complete shot gathers during QC. Middle: same trace as above but after the WAZ shot gather data had been compressed and decompressed. Bottom: difference of top and middle traces with gain of 500 applied to emphasize the differences.

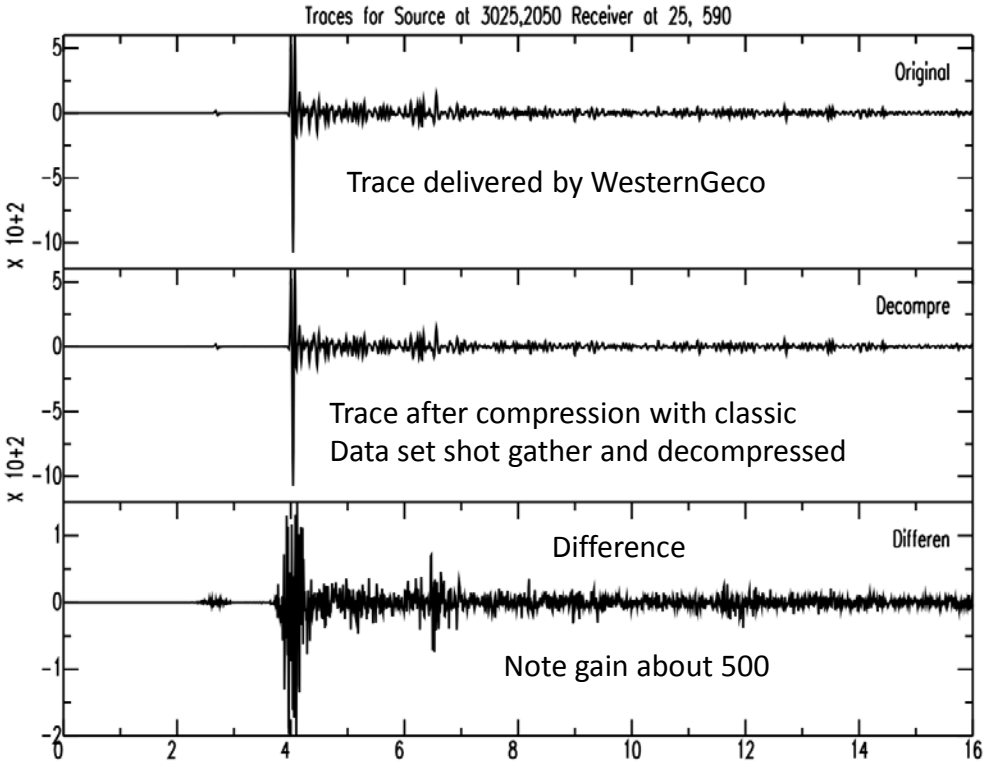

Figure 8-9. Same as Figure 8-8 except on expanded time scale to show details of traces.

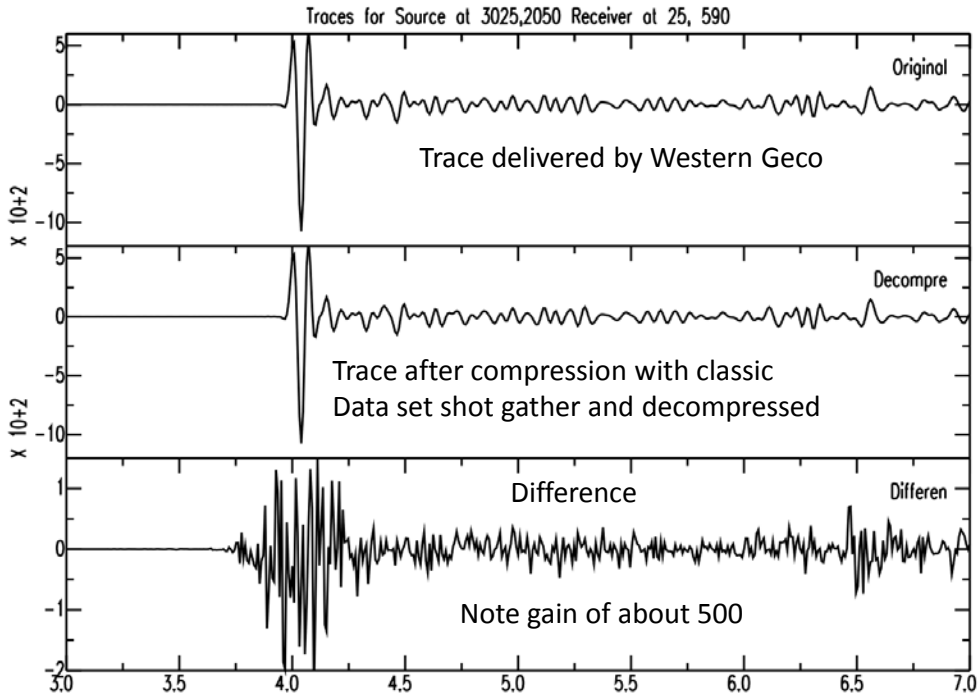

IMPACT TO PRODUCERS

The SEAM Phase I model is one of the most realistic earth models used for benchmark testing in the industry today. The salt body structure is based on an actual area of the Gulf of Mexico and includes sediment inclusions and a dirty top. The sediments are also realistic as their properties are based on rock physics such as shale content and porosity. The model has already had an impact on the industry through development of new seismic acquisition designs and operations. Some of these methods, like 'coil' acquisition, are already being utilized in the Gulf and elsewhere to enhance subsalt imaging for exploration and development. New simulation software, both acoustic and elastic, have progressed specifically to meet the simulation needs of this project. Bill Symes' acoustic code is now available to the public and Tierra (now Landmark) further developed acoustic FD code to make acoustic wave equation modeling efficient enough on a large scale to be practical for numerous applications. Hardware and software developments at AGT, to meet the demands of the SEAM elastic modeling project, have made 3D FD elastic modeling available to the industry in a time efficient manner and within reasonable cost constraints.

The simulated data are also being used, and are expected to be used more in the future, by oil and gas companies, geophysical service providers, and universities to test and develop seismic processing and subsurface imaging technology and for teaching and training. The data sets simulated by SEAM can be used to compare imaging results provided by various seismic acquisition methods including streamer, dual sensor streamer, WAZ, NAZ, RAZ, full-azimuth, and multicomponent sea floor as well as VSPs. Isotropic imaging of TTI media can be tested and compared to isotropic images. There exists the opportunity to develop Shear wave as well as P wave processing and imaging methods with this data which may provide additional information about lithology and fluids in addition to enhancing structural and stratigraphic images.

Further development of the non-seismic methods and integration with seismic methods should further advance our knowledge of the subsurface near and beneath salt bodies to enhance imaging.

Advancement of these seismic and non-seismic technologies can impact the discovery and development of additional hydrocarbon resources in the Gulf of Mexico and improve recovery of existing reserves.

TECHNOLOGY TRANSFER

There were continual efforts throughout the life of the project to transfer the technology broadly. There were several main approaches including interaction of the participants, projects using the models and data involving participants, industry service providers and universities, technical publications, and participation in industry forums and annual technical meetings.

- The project participants included 24 companies having a wide range of interests in GOM petroleum development.
- Technology Transfer through direct industry participation and publication.
- SEAM contracted for an acoustic simulation code that is publicly available, well tested, and documented.
- SEAM facilitated seismic simulation in petroleum industry via Technology Transfer.
- SEAM made regular submissions to *THE LEADING EDGE* and presentations at technical conventions including the OTC and SEG annual meetings.

SEAM Phase I RPSEA was composed of 24 member companies whose representatives met regularly to discuss progress made in SEAM work. These member companies comprise a majority of those in the petroleum industry who are interested in numerical simulation for deepwater GOM applications. Thus, SEAM activities were known to a wide segment of industry in near-real time. SEAM currently maintains an e-Community on the SEG website where ideas, results, and minutes of meetings are posted. This e-Community helps keep SEAM participants aware of our current activities and areas of technical concern. There were also regular email exchanges among members of technical working groups and across the groups. Technical communication within the SEAM project has been extensive and is illustrative of the excitement about and participation in the project by industry members.

SEG is dedicated to the dissemination of new concepts and results to the geophysical community. SEAM, as a subsidiary of SEG, shares this dedication. A link on the main web page of the SEG leads to a section of the SEG web site that discusses SEAM. This link is available to the general public.

SEAM worked with SEG and their monthly professional publication, *THE LEADING EDGE (TLE)*, to publish a regular series of articles about progress on SEAM. These articles focused on keeping the broader geophysical community aware of the activities of SEAM and how geophysical professionals might benefit from SEAM products.

SEG publishes the leading refereed journal and the most widely circulated general interest publication for applied geophysics in the world. Both publications, and much more, are also available at www.seg.org.

SEG is uniquely positioned to facilitate the delivery of results to industry and academia. SEAM contracted with Rice University to develop, characterize, and test a variable density acoustic finite difference code that was used for validation and QC of vendor calculations. Since one of the goals of SEAM is to foster the broader development and use of numerical simulation for geophysical exploration, this code was made publically available on the SEAM Phase I website. The goal was to make this code reliable, thoroughly tested, and well documented. Significant effort was not put into making this code computationally efficient as that efficiency should be the domain of the end user.

SEAM has made an effort to reach out across the geophysical community to advertise the work, to seek input and to make the community aware of our activities.

SEAM participants have made appropriate presentations at professional meetings to publicize and highlight the work. SEAM has been widely discussed at Annual Meetings of the Society of Exploration Geophysicists from 2007 through 2013. This meeting is attended by more than 8,500 exploration professionals from across the petroleum industry, academia, and government. SEAM had exhibit booths at the SEG annual meetings that were staffed by knowledgeable representatives. SEAM also helped staff the RPSEA booth at two SEG meetings and one Offshore Technology Conference (OTC).

SEAM organized “Special Sessions” at SEG Annual Meetings as well as dedicated workshops and forums to foster and encourage research using the SEAM deliverables. These meetings engaged the best minds in the global geophysical community on solving the geophysical problems of the Deepwater GOM.

To complete the SEAM Phase I project, transfer of technology, and announcement of data availability, SEAM organized a special Research Workshop in San Antonio, Texas May 21 – 24, 2013. Interested scientists from industry, and academia were invited to participate and discuss invited presentations about the SEAM deliverables and how they have been used to date.

Specific activities and publications are listed in Appendix A

CONCLUSION

Advanced modeling of synthetic geophysical data on the scale that SEAM completed would not have taken place without RPSEA support. The SEAM participants had identified the needs of the industry, research labs, and universities for test data sets

requiring computer resources and simulation algorithms not economically available at the commencement of the project. SEAM had generated a realistic acoustic earth model of a deep water subsalt environment but required financial assistance to take the model and simulations to a next level of technology needed by the industry. RPSEA funding made this possible and the data and model are now available to anyone who will use it to advance learning and technology for deep water oil and gas exploration and production. The resulting models and simulation data are already being used by industry, and there is every indication that the industry will find value in this model and data for many years into the future.

Funding for this project is provided by RPSEA through the "Ultra-Deepwater and Unconventional Natural Gas and Other Petroleum Resources" program authorized by the U.S. Energy Policy Act of 2005. RPSEA (www.rpsea.org) is a nonprofit corporation whose mission is to provide a stewardship role in ensuring the focused research, development and deployment of safe and environmentally responsible technology that can effectively deliver hydrocarbons from domestic resources to the citizens of the United States. RPSEA, operating as a consortium of premier U.S. energy research universities, industry, and independent research organizations, manages the program under a contract with the U.S. Department of Energy's National Energy Technology Laboratory.

RECOMMENDATIONS

This SEAM project funded by RPSEA UDW has successfully provided a useful earth model and simulated data sets that the industry is already using. Much has been learned about model building, simulations and working in a collaborative industry environment. As these data and model are used by industry, academia, and government groups, more will be learned and it is likely that the work on this model can be successfully leveraged by future projects. As computational methods and computers improve to allow higher resolution earth models and greater bandwidth data, more reservoir detail can be incorporated to simulate other relevant and significant exploration, production, and development problems such as time lapse reservoir characterization, pore-pressure prediction ahead of the bit to mitigate drilling hazards, micro-seismicity related to injection or production, and others.

FIGURES AND TABLES

EARTH MODELS

Table 1-1. Layer dependent parameters for setting anisotropy variables. GeoIndex is Geology unit index shown in Figure 1-4. Other parameters are defined in the text.

Figure 1-1.
Rooting the SEAM model in rock properties: from geology and petrophysics to geophysics. Figure from Joe Stefani (CVX).

Figure 1-2.
A view looking down upon the top of the complex 3D salt body. Shown around the salt is a depth slice at Z=7500 m from the gridded P-wave velocity, Vp. The white and red rectangle defines the bounds of the model 35 km E-W by 40 km N-S. The salt body surfaces extend beyond the model for gridding purposes. From Fehler and Keliher, 2011.

Figure 1-3a.
View towards the west of the eastern flank of the main salt body. Overhangs are seen from this perspective as well as the root stalk of the salt that ties to the mother salt which is not shown. The white rectangle measures 40 km by 15 km with north to south running right to left. From Fehler and Keliher, 2011.

Figure 1-3b.
View towards the east of the western flank of the main salt body. Overhangs and a grotto are seen from this perspective. The white rectangle measures 40 km by 15 km with north to south running left to right. The grotto and salt overhang area is the focus of some of the limited area data sets. Modified from Fehler and Keliher, 2011.

Figure 1-4.
GeoIndex values on model cross section. Geoindex values are:1=Basement, 2=Mother Salt, 3=Cretaceous, 4=Oligocene-Paleogene, 5=Lower Miocene, 6=Middle Miocene, 7=Upper Miocene, 8=Pliocene, 9=Pleistocene, 10=Water, 11=Inverted Lower Miocene, 12=Inverted Olig-Paleogene, 13=Inverted Cretaceous, 14=Salt Sutures, 15=Homogeneous Salt, 17=Heterogeneous Salt. From Fehler and Keliher 2011.

Figure 1-5.
Middle Miocene sheet turbidite Vshale, 35 km across. Left: Single stratigraphic slice 20 meters thick. Right: vertical average of vshale over 80 meters constituting one subsheet. From Fehler and Keliher 2011.

Figure 1-6.
Cumulative vertical sum of reservoir thickness. Black=0 m, White=800 m. Note how either salt or the northern model edge truncate the turbidite stems. From Fehler and Keliher 2011.

Figure 1-7.
A model cross-section of the original S-Velocity shows considerable variation ranging from 120 m/s – 1500 m/s in the shallow portion of the model. Note a vertical exaggeration of about 5:1 in the figure. Modified from the file Fehler_April_26_MC_reorder.ppt , 2012, in the SEAM online archive.

Figure 1-8.
Linear adjustment applied to shear velocities ranging from 100 – 1000 m/s. Modified from the file Fehler_April_26_MC_reorder.ppt , 2012, in the SEAM online archive.

Figure 1-9.
Adjusted Vs in range of 100 to 1000 m/s to be between 600 and 1000 m/s using linear scale. Note a vertical exaggeration of about 5:1 in the figure. Compare to the original Vs in Figure 6. Modified from the file Fehler_April_26_MC_reorder.ppt , 2012, in the SEAM online archive.

Figure 1-10.
A model cross-section of the original Vp/Vs shows considerable variation including very high ratios near the seafloor. Note a vertical exaggeration of about 5:1 in the figure. Modified from the file Fehler_April_26_MC_reorder.ppt , 2012, in the SEAM online archive.

Figure 1-11.
A model cross-section of the adjusted Vp/Vs shows reduced variation but as depth increases the Vp/Vs ratio varies less. Note the vertical exaggeration of 5:1 and that the color scale differs from the one used in Figure 10. Modified from the file Fehler_April_26_MC_reorder.ppt , 2012, in the SEAM online archive.

Figure 1-12.
SEG logo diffraction test pattern. Blue = no density deviation from the background, green = 0.13 g/cc above background, red = 0.5 g/cc above background. In the model, the logo is aligned east-west and is centered in both X and Y. The east-west distance between the tips of the logo is 30 km, and the north-south distance between tips is 16 km. (Binary pixels file courtesy Dave Hale.)

NUMERICAL SIMULATION

Figure 2-1.
Far-field source characteristics. The source used for all SEAM Phase I seismic simulations was identical. (Reproduced from SEAM Phase I Report)

Figure 2-2.
Common-shot gather from shots simulated with a free upper surface (left), an absorbing upper surface (right), and the difference of the two.

Figure 2-3.
Common shot East-West gathers through the source for a common shot location but with different simulation approaches. Approaches are labeled in the panel identifiers. Shot is 12873 in the acoustic model. The elastic numbering scheme does not align with that used for the other simulations so shot 409 in the elastic simulation is at almost the same location as is shot 12873 in the other simulations.

SEISMIC ACQUISITION

Table 3-1.
Classic Data Set Geometries for acoustic and acoustic absorbing upper surface simulations. The two 9 NS line 2-C data sets have receivers at 15 and 17 m depths recorded as separate shots; all other data sets have only 15 m receivers with free surface upper boundary. The WAZ interleaf; pull-only data sets have a net 600 m shot spacing after interleaving both sail directions. All distances and coordinate locations are in meters. Data volume listed includes both receivers and assumes all shots have the maximum number of traces. Actual volume will be about 13% less. Data volume is listed as uncompressed but without trace headers. Headers add another 3% to the volume; compression ratio for the trace date is about 8:1. Traces/shot listed is a maximum; shots near boundaries have fewer traces.

Table 3-2.
Acoustic data with an absorbing upper surface were simulated using the isotropic earth model to provide test data without surface multiples. Processing of this data can be compared to the free surface data to evaluate effectiveness of multiple attenuation and to evaluate other processing and imaging methods without multiple interference. For these purposes, a data volume less than the free-surface volume was simulated

Table 3-3.
These data are an expansion to the north and south from the 28 EW lines acquired with the Absorbing Upper Surface (AUS) data set. This provides a significantly wider area and aperture for 3D imaging testing. This swath of lines is centered on North 23900 which is

the east-west line that the 4 VSPs are located on. The acquisition parameters are listed and the area is illustrated in Figure 3-5.

Table 3-4.
TTI VSP Classic Data Set Geometries

Table 3-5.
This elastic data set has the a similar geometry and the same location on the model as the AUS 2793 Classic Data Set and are listed in Table 4 along with the parameters and locations for all the other elastic classic data sets.

Table 3-6.
Elastic VSP Classic Data Set Geometries

Figure 3-1.
Recording and simulation patch geometry drawn to scale. The portion of any patch outside the model (shown in gray) is not computed or recorded. Only 22% of shots have a full complement of 436,921 traces. The average number of traces/shot is about 77% of the maximum. (Slide 3 from Classic_Data sets rev 7.ppt by Acquisition Committee)

Figure 3-2.
Shot locations of the 2,793 shot grid and 28 EW line AUS data sets. The color indicates the stacked thickness of the reservoirs. The 28 EW line data crosses the thickest turbidite and channels sequences.

Figure 3-3.
NAZ EW source-streamer spread geometry

Figure 3-4.
AUS WAZ EW source-streamer spread geometry

Figure 3-5.
The TTI 2793 shot set (600 m grid of shots) extends over the whole model. The 109 line 150 m shot grid extends east-west across the model between 15800 and 32000 north. This swath is centered on North 23900, the east-west line the VSPs are located on.

Figure 3-6.
The shot lines for the TTI east-west WAZ and NAZ are illustrated relative to the 150 m shot grid and the VSP locations

Figure 3-7.
The four TTI VSPs are located at north 23900 m in the model where the wells sample three shallow reservoirs away from salt and one through a salt overhang. The receiver depth range is 1000m to 7990m with a sample interval of 15 m.

Figure 3-8.
TTI VSP Source grid recorded by each well is outlined by the color boxes. The 600 m grid of shots is from the 2793-shot data set.

Figure 3-9.
Ray-tracing indicated a minimum of 14 second seismic records were needed. Sixteen seconds were simulated.

Figure 3-10.
Description of the Elastic simulation receiver area and shot patch for the 100 m grid shot set.

Figure 3-11.
Elastic 100 m grid acquisition region. Yellow box shows region containing shots and blue box outlines the simulation and trace acquisition boundary. Overlay on Cumulative Reservoir Thickness map from Joe Stefani.

Figure 3-12.
The four VSP locations for the elastic simulations are shown. The depth range of receivers is 1000 m – 7990 m at 15 m intervals.

Figure 3-13.
Elastic VSP Source grid recorded around each well with the 2793 data set and 600 m shot interval.

Figure 3-14.
Acquisition geometry and location for the Elastic NAZEW Classic Data Set.

Figure 3-15.
Comparison of acquisition geometries for acoustic and elastic narrow azimuth classic Data sets. These are push-pull data sets so half the streamer is east of the shot and half is west.

Figure 3-16.
Acquisition geometry and location for the Elastic WAZEW Classic Data Set.

Figure 3-17.
Comparison of acquisition geometries for acoustic and elastic wide azimuth classic data sets. These are push-pull data sets so half the streamer is east of the shot and half is west.

Figure 3-18.

Acquisition shot-receiver patch geometry and location on the model for the Elastic 1600 shot Classic Data Set.

Figure 3-19.
Cross-section illustrating the variation of Vs under the 1600 shot, high resolution acquisition spread.

GRAVITY

Table 4-1.
Comparison of range of values computed for components of the gravity gradients as computed using two software packages described in the text. The similarity of the values indicates little difference in the two methods.

Table 4-2.
Range of gravity anomalies and corresponding gradients.

Table 4-3.
Free-air anomalies at 0 m level, background density 2.2 g/cm^3.

Table 4-4.
Free-air anomalies at 150 m level, background density 2.2 g/cm^3.

Table 4-5.
Bouguer anomalies at 0 m level, Bouguer correction density 2.0 g/cm^3, background density 2.2 g/cm^3.

Table 4-6.
Bouguer anomalies at 150 m level, Bouguer correction density 2.0 g/cm^3, background density 2.2 g/cm^3.

Figure 4-1.
SEAM Phase I model density cube.

Figure 4-2.
Vector (black) and tensor (blue) components of gravity field. (figure from Neda Bundalo)

Figure 4-3.
Vertical slice through density volume of the SEAM Phase I model.

Figure 4-4.
Free air anomaly at sea level to simulate ship borne gravity measurement. (figure from Neda Bundalo)

Figure 4-5.
Free air anomaly at 150 above the sea surface to simulate airborne gravity. (figure from Neda Bundalo)

Figure 4-6.
Bouguer anomaly at sea level. (figure from Neda Bundalo)

Figure 4-7.
Bouguer anomaly at 150 m above sea surface. (figure from Neda Bundalo)

CONTROLLED SOURCE ELECTROMAGNETICS (CSEM)

Figure 5-1.
SEAM Phase I Resistivity models. Upper two panels show bed-parallel and bed-normal resistivity. Bedding directions change with position. Lower panels show horizontal and vertical resistivities that were derived from bed-normal and bed-parallel resistivities by a simple rotation. Vertical East-West cross sections though North 23.9 km are shown.

Figure 5-2.
CSEM acquisition geometry superimposed on a plan view of the SEAM model. Yellow dots are receiver locations. Green lines are source towlines occupied for the receiver located at East = 11,000 m, North = 26,750 m. Source locations are spaced every 100 m along each towline; the distance between the towlines is 1 km. Synthetic CSEM data were simulated for a total of 494 receivers with 22 towlines for each receiver.

Figure 5-3.
Receiver numbering scheme for CSEM simulation. Receivers were placed at 1000 m increments across the center portion of the model. CSEM receivers are a subset of those used for MT simulation. To maintain consistency between CSEM and MT receiver numbering, not all receiver numbers are used for CSEM simulation. Yellow dots show locations of receivers.

Figure 5-4.
CSEM source towline numbering scheme. Towlines for each receiver extend 10 km North, South, East, and West of the receiver position or to the model boundary if the boundary is within 10 km of the receiver. Yellow dots show receivers. Black lines show towlines. Tx001, Tx002, etc. are the towline numbers.

Figure 5-5.
Example of the comparison of CSEM simulation data provided by EMGS and that conducted by a SEAM participating company. Data for receiver Rx177 are shown for 2

Hz. Sources are located along an East-West line passing through the receiver. Red line shows EMGS result and black line shows benchmark simulation result. Comparison is quite good except at offsets larger than about 6 Km to the East of the receiver where field amplitude is several orders of magnitude smaller than it is near the source. Due to the small field values, the comparison of phases at this range is not reliable.

Figure 5-6.
Top Row: Cumulative reservoir thickness (left) and 2.5 km vertical resistivity in Ωm (right) maps for the portion of the model over which CSEM data were simulated. Subsequent Rows: Maps of log values of the East-West component of horizontal electric field magnitude (E_x in V/m) at 5 km source-receiver offset. Note that log values are all negative so regions with higher field are shown in red. Source is located due West of receiver. Field is plotted at location of midpoint between source and receiver. Results for various frequencies are shown. Note the area of a relatively higher field to the east of the salt body, indicative of resistive hydrocarbon-filled reservoirs.

MAGNETOTELLURICS

Figure 6-1.
Receiver numbering. A receiver at a given location in the CSEM simulation has the identical number in the MT simulation.

Figure 6-2.
Seafloor depth in meters in the SEAM resistivity model.

Figure 6-3.
Example of MT simulation results. Data from CGG (below) and EMGS (top) are shown. The values of the impedance tensor component Zxx is plotted as a function of position on the SEAM model. CGG data have been rotated and scales to match the convention used by EMGS.

QUALITY CONTROL

Figure 7-1.
East-West shot gathers passing through the source position for Shot 12873 in the acoustic simulation (a) and for the TTI simulation (b). Plots like this were used as part of the vendor qualification procedure for the TTI simulation. The plots show remarkable similarity in spite of the simulations having been conducted by independent vendors. Notable differences are slight changes in arrival time and amplitudes of events. The source insertion approach used in the two simulations was quite different and this resulted in differences in the gathers for the first few seconds of the simulation at locations near the source.

Figure 7-2.
Traces resulting from simulations conducted on a layered elastic vendor qualification model using reflectivity (a) and by simulation vendor AGT (b). These traces are for the vertical component of acceleration measured along a vertical line that penetrates the seafloor located at a depth of 1650 m. Receiver depth in meters is given next to the right hand side of each trace.
Figure 7-3.
Same as Figure 7-2 except that the East-West component of acceleration is plotted.

Figure 7-4.
East-West gathers for simulation on the seam elastic model conducted by Sandia National Laboratories (a) and AGT (b). The pressure on the seafloor is plotted. The Sandia simulation did not cover as large a portion of the model as did the AGT simulation. Images are scaled so that overlapping portions of the gathers from the two simulations are on the same scale

DATA COMPRESSION

Table 8-1.
Listing of various seismic data sets generated during the SEAM Phase I RPSEA project and whether or not each data set was compressed.

Figure 8-1.
East-West gather of traces for the elastic vendor qualification shot surface trace data provided by AGT. Gathers are taken 30 m North of the source position. Trace spacing is 15 m.

Figure 8-2.
Gather from Figure 8-1 after entire shot gather had been compressed and decompressed.

Figure 8-3.
Difference of gathers shown in Figure 8-1 and 8-2. Amplitude has been multiplied by 100 to emphasize differences.

Figure 8-4.
East-West gather of traces for the vendor qualification elastic shot surface data provided by AGT. Gathers are taken 30 m North of the source position. Trace spacing is 30 m.

Figure 8-5.
Gather from Figure 8-4 after entire shot gather had been compressed and decompressed.

Figure 8-6.
Difference of gathers shown in Figure 8-4 and 8-5. Amplitude has been multiplied by 100 to emphasize differences.

Figure 8-7.
Difference of gathers shown in Figure1 8-4 and 8-5. Plot is on same scale as Figures 8-4 and 8-5.

Figure 8-8.
Top: Trace from one shot in WAZ data set for AUS simulation that was extracted from complete shot gathers during QC. Middle: same trace as above but after the WZ shot gather data had been compressed and decompressed. Bottom: difference of top and middle traces with gain of 500 applied to emphasize the differences.

Figure 8-9.
Same as Figure 8-8 except on expanded time scale to show details of traces.

REFERENCES

Fehler, M. and P. J. Keliher, SEG 'SEAM Phase I: Challenges of Subsalt Imaging in Tertiary Basins, with Emphasis on Deepwater Gulf of Mexico, SEG, online ISBN 978-1-56080-294-5, 2011.

Mackie, R. and T. Madden, Three-dimensional magnetotelluric inversion using conjugate gradients, *Geophysical Journal International* 115, 215-229, 1993.

Mavko, G., T. Mukerji, and J. Dvorkin, The Rock Physics Handbook: Tools for Seismic Analysis in Porous Media, Cambridge University Press, ISBN 0 521 62068 6, 1998.

Moldoveanu, N., Y. Ji, C. Beasley, Multivessel coil shooting acquisition with simultaneous sources, SEG Extended Abstract Las Vegas, 2012

Moldoveanu, N.,and J, Kapoor, What is the next step after WAZ for exploration in the Gulf of Mexico? SEG Extended Abstract Houston, 2009

J. Stefani, M. Frenkel, N. Bundalo, R. day, M. Fehler, SEAM Update: Models for EM and Gravity Simulations, The Leading Edge, 132-135, 2010.

Stork, C. , Seismic acquisition is moving from a "CMP Fold" perspective to a "Wavefield Recording" perspective which has significant implications on acquisition design, SEG Extended Abstract, San Antonio, 2011.

Thomsen, L., Weak elastic anisotropy, Geophysics, Vol 51, No 10, pp 1954-1966, 1986.

LIST OF ACRONYMS AND ABBREVIATIONS

2D – two dimensional

3D – three dimensional

AGT – Advanced Geophysical Technology, Inc.

AUS – Absorbing Upper Surface

BHP - BHPBilliton Petroleum (Americas), Inc

COP – ConocoPhillips

CSEM – Controlled Source ElectroMagnetics

EM - electromagnetic

FD – finite difference

GB – Gigabytes

g/cm^3 - grams/cubic centimeter (density)

GOM – Gulf of Mexico

GPU – graphics processing unit

Hz – hertz (cycles/second)

km – kilometer

m - meter

MB – Megabytes

Md5sum – a data verification algorithm

mgal - gravity values in milligals

MIT – Massachusetts Institute of technology

m/s - velocity

MT – Magnetotellurics

NAZ – narrow azimuth

OTC – Offshore Technology Conference

PGS – Petroleum Geo-Services

QC – quality control

RAZ – rich azimuth

RPSEA – Research Partnership to Secure Energy for America

s - second

SEAM- SEG Advanced Modeling Corporation

SEG- Society of Exploration Geophysics

SEGY – a standard seismic data format developed by the SEG

SP – shot point

TB – Terrabytes

TLE – The Leading Edge

TTI – Tilted Transverse Isotropy

UDW – Ultra-Deepwater

VSP – Vertical Seismic Profile

VTI – Vertical Transverse Isotropy

WATS – wide azimuth towed streamers

WAZ – wide azimuth

XOM - ExxonMobil

Ωm - ohm-meter

TABLE OF SYMBOLS

D = Depth measured from sea surface

delMax = maximum value of δ for each model layer

dx = grid interval in x (East) direction

Dx = x component of bed dip

D_x^{tti} = x-component of dip vector

dy = grid interval in y (North) direction

Dy = y component of bed dip

D_y^{tti} = y-component of dip vector

dz = grid interval in z (depth) direction

E = East

epsMax = maximum value of ε for each model layer

E_x = x component of electric field

E_y = y component of electric field

E_z = z component of electric field

gamMax = maximum value of γ for each model layer

Gz = vertical gravity

H_x = x component of magnetic field

H_y = y component of magnetic field

H_z = z component of magnetic field

N = North

P = compressional wave

PS = shear wave converted from an incident P wave

PSv = a vertically polarized shear wave converted from an incident P wave

Q = attenuation

R_h = horizontal resistivity

Rn = resistivity normal to bedding

Rp = resistivity perpendicular to bedding

R_v = vertical resistivity

S = Shear wave

S = south

Sv = vertically polarized shear wave

T_x, T_y = complex values of MT Tipper vector

Txx, Txy, Txz, Tyy, Tyz and Tzz = components of gravity gradient tensor

Vp = Compressional wave velocity

Vs = Shear wave velocity

v-shale, Vsh, vshale = fractional volume of shale

W = west

W_s = weight factor for each model layer (0.0 – 1.0) applied to bed dip to determine TTI dips

X = East

Y = North

Z = Depth

Z_{xx}, Z_{xy}, Z_{yx}, Z_{yy} = complex values of MT impedance tensor

γ = S-wave anisotropy; the fractional difference of Vs in the vertical (or bed-normal) and horizontal (or bed parallel) directions. Thomsen's weak anisotropy parameters (Thomsen, 1986).

δ = the crucial anisotropic parameter for near-normal P-wave propagation. Thomsen's weak anisotropy parameters (Thomsen, 1986).

ε = P-wave anisotropy; the fractional difference of Vp in the vertical (or bed-normal) and horizontal (or bed parallel) directions. Thomsen's weak anisotropy parameters (Thomsen, 1986).

θ = Dip angle for TTI model

ρ = density

ϕ = Dip angle for TTI model

ϕ^{ε} = Effective porosity

ϕ^{τ} = Total porosity

APPENDICES

Appendix A - Technology Transfer

Workshops

Workshop about SEAM and SEAM RPSEA project held at Society of Exploration Geophysicists in Houston on October 29, 2009.

A workshop about the SEAM project was held May 21-24, 2013. The workshop was attended by approximately 50 people. Presentations about the SEAM simulations, SEAM data, and use of the data by several investigators were made at the workshop.

Presentations

Poster about project was prepared and posted at RPSEA booth during annual meeting of the Society of Exploration Geophysicists in Houston on October 25-28, 2009.

Poster about SEAM and SEAM results presented at SEG Summer Research Workshop on Subsalt Imaging in July 2010.

An oral presentation about SEAM was made at the Fall Annual Meeting of the American Geophysical Union in San Francisco, CA between 13-17 December, 2010.

A presentation about iWave development and application for SEAM at the HPC in O&G Workshop, at Rice University, Houston, TX 1 March, 2012.

An oral presentation about SEAM was made at the May 2012 Offshore Technology Conference.

A presentation about challenges in deepwater exploration and the SEAM contribution in meeting those challenges was made at the January, 2013 meeting of the Texas Academy of Medicine, Engineering and Science. A video of the talk is available on youtube.

Publicity

Jan Madole and Michael Fehler of the SEAM project helped staff the RPSEA booth on the afternoon of October 27, 2009 to answer questions and engage in discussions about the SEAM RPSEA activities.

SEAM staff participated in a Technology Transfer booth that was run by RPSEA at the Annual Meeting of the Society of Exploration Geophysicists held in October, 2010.

SEAM staff participated at the RPSEA booth at the May 2011 Offshore Technology Conference. A poster about SEAM was exhibited at the booth.

SEAM had a booth at the Annual Meeting of the Society of Exploration Geophysicists that was held in Las Vegas, NV in early November, 2012.

RPSEA-supported meetings

Ultradeepwater workships – attended and made presentations at these worshops
June, 2010
July, 2011
Sept. 2012
2013.

TAC meeting presentations:
Sept, 2009
Nov, 2009
May, 2011
Sep, 2011
Jan., 2012
May, 2012
Jan., 2013
May, 2013

Publications

J. Stefani, M. Frenkel, N. Bundalo, R. day, M. Fehler, SEAM Update: Models for EM and Gravity Simulations, The Leading Edge, February 2010, pp 132-135.

M. Fehler, SEAM Update: SEG advanced modeling Corp: Completion of Phase I acoustic simulations, The Leading Edge, June 2010, pp132-134.

M. Fehler, SEAM Update: Absorbing upper surface simulations on the SEAM Variable-Density Acoustic Model, The Leading Edge, October 2010, pp 1200-1201

M. Fehler, R. Day, SEAM Update: Construction of a Tilted Transverse Isotropic Model, The Leading Edge, March 2011, pp 1204-1205.

M. Fehler, SEAM Update:Phase I-RPSEA progress includes new activities, The Leading Edge, September 2011, pp 892-893.

M. Fehler, SEAM Update: Elastic Simulations, The Leading Edge, January 2012, pp 24-25.

M. Fliedner, S. Treitel, L. MacGregor, Full-waveform inversion of seismic data with the Neighborhood Algorithm, The Leading Edge, May 2012, pp 570-579.

M. Fehler, SEAM Update: TTI Simulations, The Leading Edge, May 2012, pp 510-512.

J. Morten and K. Kumar, Salt Flank Exploration - 3D CSEM Imaging in the SEAM Model, 74th EAGE Conference & Exhibition, Copenhagen, Denmark, June 2012.

M. Fehler and M. Frenkel, SEAM Update: Controlled-source Electromagnetic Simulations, The Leading Edge, September 2012, pp 1012-1014.

Fehler, M. and P.J.Keliher, 2011, SEAM Phase 1: Challenges of Subsalt Imaging in Tertiary Basins, with Emphasis on Deepwater Gulf of Mexico, SEG, 166pp, ISBN print 978-1-56080-287-7, ISBN online 978-1-56080-294-5.

M. Fehler, SEAM Phase I-RPSEA Update: Status of Simulations, The Leading Edge, December 2012, pp 1424-1425.

M. Fehler, SEAM Phase I-RPSEA Update: Elastic Simulations, The Leading Edge, April 2013, pp 466-467.

APPENDIX B - Shot & Receiver Locations and Numbering

For acoustic and TTI simulations, portions of the receiver patch that fall outside the model are not computed or recorded. The final receiver geometry for all acoustic simulations, shown in Figure B-1, used a 19.8 km receiver patch to ensure that the receivers were centered on the shot and we got a zero offset trace. There are 661 receivers in each direction for a maximum of 436961 traces per shot. Receiver channel number is stored in trace header bytes 13-16. The location of channel number M can be calculated using:

East coordinate in meters = (Source East Coordinate - 9900) + 30*ifix((M-l)/661)
North coordinate in meters = (Source North Coordinate - 9900) + (M-1-661* ifix((M-1)/661))*30
where ifix means the rounding the variable down to nearest whole integer.

(Header also contains a sequential trace number in bytes 1-4 that always starts with 1 and proceeds through the total number of actual traces present within each shot record.)

Initial plans had shot locations starting on the model boundaries near the origin. Based on suggestions from the simulation vendor, shots were repositioned so the shot grid is centered on the model and no shots are on the model boundary. As shown in Figure B-2, the shot grid is 25 m inside the east and west boundaries and 50 m inside the north and south boundaries. Shot locations are numbered 1 to 62478 based on their east and north coordinates. The location of shot number N can be calculated using:

East coordinate in meters = 150*ifix((N-1)/267*)* + 25.
North coordinate in meters = (N-1-267*ifix((N-1)/267))*150 + 50.
where ifix means the rounding the variable down to nearest whole integer and where N is the first 5 digits of shot number 1 to 62478.

Shot numbers are used for “original field record number” in trace header bytes 17-20 (aka ESPN or “energy source point number”) for the free surface shots with receivers at 15 m depth. For shots with receivers at 17 m, 100,000 is added to ESPN. For data sets simulated after the acoustic free-surface except the elastic data, a constant was added to the ESPN as stated in the EBCDIC header. These constants are listed.

Acoustic Free Surface shots at 15 m depth	0 is added	first shot number is 1
Acoustic Free Surface shots at 17 m depth	100000 is added	first shot number is 100001
Acoustic Absorbing Upper Surface at 15 m	200000 is added	first shot number is 200001
Acoustic Absorbing Upper Surface at 17 m	300000 is added	first shot number is 300001

Acoustic TTI	400000 is added	first shot number is 400001

If you remove the leading digit on the shots with numbers > 100000, the resulting number give the number of the Acoustic Free Surface shot at the same location. The Elastic shot numbers begin at 1 and the numbers have no relation to those in the other simulations. The shot x,y coordinates in the headers can be used to correlate the elastic shots to shots in the other data sets.

Figure B-3 shows the receiver numbering scheme used for all acoustic and TTI simulations. Receivers are numbered by their position relative to the source. If a given receiver location is outside of the model, that receiver is not recorded and the receiver number is not used. Thus shots near the model boundaries do not have all receiver numbers used.

Figure B-4 illustrates shot and receiver locations near the model origin. Inline and Cross-line numbers are defined on 5 m bin spacing in east and north directions, respectively, with starting value of 1001 at model origin. The first column of shots is at Inline 1006. Inline and Cross-line values in the trace headers represent the midpoint location for each trace. The "X-Y Locations" tab of spreadsheet QC_ChapterTables.xls calculates the X,Y coordinates, inline and cross-line coordinates, midpoint, and offset for any trace by shot number and channel number.

The source and receiver depths were placed at 15 m, as this is the most common depth used in multi-azimuth field acquisition today.

For the elastic simulation, shot numbering began at shot 1 and shots were numbered as follows:

Data Set	First Shot Number
2793-shot data set	1
15 by 8 km shot grid	3001
1600 shot set	11001

Figures B-5 and B-6 illustrate the receiver numbering scheme for the elastic 2793-shot set and the 15 km by 8 km shot set for both seafloor and surface traces. The receivers are numbered in a manner similar to that for the acoustic data sets. Receiver 1 is the furthest one southwest of the source. Receivers are numbered increasing from South to North and then from West to East. For the 2793-shot set, receivers are numbered within a grid centered on the source. A fixed receiver grid was used for the 15 by 8 km shot grid so a receiver with a given number has a fixed location.

See the list of headers defined for the data in APPENDIX B at the end of this section.

Figure B-1. Recording and simulation patch geometry drawn to scale. The portion of any patch outside the model (shown in gray) is not computed or recorded. Only 22% of shots have a full complement of 436,921 traces. The average number of traces/shot is about 77% of the maximum. (Slide 3 from Classic_Data sets rev 7.ppt by Acquisition Committee)

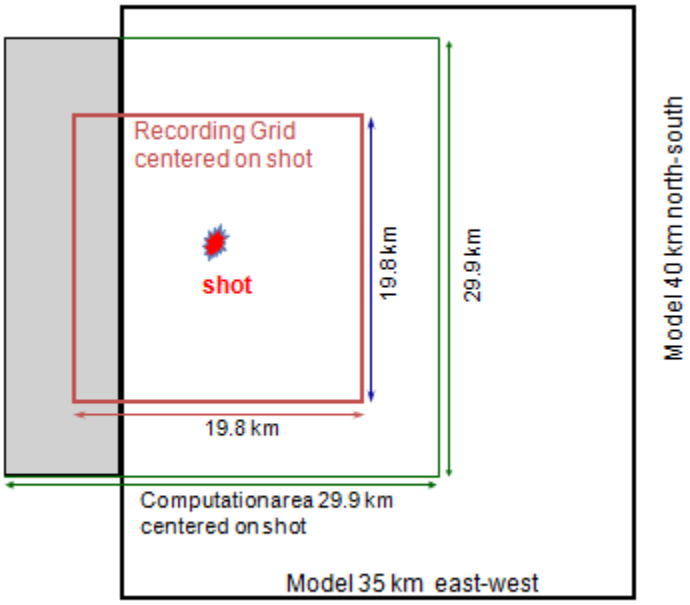

Figure B-2. Shot numbering scheme for acoustic shots including TTI. Shot locations are numbered 1 to 62478 based on East and North coordinates. Inline and Cross-line numbers are defined on 5 m bins in east and north directions respectively with value of 1001 at model origin. (Slide 4 from Classic_Data sets rev 7.ppt by Acquisition Committee).

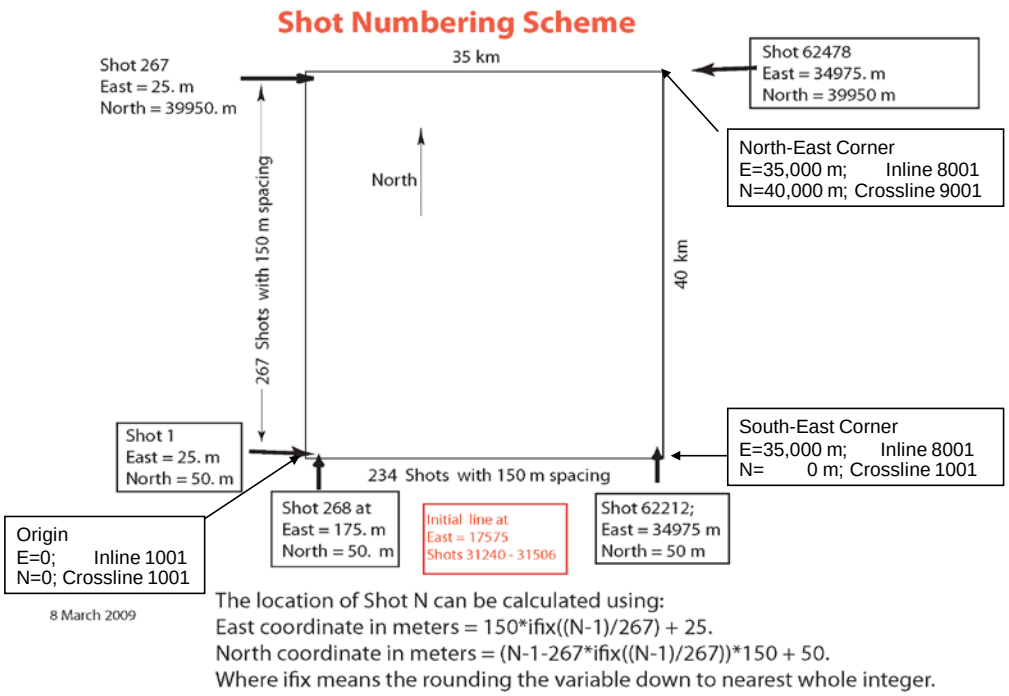

Figure B-3. Channel numbering scheme for acoustic and acoustic TTI shots. Shots closer than 9900 m to a model edge have missing channel numbers. Channel number is NOT sequential trace number within the shot record. (Figure by Mike Fehler).

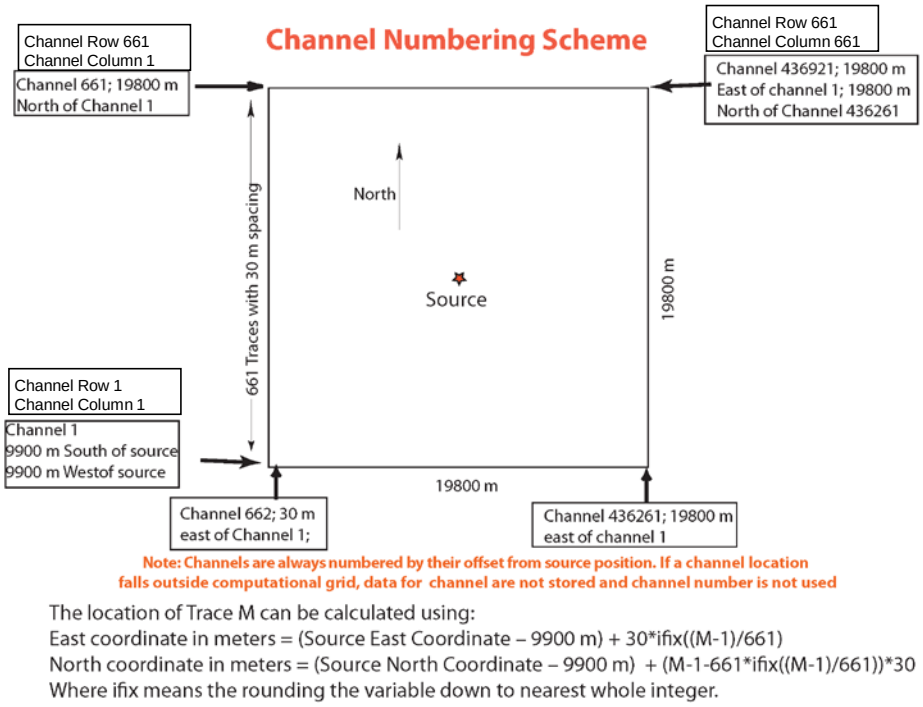

The location of Trace M can be calculated using:
East coordinate in meters = (Source East Coordinate – 9900 m) + 30*ifix((M-1)/661)
North coordinate in meters = (Source North Coordinate – 9900 m) + (M-1-661*ifix((M-1)/661))*30
Where ifix means the rounding the variable down to nearest whole integer.

Figure B-4. Shot and Receiver locations near the model origin (0,0) for acoustic data sets. Shot 1 is at E=25 m, N=50 m. Inline and Cross-line numbers are defined on 5 m bin spacing in east and north directions respectively with value of 1001 starting at model origin. Shot 1 is at Inline 1006, cross-line 1011.

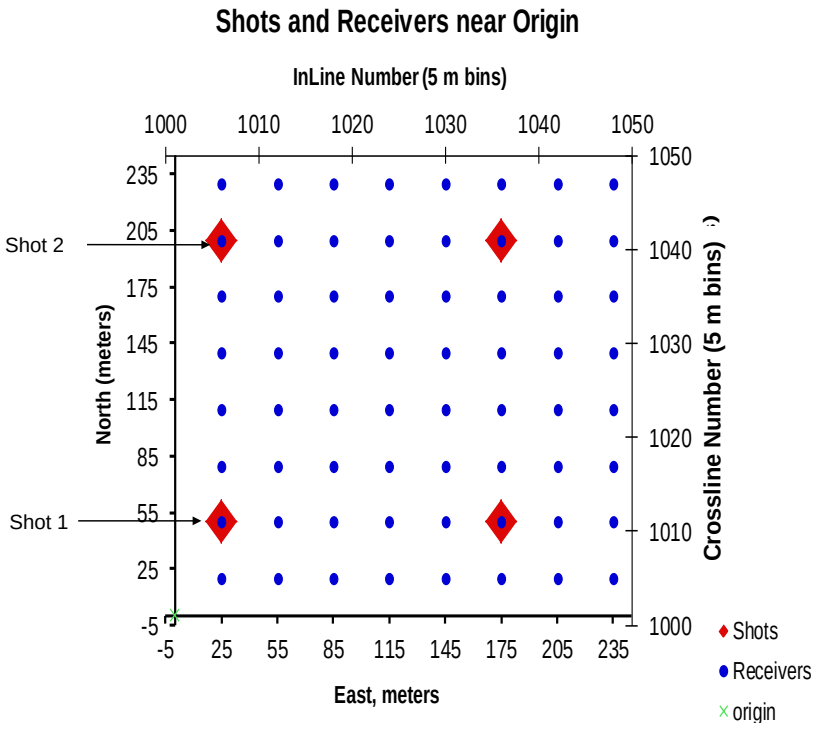

Figure B-5. Channel numbering scheme elastic 2793-shot set and the 15 km by 8 km shot set for seafloor data. If Channel location falls outside model, the number associated with this channel is not used (Figure by Mike Fehler**).**

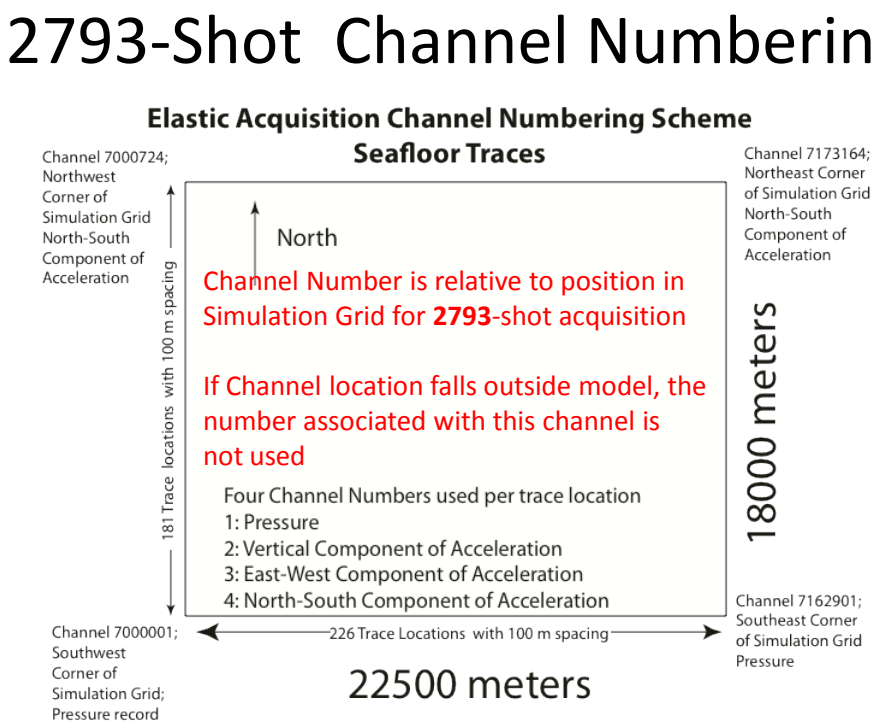

Figure B-6. Channel numbering scheme elastic 2793-shot set and the 15 km by 8 km shot set for surface data. If Channel location falls outside model, the number associated with this channel is not used (Figure by Mike Fehler).

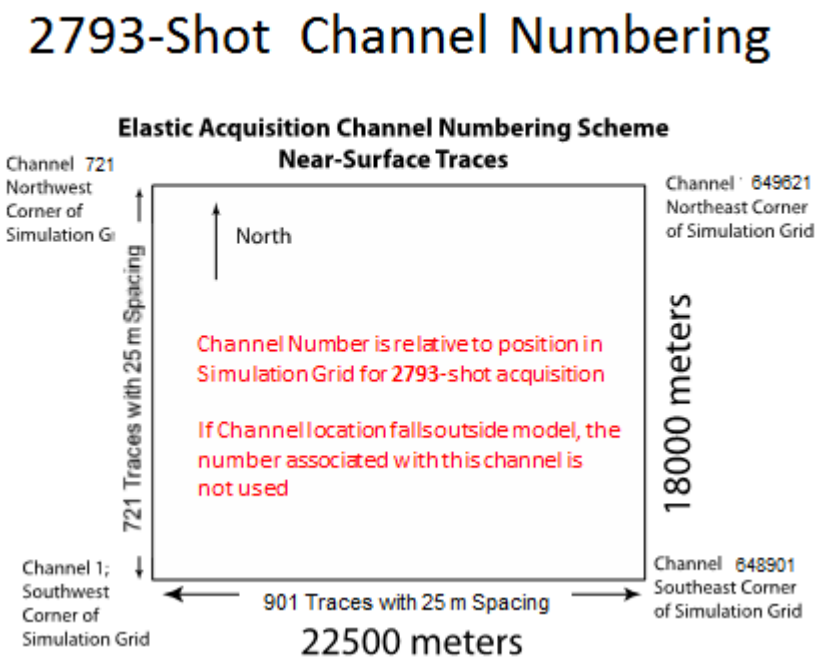

Appendix C – SEG-Y Header Definitions

This appendix list headers actually used taken from a Promax header dump for shot 05361, file Shot05361_Promaxhdrdump.txt in the report archive. The raw SEAM data is one shot per SEG-Y file so every shot has its own EBCDIC textual header and binary file header followed by the trace headers. The WAZ and NAZ Classic Data Sets have the same binary trace headers but different sort order as well as different EBCDIC and Binary File headers.

Headers for Simulated Shot Records

Textual File Header, aka EBCDIC header.

```
C 1 Client: SEAM Phase 1   Vendor: Tierra Geophysical   Date: May 11, 2009
C 2 Project Description: SEAM Phase 1 Numeric Simulation
C 3 SEGY Data Format: IEEE                    XY Units: Meters
C 4 Data Description: Full azimuth shot records      Source(s): 005361
C 5 Data Type:  Shot record amplitudes in time       Units: Pascals
C 6 Specified Amplitude: RMS value of 100 Pascals over a window from .664-.984s
C 7   at an offset of 990m (the direct arrival through water)
C 8 Observed Amplitude: Approximately 260 Pascals for postive peak at 990m for
C 9   direct arrival through water
C10 Wavelet Description: Npoles, f3db pairs  (4,22) (2,20) (1,5)
C11 Projection: UTM Zone 16              Spheroid: WGS84
C12 Geodetic datum: WGS84                Central meridian: 87 degrees W
C13 Grid origin coor.: 401,674.66E 3,097,605.23N   Scale factor: .9996
C14 Grid origin lat long: 28:00:00N  88:00:00W
C15 Corner      X       Y  Iline  Xline  Given in Local Coordinates
C16   1         0       0   1001   1001
C17   2         0    40005   1001   9002
C18   3     34995    40005   8000   9002
C19   4     34995       0   8000   1001
C20 Shot Depth:        15 m                Receiver Depth:     15 m
C21 Inline bin size:     5 m               Max time:          16000 ms
C22 Cross-line bin size:  5 m              Sample interval:    8 ms
C23 First Sample:        0 ms              Samples/trace:      2001
C24 Receiver patch: -9900 to 9900 in both X and Y directions
C25 Channel interval: 30 m in both X and Y      Number of Channels: 436921
C26 Number of gun arrays: 1                  Shot Pattern:       Single
C27 Shot interval: 150 m in both X and Y       Shot columns: 234
C28 Coordinates at first shot: X=25 Y=50       Shot rows: 267
C29 Polarity: +RC peak                       Phase: Mixed/causal
C30 Conventional data: Shots 1-62478, 2nd cable (17m depth): Shots 100001-162478
C31 Absorbing surface: Shots 200001-262478,
C32 Absorbing surface second cable (17m depth): Shots 300001-362478
C33 HEADER NAME       POSITION   LENGTH     HEADER NAME       POSITION   LENGTH
C34 CHANNEL ROW       181        4I         VENDOR NUMBER       197        4I
```

C35 CHANNEL COLUMN 185 4I SOFTWARE CHECKSUM 201 4I
C36 INLINE 189 4I DATE AND TIME 205 8I
C37 CROSS-LINE 193 4I
C38 PROCESSING FLOW:
C39 Data compressed approximately 10:1 using method of US Patent 6,160,919
C40 SEGY REV1

Binary File Header

Binary Header length in bytes = 400
Job Identification Number ..... = 0
Line Number ..... = 0
Reel Number ..... = 0
Traces per Ensemble ..... = 661
Sample interval (micro sec) ..... = 8000
Recording sample interval ..... = 0
samples per trace ..... = 2001
recording samples per trace ..... = 2001
Data sample format ..... = 4 Byte IEEE floating point
Correlated data traces ..... = Yes
Binary gain recovery ..... = Yes
Amplitude recovery method ..... = Other
Measurement system ..... = Meters
Impulse signal recovery code ..... = 0
SEG-Y format revision number ..... = 1. 0
Fixed trace length flag ..... = 1
Extended Textual File Headers .... = None
Sample rate of recorded data (ms) .. = 8.
Number of samples per trace ..... = 2001
Data sample format ..... = IEEE FLOATING POINT

Binary Trace Header

1-4: Sequential trace number within this file. Since 1 shot/file, this is also sequential trace for shot
13-16: Channel number within full shot record (before positions off the edge of the model are discarded)
17-20: Shot number, aka “Energy Source Point Number”
21-24: Sequential row number – values are all zero
25-28: Sequential trace number within row – set properly
29-30: Trace type = 1 (seismic)
33-34: Horizontal stack fold = 1
37-40: Signed offset from source to receiver (convention for sign unclear when in 3D)
41-44: Receiver elevation * 10000 (always a negative constant)
45-48: Surface elevation at source * 10000 (set at negative constant -150000, instead of zero!)
49-52: Source depth * 10000 (always positive constant) = 150000
53-56: Datum elevation at receiver (=0)

57-60: Datum elevation at source (=0)
69-70: Scalar for elevations and depths (= -10000, meaning divide by 10000)
71-72: Scalar for coordinates (= -10000, meaning divide by 10000)
73-76: Source X * 10000
77-80: Source Y * 10000
81-84: Receiver X * 10000
85-88: Receiver Y * 10000
109-110: Delay recording time (=0)
115-116: Number of samples per trace (constant 2001)
117-118: Sample interval in microsec (constant 8000)
181-184: Channel Row 1-661 in the Y direction
185-188: Channel Column 1-661 in the X direction Channel Number = Row+661*(Column-1)
189-192: Inline Common Mid Point Location 1001 to 8000 in X direction on 5 m bin
193-196: Cross-line Common Mid Point Location 1001 to 9002 in Y direction on 5 m bin
197-200: Vendor Number = 7
201-204: Software checksum
205-212: Date and Time the SEG-Y file was created and compressed (not same as date of simulation)

The above header dump reveals a few non-standard SEG-Y header definitions or locations:

Bytes 21-24 (Sequential row number) are all zero but bytes 25-28 (Sequential trace number within a row) were set. The simulation contract did not require either of these headers to be set. However, since they are a linked pair, if one is set the other should be also to avoid confusion.

Bytes 45-48: The simulation contract defined this location as: “Source elevation from sea level” so it was set to -15, 000 (elevation times the scalar 10000). However, the standard definition for bytes 45-48 is “Surface elevation at source”, i.e., the elevation of the surface of the earth at the source XY = zero for ocean data.

Bytes 181-188: Channel Row and Channel Column increment from 1 to 661 for each row and column in the receiver array as shown in Figure 14 in the Acquisition chapter. These two headers occupy the locations normally reserved for “X and Y coordinate of the ensemble position of this trace”. (“Ensemble position” depends on whether the ensemble represents a shot record, a CMP, CRP, etc.)

Bytes 197-200 Vendor Number is 7. These bytes are normally reserved for Shotpoint Number. “Shot Number” in bytes 17-20 is the same as Shotpoint number for the free surface, 15 m receiver data, but not for the 17 m receiver data or the absorbing upper surface data.

Bytes 201-204: Software Checksum is the auto-computed checksum of the currently installed software binaries to detect any changes in the software. It occupies the bytes normally reserved for two standard headers “Scalar to be applied to the shotpoint number” and “Trace value measurement unit” (Pascal for this data).

Bytes 205-212: Date and Time format is a 64-bit integer that represents Unix/POSIX time, which is the number of seconds since January 1, 1970. The upper 4 bytes are stored as an integer in bytes 205-208 and the lower 4 bytes are stored as an integer in bytes 209-212. Java code to extract it would look something like this:

```
int[] traceHeader = new int[60];  // 240 bytes long
read_a_trace_header(traceHeader);
long upper = (long)traceHeader[51];  // Bytes 205-208
long lower = (long)traceHeader[52];  // Bytes 209-212
long time = lower + (upper << 32);  // Note use of bit-shift operator
Date date = new Date(time);
```

The value represents the date and time the SEG-Y files were created and compressed. This is generally two to four weeks after the data was simulated, but could be more or less for any particular shot file.

This Date/Time stamp occupies bytes normally reserved for two standard headers: Transduction Constant (205-210) and Transduction Units (211-212) intended to define units for the trace amplitudes like pascals, millivolts, m/s, etc., in machine readable form. The data was computed in pascals. The dual depth files allow computation of vertical component of velocity. The standard location for day of year is bytes 159-160 and time (hours, min, sec) is bytes 161-168.

All length units are in meters *after* the scalar for XY coordinates or depth is applied. That scalar is -10000 meaning all values are divided by this number. This is as per SEG-Y standard, but all processing packages may not automatically apply the scalar.

The Binary file header dump for shot 5361 shows the "number of traces/ensemble = 661" whereas it should be 123201. This header has the same value of 661 on shot 35265. Hence is may be incorrect on all shots. The statement in the EBCDIC header of "Number of Channels: 436921" is the maximum number for shots near the center of the model, not the number of traces for a particular shot. The only information in the EBCDIC header that changes with each shot is the Source number and the date.

The contract specified "Files must be readable by SeismicUnix. However, when there is a discrepancy between SEGY standard and SeismicUnix, the SEGY standard must be chosen. "

References for SEGY Format:

http://www.seg.org/SEGportalWEBproject/prod/SEG-Publications/Pub-Technical-Standards/Documents/seg_y_rev0.pdf

http://www.seg.org/SEGportalWEBproject/prod/SEG-Publications/Pub-Technical-Standards/Documents/seg_y_rev1.pdf